Selection of Vegetation and Flexible Vegetal Drag Coefficients for Erosion Control in Lacustrine Wave Environments

A DISSERTATION
SUBMITTED TO THE FACULTY OF THE GRADUATE SCHOOL
OF THE UNIVERSITY OF MINNESOTA
BY

John A. Chapman

IN PARTIAL FULFILLMENT OF THE REQUIREMENTS
FOR THE DEGREE OF
DOCTOR OF PHILOSOPHY

John S. Gulliver, Bruce N. Wilson

June 2014

Acknowledgements

This dissertation could not have been possible without the help and support of so very many people. My wife and daughters and mother have supported and encouraged me throughout this endeavor and without their support this could not have been accomplished. Bruce Wilson and John Gulliver have been invaluable for their ideas and experience in research and academics. Mary Blickenderfer was a strong catalyst in initiating my work and this could not have been done without her expertise and experience with plants and shoreline restorations. I also want to thank Chris Paola, an exemplar of teaching and research I can only strive to follow, who always pressed me to do more. I also want to thank all of those at Saint Anthony Falls Laboratory and Bioproducts and Biosystems Engineering who helped make the research happen, including Brad Hanson, Stephanie Nappa, Chris Ellis, and Dick Christopher.

The U.S. Environmental Protection Agency provided funding for this research through the Minnesota Pollution Control Agency's 319 projects.

Dedication

This dissertation is dedicated to my family; those who supported me up to now and those who inspired to achieve more in the future. To Alvin, Karen, Sara, Abigayle, Kailey, and Erica.

Abstract

The restoration of plant communities in littoral zones often fails. Because littoral habitats around the world often are subject to changing water regimes and potentially changing future climates, a better understanding of species competitive interactions under such conditions is needed for restoration plant selection. To represent shoreline plant communities, we grew eight freshwater species used in shoreline restoration projects in Minnesota and Wisconsin, USA, in outdoor basins and manipulated water levels to determine the effect on above ground biomass. Biomass production of some species in the competing environment was related to the proximity to water or inundation depth and frequency. *Sparganium eurycarpum* and *Bolboschoenus fluviatilis* dominated the total biomass in all water manipulations. These findings allow for better design of plant community composition and better vegetative erosion control under a variety of water conditions.

This thesis also investigates the ability of plants to reduce waves and flow, through a comparison of parameters that characterize vegetation flexibility effects on flow resistance and drag. Drag forces measured in a flume for simple cylindrical obstructions of the same shape and size but with different flexibility under several flow conditions. A novel formulation is developed where the drag coefficient is evaluated as a function of the relative velocity and the elastic modulus of the obstruction.

Current methods for estimating energy dissipation require plant specific parameters that are difficult to estimate for the large variety of plant morphologies used in shoreline protection, requiring testing on each species of interest. The method

developed herein directly measures hydrodynamic forces on individual plant shoots using a torque sensor mounted beneath the bed of a flume. The data collected also suggests that more flexible objects result in less drag force on each element and suggests that frequency response is related to the frequencies existing in the driving wave and the natural frequency of the obstruction element, although harmonic synchronization appears to occur in some cases, doubling the expected drag force magnitude.

A case study is also included as an example of how the findings presented here can be applied to a shoreline erosion control evaluation. The case study is an inland lake in northern Minnesota currently having erosion soil losses. Data from this research is used to develop a vegetation scenario that is predicted to limit the erosion.

Table of Contents

List of Tables

List of Figures

Chapter 1
Introduction and Background

Introduction

Evolution has been occurring in nature for millions of years and established a balance in dynamic systems. Species and processes may be unbalanced temporarily, but evolution tends to restore a balance in the systems. An invasive or aggressive species may dominate a system, but eventually a competitor emerges and balance is restored. Engineering designs that utilize natural materials can take advantage of the evolution which has already optimized the systems, but the systems are complex and deeper understanding is needed for reliable designs. Vegetation is one of these natural materials that has advantages for engineered erosion control, but our understanding of the material needs to be improved.

Water, energy, air, and nutrients are the most important resources for life. Shoreline erosion impacts two of these; our soil (and nutrient) resources, as well as the quality of our water resources. Soil erosion is a critical part of a natural cycle of land formation, yet it is also a natural hazard resulting in the loss of resources, infrastructure, property and even life.

The official length of the United States shoreline is over 153,600 km (NOAA, 2014) and 123 Million people, or 39% of the population of the United States was living in coastal counties in 2010 (NOAA, 2013a). Approximately 350,000 structures are currently located within 152 meters of the United States shoreline (NOAA, 2013b). These figures showing the concentration of people and property within shoreland zones reflect

the large hazard potential of shoreline erosion, yet these figures do not include inland lakes and water resources.

The Minnesota Department of Natural Resources (MnDNR) accurately tracks the length of Lake Superior coastal shoreline (304 km), number of lakes (11,842 over 10 acres), and the number of natural rivers and streams (6,564 totaling 111,366 km), along with the total area covered by lakes and rivers (1,036,116 ha), (MnDNR website). However, the MnDNR does not officially measure the length of the inland lake shoreline or the population, structures, or other features within the shoreland zone. Using the data on area and quantity of lakes it can be estimated that Minnesota has between 80,500 km and 144,800 km of inland lake shoreline which is on the same order of the length of the total U.S. coastal shoreline, suggesting the amount of property and potential losses from shoreline erosion is significant.

The fundamental soil particle detachment that is erosion can occur for many reasons, including gravity, wind flow, water flow, water waves, vehicle tires or any impact force large enough to dislodge a soil particle. The fundamental soil erosion process becomes more complex and specific as the displacement forces and environments of erosion are explored.

In a shoreline environment, erosion is often most significant from wave action which may be induced by winds or in some cases anthropogenic activity such as boat navigation. In deeper water, waves do not have fluid particle orbital motion that extends to the soil bed at the bottom of the water column to cause erosion, but obstructions in deep water can dissipate wave energy and reduce the erosion potential closer to the

shoreline. Near the shoreline, shallow water waves create fluid particle oscillations along the soil bed resulting in shear stresses that may dislodge soil particles and allow for sediment transport away from the shoreline. Additionally, breaking-wave forms have additional fluid dynamics, such as plunging, that are highly erosive in nature.

Soil particle removal along the near shore soils or toe of the shoreline can result in undercutting and over-steepening of the littoral zone slope above the waterline. Over-steepening of the slope can result in additional slope failures and erosion that threatens property and lives.

Soil particle stabilization at the shoreline can be achieved through several methods. Hard armoring with rock or concrete may be appropriate in some conditions (USACE, 2002), but lacks additional environmental benefits (Wilcox and Meeker, 1992) that can be achieved using vegetation. Future climate conditions (IPCC 2007) may result in hard armoring to be located too low or too high to be effective, where vegetation has the potential to migrate with water level changes.

Stabilization through engineered vegetation is often not recommended in areas where significant property loss is possible (USACE 2002). Challenges on using vegetation in engineered solutions stem from the highly variable nature of vegetation. Each vegetation species has its own morphology, growth cycle, establishment needs, and from these attributes each vegetation species has a different potential for providing erosion stabilization at any one specific site.

The overall goal of this research is to improve our understanding of shoreline erosion control using vegetation. The specific research questions address a few of the

barriers to using vegetation for engineering shoreline stabilization by providing a better understanding of how shoreline species grow in current and future climates so we can better select species for shoreline restoration and provide a better understanding of the drag occurring due to the vegetal elements.

The fundamental concepts of this research can be applied to any shoreline in the world, but the vegetation of interest has been selected to be common in lake shoreline restoration projects in Minnesota and the flow conditions have been selected to be common for inland lakes.

Approach

There are many questions that have not been answered regarding using vegetation for shoreline erosion control. The complex interaction of vegetation with the environment leads to many unknowns when evaluating natural sites and useful conclusions that can be applied to other sites are rare. This thesis uses experiments in engineered vegetation plots and flumes to attempt to isolate key aspects of vegetation to provide more useful predictions for engineering use.

Experimental outdoor vegetation plots were established at the University of Minnesota St. Anthony Falls Laboratory (SAFL) to evaluate species growth. Experimental indoor wave flume experiments were conducted at SAFL and the University of Minnesota Bioproducts and Biosystems Engineering Department (BBE) hydraulics laboratory to evaluate the drag occurring from vegetal elements.

Thesis Layout

This thesis is an assembly of several research articles. This chapter provides an introduction to the collection of work, the second, third, and fourth chapters are reproductions of research articles, the fifth chapter includes a case study of calculation examples, and the last chapter provides an overall conclusion to the thesis.

The second chapter entitled "Competition and Growth of Eight Shoreline Restoration Species in Changing Water Level Environments" has been published in the December 2013 issue of Ecological Restoration. This chapter explores how eight different shoreline vegetation species grow under different water level conditions in an effort to determine if some species can be better established to provide shoreline erosion control. I was the first author and drafted this article in addition to processing and analyzing the data collected. Mary Blickenderfer assisted with editing the vegetation information; Bruce Wilson assisted with guidance and editing of the statistics. The data collected for this chapter required significant work of many people, although I did participate in plant establishment, experimental design, and data collection.

The third chapter entitled "Drag force parameters of rigid and flexible vegetal elements" has been submitted to Water Resources Research in February 2014. This chapter explores how flexibility alters vegetal element drag and provides a predictable physical relationship between vegetation modulus of elasticity and the drag coefficient that should be used for that element. I was the first author and drafted this article. I designed the experiment, assembled the flume apparatus, and collected the data for this chapter.

The fourth chapter entitled "Flume Instrumentation for Measurement of Drag on Flexible Elements Under Waves" has been accepted for publication in Experiments in Fluids in March 2014. This chapter explores how element flexibility affects the drag occurring in wave flow, and illustrates how the frequency of the wave and the natural frequency of the element can interact to affect the drag forces. The drag response under waves is more complex than directional flow as expected, and predictions of drag coefficient are related to the Keulegan-Carpenter number and the modulus of elasticity. I was the first author and wrote this article. I designed the experiment, assembled the flume apparatus, and collected some of the data. A student worker assisted with some of the data collection.

The fifth chapter entitled "A Case Study of Shoreline Erosion Calculations" provides an example of how the information provided in this body of work can be used with information from the literature to better evaluate shoreline erosion potential. The sixth chapter is provided as a summary and conclusion of this research. Appendices contain the data used in each of the experiments.

Chapter 2
Vegetation Selection

Summary

The restoration of plant communities in littoral zones often fails. Because littoral habitats around the world often are subject to changing water regimes and potentially changing future climates, a better understanding of species competitive interactions under such conditions is needed for restoration plant selection. To represent shoreline plant communities, we grew eight freshwater species used in shoreline restoration projects in Minnesota and Wisconsin, USA, in outdoor basins and manipulated water levels to determine the effect on above ground biomass. Biomass production of some species in the competing environment was related to the proximity to water or inundation depth and frequency. *Bolboschoenus fluviatilis* had biomass differences related to inundation under dry, fluctuating, and normal water manipulations and *Schoenoplectus tabernaemontani* had biomass differences related to inundation under wet and fluctuating water manipulations, while *Carex comosa* and *Carex lacustris* had biomass differences related to placement location under only the wettest water manipulation and *Sparganium eurycarpum* had biomass differences related to placement location under only the driest water manipulation. *Spartina pectinata, Carex vulpinoidea,* and *Juncus effusus* appeared to not have biomass differences related to placement location under any of the water manipulations used. *Sparganium eurycarpum* and *Bolboschoenus fluviatilis* dominated the total biomass in all water manipulations. *Carex vulpinoidea* and *Carex lacustris* had

the least total biomass production in all but one water manipulation. These findings allow for better design of plant community composition and better vegetative erosion control under a variety of water conditions.

Introduction

The establishment of vegetation along inland lake shorelines when restoring these dynamic environments is often critical for sediment stabilization and erosion prevention. Sediment stabilization is often a prerequisite to site restoration (USDA 1996), if not a primary goal of the restoration. The use of rock and concrete for erosion control may be more reliable in the short term, but vegetation provides additional benefits to the ecosystem (Wilcox and Meeker 1992). Revegetation projects in littoral areas commonly plant a single species or limited species in single beds (Henderson et al. 1999) and water depth amplitude, depth duration, and depth frequency are all critical factors for plant species survival in restorations along lakes and reservoirs (Bunn and Arthington 2002). Either a lack of understanding of species response to water regime, or a lack of understanding of water regime could result in failure of the entire restoration project where only a few species are present. Recent surveys suggest an 80% failure rate for littoral vegetation restoration (Vanderbosch and Galatowitsch 2010).

Plant species have different adaptation strategies for coping with various water regimes. These strategies may result in taller vegetation (Squires and Van Der Valk 1992), changes in growth cycle (Blom and Voesenek 1996), or changes in characteristics of the root system (Visser et al. 1996). Failure to understand how species will respond to

different water regimes can result in plant communities that do not meet restoration goals (Galatowitsch et al. 1999).

With a better understanding of how water depth influences the establishment of plant communities and competition between commonly planted species, we can promote greater use of vegetation for erosion control on shorelines and take advantage of the additional habitat and adaptability vegetation provides. Existing seed banks and competition between species have been shown to limit success of restorations with fluctuating water levels (Budelsky and Galatowitsch 2000). For example, Budelsky and Galatowitsch (2000) found that competition between the planted *Carex lacustris* and plants in the existing seed bank limited the success of *C. lacustris* in the highest elevations. Failure of vegetation establishment can also be the result of improper location of the planting in relation to water depth (Vanderbosch and Galatowitsch 2011).

While many studies have evaluated how water level influences growth, survival, and species richness (Wilson and Keddy 1988, Kirkman and Sharitz 1992), the literature is inconsistent particularly regarding species diversity and competition (Webb et al. 2012). Studies have focused on a single species or limited numbers of species (Seabloom et al. 1998), but only a few studies have evaluated larger communities of species (Squires and Van DerValk 1992). In addition, some previous studies of water depth impacts on macrophyte communities (Neilson and Chick 1997, Casanova and Brock 2000) provide insight to establishment and competition, but studies on additional species are needed to understand impacts in other geographic regions.

Additionally, future changes in water regimes may be influences by factors, such as local flow alteration and climate (IPCC 2007), which may favor the survival of some plant species over others (Bailey-Serres and Voesenek 2008). In the upper Midwestern United States, fluctuating water regimes from increasing storm event precipitation magnitudes and prolonged dry periods are predicted. Data available for individual plant survival with water regime changes may not be representative of plant communities established for restorations. Experiments that examine the response of restorations to predicted changes in water regime are necessary to establish successful restoration projects resilient in the face of climate change.

Our study evaluated the growth of, and competition between, eight shoreline plant species commonly used in restoration projects in the upper Midwestern United States when subjected to different water regimes or inundation patterns. We included both rhizomatous and caespitose species typical of littoral habitats and commonly used for inland lake shoreline restoration in Minnesota and Wisconsin. We subjected these plants to wet, dry, normal, and fluctuating water levels that could result from potential future climate scenarios and measured plant biomass to understand how restoration plantings will survive and adapt to future climate induced water level depth and fluctuation stressors.

Methods

We performed this study at the University of Minnesota's St. Anthony Falls Laboratory (SAFL), which is located along the Mississippi River at St. Anthony Falls in

Minneapolis, Minnesota. We selected eight species commonly used in inland lake restoration in Minnesota and Wisconsin to represent caespitose and rhizomatous grown forms of littoral plant communities, as shown in Table 2.1. *Sparganium eurycarpum, Bolboschoenus fluviatilis, Schoenoplectus tabernaemontani,* and *Carex lacustris* are species commonly planted below the water surface and will be referred to as "littoral species" in this study. *Carex vulpinoidea, Carex comosa, Juncus effuses,* and *Spartina pectinata* are species commonly planted above the water surface and will be referred to as "wet-transition species" in this study. The 2-year old plants were grown off-site by Natural Shore Technologies of Maple Plain, Minnesota and were delivered in 0.1 m pots with a 0.3 m minimum plant height. The typical mature height of the plants ranges from 0.4 to 3 meters, as shown in Table 2.1.

Table 2.1. The plant species used in this study with their growth form and common shore zone planting location.

Species Group	Scientific name (Common name)*	Growth Form	Typical Mature height* (m)
Wet-Transition	*Carex vulpinoidea* (Fox sedge)	Caespitose	1
	Carex comosa (Bottlebrush sedge)	Caespitose	0.5-1.2
	Juncus effusus (Common rush)	Caespitose	0.4-1.3
	Spartina pectinata (Prairie cordgrass)	Rhizomatous	2-3
Littoral	*Sparganium eurycarpum* (Giant bur-reed)	Rhizomatous	2.5
	Bolboschoenus fluviatilis (River bulrush)	Rhizomatous	1-2
	Schoenoplectus tabernaemontani (Softstem bulrush)	Rhizomatous	0.5-3
	Carex lacustris (Lake sedge)	Rhizomatous	0.5-1.35

* Nomenclature and height according to *Flora of North America*: http://fna.huh.harvard.edu/

We investigated the impacts of water regime, planting elevation in relation to water level, and species on the above ground biomass generated during the first growing season after transplanting. We established wet, dry, and normal water level regimes through review of historical water levels for over 26 lakes in Minnesota in dry, wet, and normal years as classified by the Minnesota State Climatology Office. We established the fluctuating regime through a review of climate change scenarios and modeling (Liukkonen 2012) where precipitation increases are predicted in September and October. Within each water regime, we planted the four littoral species randomly in seven horizontal rows at equally spaced elevations in the lower half of the regime plot. We planted the wet-transition species in a similar pattern into seven horizontal rows in the upper half of the regime plot. We did not replicate the water regimes, but the planting pattern across each row included four individual plants of each species alternated with the other species, resulting in four four-species units. We created all four water regime plots with identical species planting locations.

We constructed the four outdoor planting basins in the dry sediments filling retired Spillway One of the St. Anthony Falls Dam. We diverted water from the Mississippi River above the St. Anthony Falls Dam, which effectively creates a reservoir or lake at this reach, to create one water regime within each basin according to the experimental design.

We constructed the four basins identically and placed them adjacent to each other with minimal shading from surrounding structures. Basins were 4.9 m by 4.9 m square in size with a 0.9 m depth. We constructed the basin walls of CDX plywood with wood framing reinforcement and sealed with a 45mil EPDM rubber membrane. We placed backfill around the basin exterior to a depth of 0.3 m to 0.6 m for structural support. A schematic of the basin is shown in Figure 2.1.

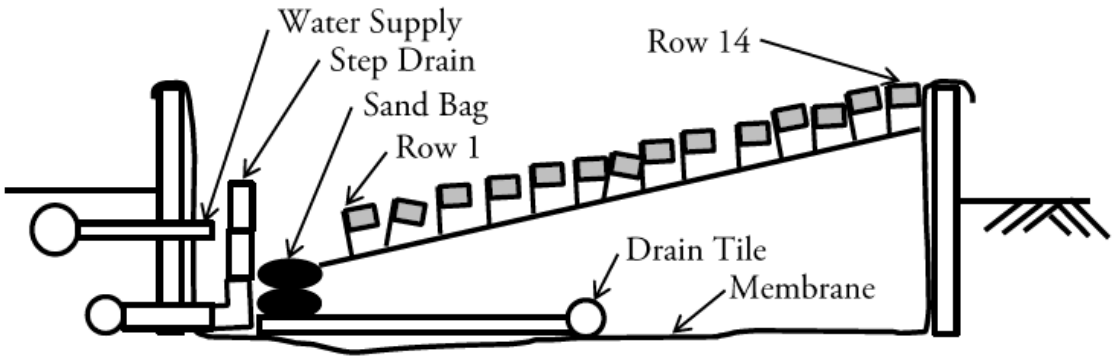

Figure 2.1. The basin schematic showing the overall cross section of the four identical basins with plumbing, retaining walls, and impervious membrane and flagged planting rows.

We supplied the basins with water through a 0.15 m diameter PVC header pipe from the SAFL main channel sump. We connected each basin to the supply line header pipe by a separate 0.05m gate valve and we drained each basin by a 0.1 m PVC pipe. We used a drain pipe turned in a vertical orientation using a 90-degree pipe bend to act as a weir outlet. We adjusted the drain pipe vertically using a slip fit coupling for control of

water level. We sealed pipes passing through the rubber membrane using a flange and gasket on each side of the membrane along with Valkem sealant. We also placed a 0.1 m HDPE perforated drain line in the bottom of the basin running parallel to the artificial shore, above the membrane, to provide nearly uniform water conditions through the basin soils. We continuously cycled water from the Mississippi River through the basins during the experiment and used a Hach Hydrolab Data Sonde 5 to monitor the basin water for temperature, pH, and dissolved oxygen.

We filled the basin interior with the planting medium at approximately a 7.5-horizontal: 1-vertical slope with the lowest elevation along the north east side (approximately 60 compass degrees) and the highest elevation along the south west side (approximately 240 compass degrees). The sloping planting medium had an overall elevation change of approximately 0.5 meters over a length of 3.9 meters. The four basins had uniform slopes, except the basin used for the normal water regime unintentionally was 0.1 meter lower in the upper rows. We placed a row of sand bags 0.32 m from interior of the basin wall between the inflow and outflow pipes and the sloping planting medium to prevent the plumbing network from clogging from possible soil movement. We used an engineered soil planting medium consisting of 50% sand and 50% Mn/DOT Grade 2 compost (Mn/DOT 2005) by volume. The purpose of the relatively high compost fraction was to assure that no nutrients became limiting. We mixed the sand and compost on site during soil placement. To verify uniform conditions, we collected soil samples from each basin and analyzed them for total nitrogen, total phosphorus, and loss on ignition.

Between June 14 and June 16, 2010, we transplanted two hundred twenty-four plants from pots into the basin planting medium. Each plant was spaced 0.32 m from the next plant in the row, and each row was 0.32 m from the next row. Each row was located 0.038m apart in elevation, with row 1 at the lowest elevation and row 14 at the highest elevation, as shown in Table 2.2. We planted the littoral species in the lowest 7 rows and wet-transition species in the highest 7 rows. Individual species were able to migrate within the basin to allow for competition comparisons.

Table 2.2. Soil elevations and example inundation depth of plant base for each row of the four basins. A negative inundation value indicates the height above the water surface.

	Soil Elevation (m)				Average Inundation level (m)			
Row	Wet	Dry	Fluctuating	Normal	Wet	Dry	Fluctuating	Normal
1	0.250	0.250	0.230	0.250	0.453	0.224	0.329	0.342
2	0.290	0.280	0.265	0.270	0.413	0.194	0.294	0.322
3	0.330	0.310	0.300	0.290	0.373	0.164	0.259	0.302
4	0.380	0.360	0.350	0.390	0.323	0.114	0.209	0.202
5	0.405	0.425	0.400	0.450	0.298	0.049	0.159	0.142
6	0.430	0.455	0.443	0.465	0.273	0.019	0.116	0.127
7	0.480	0.496	0.487	0.480	0.223	-0.023	0.072	0.112
8	0.530	0.510	0.530	0.495	0.173	-0.037	0.029	0.097
9	0.573	0.555	0.566	0.510	0.130	-0.082	-0.007	0.082
10	0.615	0.565	0.611	0.535	0.088	-0.092	-0.052	0.057
11	0.645	0.627	0.615	0.560	0.058	-0.154	-0.056	0.032
12	0.675	0.665	0.684	0.578	0.028	-0.191	-0.125	0.015
13	0.705	0.702	0.726	0.595	-0.002	-0.229	-0.167	-0.003
14	0.735	0.740	0.767	0.625	-0.032	-0.266	-0.208	-0.033

We began filling the basins with water on June 23, 2010 to achieve the mid-basin level on June 29, 2010. We controlled the water levels of each basin by manually adjusting the weirs weekly according to targeted water level regimes. The actual water

levels that occurred in the basins deviated from the targeted levels due to a shorter experimental time of operation, rain events and other climate factors. The fluctuating water regime shows the greatest deviation from the targeted level and does not have an even frequency and amplitude. The actual water level regimes are shown in Figure 2.2. The water elevation shown in Figure 2.2 corresponds to basin soil elevations provided in Table 2.3.

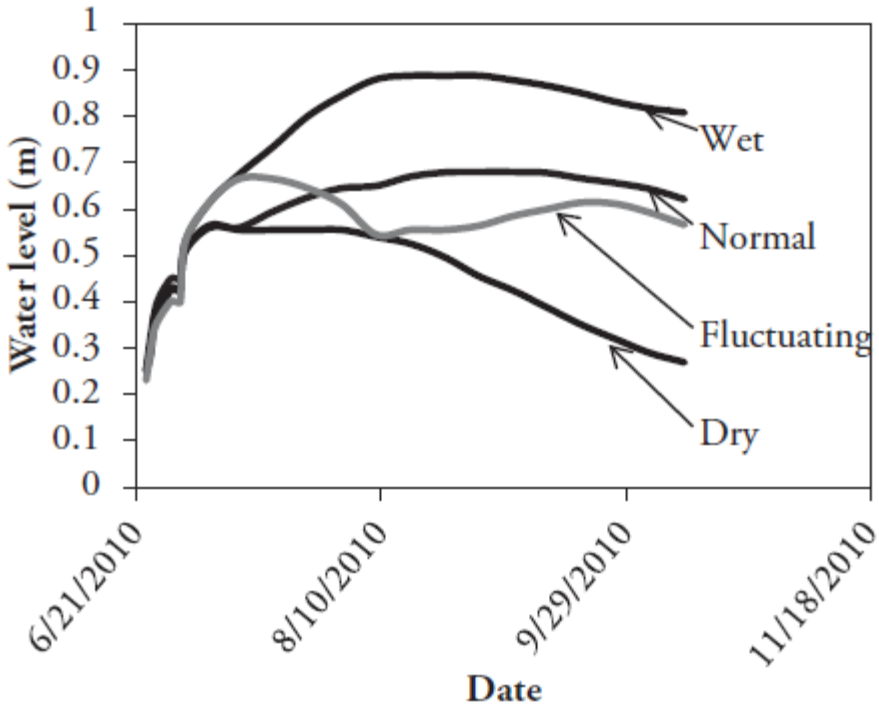

Figure 2.2. The water levels occurring at each date of the study for the four water level regimes. The wet regime resulted in all rows being inundated for much of the growing season, while the dry regime resulted in the water level ending below all rows by the end of the study.

Table 2.3. The split plot analysis results for plant biomass with nesting in rows of inundation level for each basin. The degrees of freedom (Df), F-value, and p-values for each water regime are shown as well as the level of significance where applicable.

Type	Species	Factor	Wet	Dry	Fluct.	Normal
Wet-Transition Species	*Carex vulpinoidea*	Df	6	6	6	6
		F	1.0858	0.9917	1.1802	1.0175
		p	0.4075	0.4601	0.36	0.4451
		Significance				
	Carex comosa	Df	6	6	6	6
		F	4.075	1.388	1.1452	1.618
		p	.009354	0.2723	0.377	1.994
		Significance	1%			
	Juncus effusus	Df	6	6	6	6
		F	1.0667	1.3875	1.8637	0.254
		p	0.4178	0.2727	0.1429	0.9512
		Significance				
	Spartina pectinata	Df	6	6	6	6
		F	0.7093	1.1104	1.2559	0.3427
		p	0.6465	0.3946	0.3255	0.905
		Significance				
Littoral Species	*Sparganium eurycarpum*	Df	6	6	6	6
		F	1.3245	3.3945	1.7096	0.3676
		p	0.29685	0.020324	0.1761	0.6989
		Significance		5%		
	Bolboschoenus fluviatilis	Df	6	6	6	6
		F	0.9496	6.8396	3.6706	6.489
		p	0.485185	0.00066	0.01474	0.00089
		Significance		0.1%	5%	0.1%
	Schoenoplectus tabernaemontani	Df	6	6	6	6
		F	14.756	1.1013	3.3656	1.8264
		p	4.44E-06	0.39935	0.02103	0.150276
		Significance	0.1%		5%	
	Carex lacustris	Df	6	6	6	6
		F	4.8916	1.3375	1.7605	0.6448
		p	0.003958	0.2917	0.16431	0.69363
		Significance	1%			

From June 30 to October 29, 2010 we measured plants monthly for leaf height, stem diameter, and number of flower heads. After senescence, we harvested all the above-ground biomass from the basins between October 18 and 29, 2010. At harvest we recorded the leaf height and number of stems for each plant. Some plants spread beyond their original 0.32 m by 0.32 m designated location, and the recorded plant information within the 0.32 m by 1.28 m four-plant-unit-cell was used to represent the plant for that location. We delineated the 0.32 m by 1.28 m plant-unit-cell by a PVC frame placed around the plants during the harvest procedure. We placed all harvested material in paper bags and dried it at 55°C for a minimum of four days, at which time we weighed the samples to determine the dry above-ground biomass, after subtraction of the average bag weight. The resulting above ground dry biomass is presented in grams corresponding to the mass per 0.32 m by 0.32 m species planted area, and for this paper is simply stated as biomass. For quality control purposes, we reweighted all dried samples on June 1 through 3, 2011 to confirm the measurements.

We used a split-plot analysis with nesting in surface elevation, or rows, to evaluate each of the replicate basins in this study (Montgomery 1997). The water regime treatment (whole plot) was unreplicated, so we did not calculate an error term for this factor. We have used less rigorous comparisons between species biomass in each water regime to gain additional insight to water regime impacts. The surface elevation is a surrogate for water inundation within the basin, as plants in the lower row numbers were subjected to deeper water as shown in Figure 2.2. The amount of inundation at a given surface elevation for each basin fluctuated throughout the season by design, but an

average inundation value was assigned to each surface elevation, or row, of each basin. We only used the locations of the initial planting this analysis, and not the locations that would include migration of plants. We performed the statistical analysis for each plant species independently using the R version 2.14 software. The number of stems was used to calculate the Shannon-Weiner Index of diversity (Kent and Corker 1992).

Results

Analyses indicated that surface elevation, or average inundation, as a main factor significantly affected biomass in one of the wet-transition species, and all of the littoral species, as seen in Table 2.3. The above ground dry biomass in the littoral species tended to increase with increasing inundation (Figure 2.3a); in contrast the wet-transition species tended to have decreasing aboveground dry biomass with increasing inundation (Figure 2.3b).

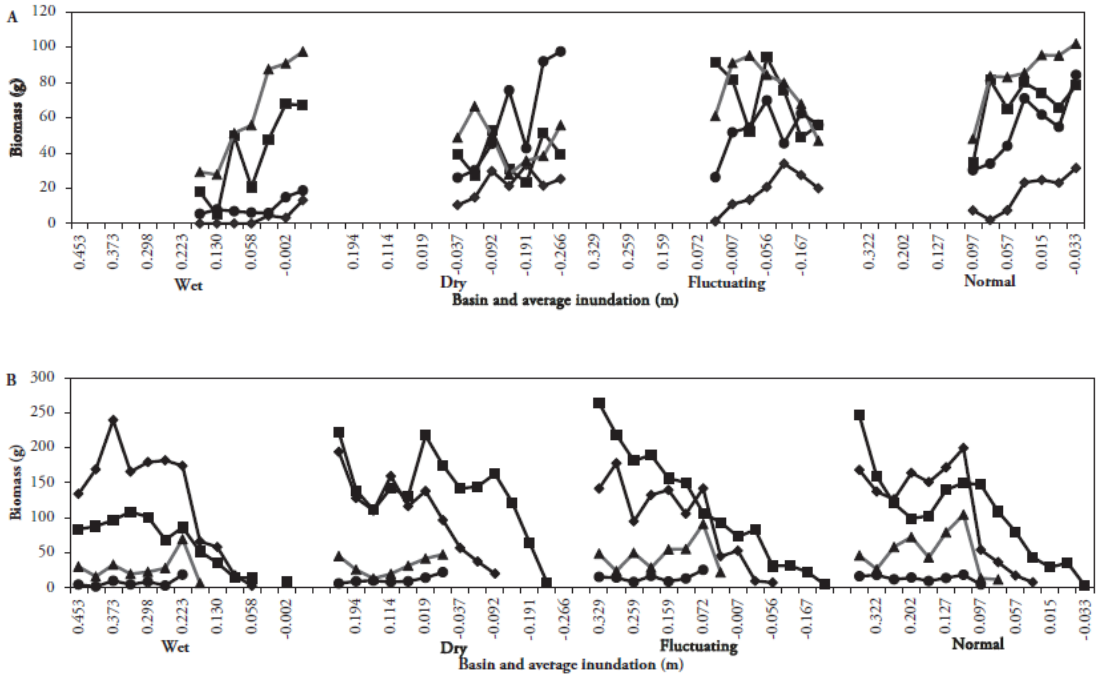

Figure 2.3. Average wetland species biomass (in grams) for wet, dry, fluctuating, and normal water regime basins. The wet-transition species are shown in (A) where *Carex vulpinoidea* is indicated by diamonds, *Carex comosa* is indicated by squares, *Juncus effusus* is indicated by triangles, and *Spartina pectinata* is indicated by circles and littoral species are shown in (B) where *Sparganium eurycarpum* is indicated by diamonds, *Bolboschoenus fluviatilis* is indicated by squares, *Schoenoplectus tabernaemontani* is indicated by triangles, and *Carex lacustris* is indicated by circles. The data is presented by average inundation for wet, dry, fluctuating, normal water regime basins.

The biomass of *Bolboshoenus fluviatilis* was affected by average inundation in the dry, fluctuating, and normal regime (Figure 2.4a, 2.4b, and 2.4c), with a consistently increasing biomass trend with more inundation. The biomass of *Carex comosa* was affected by average inundation only in the wet regime (Figure 2.4d), with a consistently increasing biomass trend with less inundation. The biomass of *Carex lacustris* was also

affected by average inundation only in the wet regime (Figure 2.4e), but a defined trend of biomass change with inundation is not apparent. The biomass of *Schoenoplectus tabernaemontani* was affected by average inundation in the wet and fluctuating regimes (Figure 2.4f and 2.4g), but a defined trend of biomass change with inundation is also not apparent. The biomass of *Sparganium eurycarpum* was affected by average inundation in the dry regime (Figure 2.4h), with a consistently increasing biomass trend with more inundation.

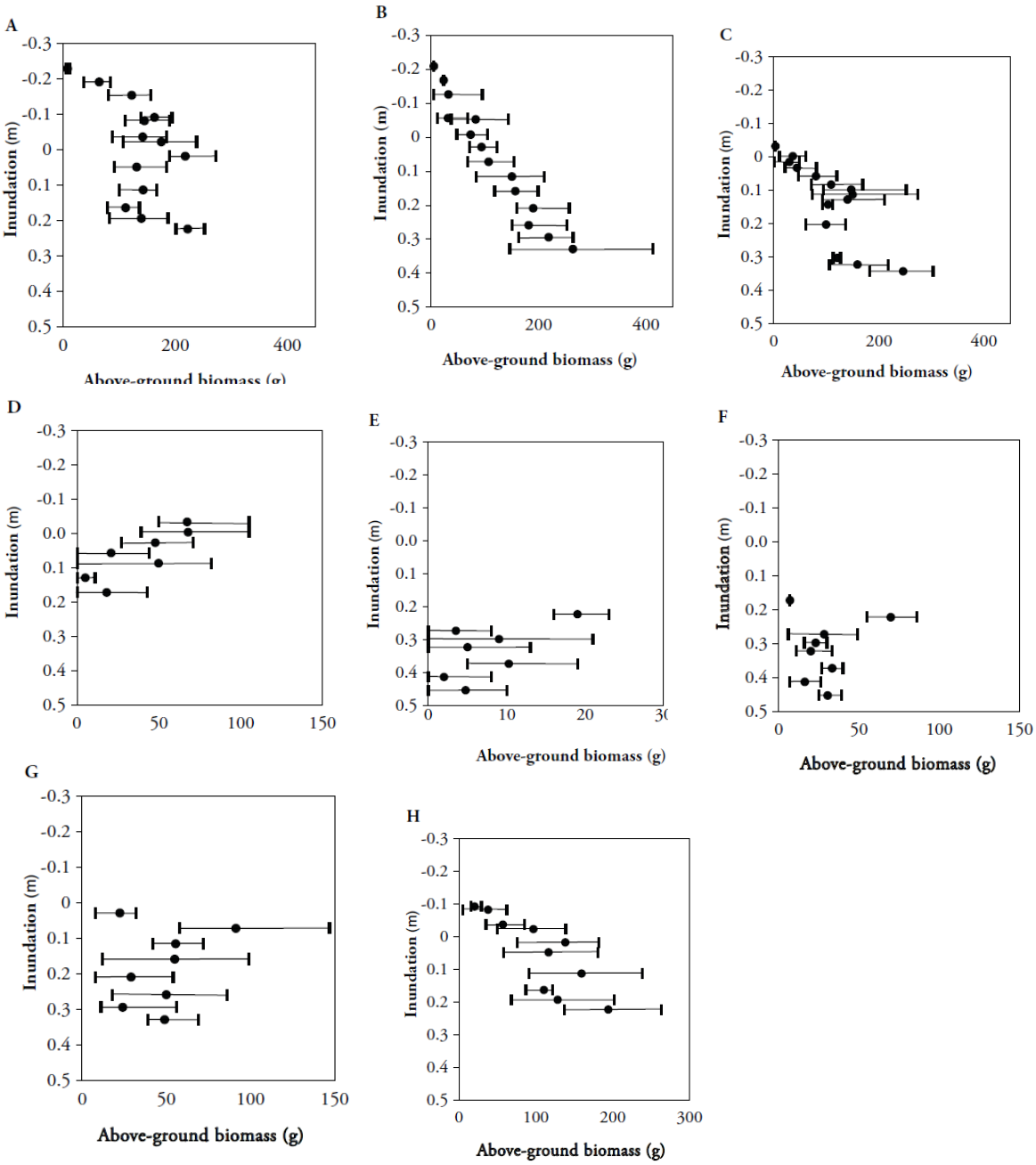

Figure 2.4. Species above ground dry biomass (in grams) average, maximum, and minimum values for (a) *Bolboschoenus fluviatilis* in the dry regime, (b) *Bolboschoenus fluviatilis* in the fluctuating regime, (c) *Bolboschoenus fluviatilis* in the normal regime, (d) *Carex comosa* in the wet regime, (e) *Carex lacustris* in the wet regime, (f) *Schoenoplectus tabernaemontani* in the wet regime, (g) *Schoenoplectus tabernaemontani* in the fluctuating regime, and (h) *Sparganium eurycarpum* in the dry regime, which are species and water regimes with significant differences

in row, or surface elevation. The average inundation of the plant location on the vertical axis, where negative values of inundation indicate the plant base was above the water level.

All eight species were present in each basin resulting in the same species richness for all water regimes. The Shannon-Weiner Index of diversity calculated was 3.78 for the wet water regime, 4.84 for the dry water regime, 4.69 for the fluctuating water regime, and 4.87 for the normal water regime.

The total sum of biomass in Figure 2.5 indicates three species are minimally present in the wet regime, and the Shannon-Weiner Index shows this regime has the least diversity. *Sparganium eurycarpum* accounts for 42.4% of the biomass, and *Bolboschoenus fluviatilis* accounts for 23.6% of the biomass, with the *Carex vulpenoidea* having only 0.7% of the total biomass in the wet regime. The amount of diversity in the dry water regime was almost as high as the normal regime according to the Shannon-Weiner Index, with 24.5% of the total biomass being from *Sparganium eurycarpum*, 41.5% from *Bolboschoenus fluviatilis* and *Carex lacustris* having only 1.9% of the biomass. The normal water regime was the most diverse of the four according to the Shannon-Weiner Index, with *Bolboschoenus fluviatilis* accounting for 30.2% of the total biomass, *Sparganium eurycarpum* accounting for 25.7% of the total biomass and *Carex lacustris* having the least biomass at 2.3%. The total sum of the collected above ground dry biomass for each species shows that *Sparganium eurycarpum* and *Bolboschoenus fluviatilis* have more biomass than other species regardless of water regime.

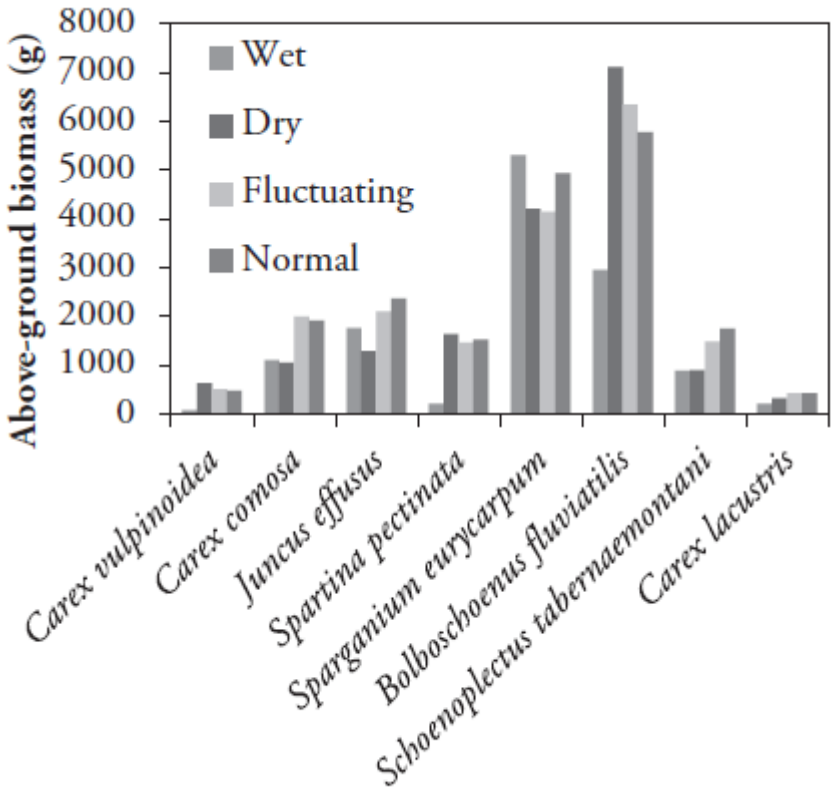

Figure 2.5. Total sum of above ground dry biomass for each basin and species.

Discussion

Generally our results support previous studies of fewer species where inundation depth, frequency and duration influence the production of plant biomass (Casanova and Brock 2000, Vanderbosch and Galatowitsch 2010, Webb et al. 2012), but our results provide additional insight to species response to inundation in the presence of other species. This study evaluated the factor of inundation depth applied through a seasonal water regime, and with the experimental design the plant location, surface elevation, and inundation depth were all associated and were not evaluated separately. Wilson and

Keddy (1988) found the placement of plants in a restoration has the potential to affect the biomass of the plants, which was also supported by these findings.

While *Bolboschoenus fluviatilis* biomass was affected by inundation under the dry, fluctuating, and normal water regimes, but there was still more total above ground dry biomass than most other species compared. This species could be a good choice for providing erosion protection on restorations where inundation changes are possible due to the overall vigor and migration observed. The relationship and significance levels of biomass to inundation levels appears different for the dry, fluctuating and normal water regimes, although this was not tested statistically, likely due to inundation duration and frequency.

Sparganium eurycarpum could also be a good choice for establishment on restoration projects where inundation changes are possible in future climate, as more biomass was generally created by this species compared to most others studied here. While many species had their poorest biomass production under a wet regime, *Sparganium eurycarpum* generated the most total biomass of all of regimes tested on this species, and the most biomass of all the species under the wet regime. This species also appears to migrate and adapt to the water inundation, and only showed a decrease in biomass due to inundation levels in the dry regime.

Caution may be advised when planting *Schoenoplectus tabernaemontani* where future climates may result in wet or fluctuating inundation regimes, as these conditions did affect the biomass. The portion of total biomass produced compared to the other

species was moderate, suggesting this species is able to compete moderately well against the others studied here.

Two of the *Carex* studied, *Carex lacustris* and *Carex comosa*, were both affected by the inundation levels under the wet regime, which has been shown in other studies on *Carex* (Nielson and Chick 1997). While the wet regime appears to result in less biomass with greater inundation, *Carex comosa* appears to compete moderately well against the other species studied here and may still be moderately effective in providing soil stabilization. The total biomass of *Carex lacustris* was low when compared to the other species for all water regimes suggesting it did not compete well and may not be a good choice for soil stabilization at a restoration site. *Carex lacustris* has been found to be sensitive to competition from the planted species and weed seed banks (Budelsky and Galatowitsch 2000) and inundation timing (Yetka and Galatowitsch 1999). Budelsky and Galatowitsch (2000) also found *Carex lacustris* to become better established if it survives into a third year of growth and a longer study three or more years, as recommended by Squires and van der Valk (1992), is needed to better evaluate the response. Our measurements of the above ground biomass may not reflect the plant survival, as below ground biomass has been found to increase relative to the above ground biomass as a survival strategy in water regime stress (Squires and van der Valk 1992). Our study did not isolate different strategies species may have to manage inundation (Blom and Voesenek 1996), and their long term resilience to inundation may not have been apparent.

Wetter regimes resulted in lower diversity, which has been observed in other studies (Casannova and Brock 2000) but not consistently in the literature (Webb et al. 2012). The strong biomass production of *Bolboschoenus fluviatilis* and *Sparganium eurycarpum* appear to contribute to low diversity and care should be taken where these are heavily planted. Squires and van der Valk (1992) found that water depths of less than 0.2 meters can impact biomass productions in some species while other species are marginally impacted by depths greater than 0.7 meters. In our study, the largest average inundation on the plants was 0.45 meters, and it is possible a greater magnitude of inundation would have resulted in significant differences in more species, such as *Spartina pectinata* which has been affected by inundation in other studies (Miller and Zedler 2003).

While our study included both rhizomatous and caespitose species, our initial results do not suggest a difference in growth related to the rooting form under these conditions. The two species with the most biomass and apparently the most adaptable to water level regimes were both rhizomatous and root response to water regime has been found to improve plant vigor (Visser et. al. 1996), but there does not appear to be a consistent trend among rhizomatous species. Blom and Voesenek (1996) found that rhizomatous plant species may also be more effective for revegetation and erosion control in near-shore areas due to their rooting strategies, and with the biomass responses presented here it is advisable to not rely heavily on the caespitose species used in this study.

Implications for practice

The following implications for restoration practice can be summarized from this study.

- Care should be taken when choosing plants in a fluctuating water environment, as it can impact project success.
- Water level fluctuations of 0.2 m to 0.4 m does not appear to impact the establishment of the eight species in this study.
- Long duration water inundation of 0.4 m or more does appear to reduce the plant biomass generated in the first year of establishment of seven of the eight species in this study, with *Spartina pectinata* and *Carex vulpinoidea* having the least biomass.
- *Carex vulpinoidea* and *Spartina pectinata* should be planted in areas that experience less frequent flooding since these species were least tolerant of extended inundation during plant establishment.
- *Carex comosa* and *Juncus effusus* establish well just above the average water level where plants experience intermittent, seasonal flooding.
- *Bolboschoenus fluviatilis*, *Carex lacustris*, and *Schoenoplectus tabernaemontani* establish well in shallow water just below the average water level where plants are inundated most or all of the first season.
- *Sparganium eurycarpum* tolerates slightly deeper water for establishment, providing that plants are tall enough to emerge from the water when they are initially planted.

- Given the environments created in this study, *Bolboschoenus fluviatilis* and *Sparganium eurycarpum* dominated the plant community in all water regimes.
- *Bolboschoenus fluviatilis* and *Sparganium eurycarpum* may establish under a range of water conditions, but their aggressiveness could limit diversity.
- Consider rhizomatous plant species for restoration and erosion control in near-shore areas, including those experiencing water level fluctuations. However care should be taken as this planting strategy could lead to potential monocultures, which are ecologically less stable over time than diverse plant communities.

Chapter Acknowledgements

This study was made possible by Clean Water Act Section 319 Funding through the U.S. Environmental Protection Agency and the Minnesota Pollution Control Agency. This study would also not have been possible without the hard work and dedication of Camilla Correll, Miki Hondzo, Barbra Liukkonen, Mary Pressnail, and Karen Terry.

Additional Discussion

This study was originally published under the title “Competition and Growth of Eight Shoreline Restoration Species in Changing Water Level Environments” in the December 2013 issue of Ecological Restoration, Copyright 2013 by the Board of Regents of the University of Wisconsin. Reproduced with permission.

The experimental study did not fully explore differences between caespitose and rhizomatous species due to plant availability, but it appears that rhizomatous species in addition to being more aggressive and potentially more capable of producing more

biomass in future climates have a root structure that is like more beneficial for erosion control. The rhizomatous shoots should be able to provide additional soil reinforcement and remain intact in the event of a localized erosion incident. The migration through shoots is also potentially more reliable in a fluvial environment, where other mechanisms such as seed dispersal could be more influenced by water conditions and be less reliable.

Chapter 3
Flexible Vegetation Drag in Unidirectional Flow

Summary

This paper compares parameters that characterize vegetation flexibility effects on flow resistance and drag. Drag forces have been measured in a flume for simple cylindrical obstructions of the same shape and size but with different flexibility under several flow conditions. This data set is used to fit drag parameters and to relate their value to flexibility through the Cauchy Number. A novel formulation is presented where the drag coefficient is evaluated as a function of the relative velocity and the elastic modulus of the obstruction. While the use of a Vogel exponent and reference velocity provides a similar response, the reference velocity when used is somewhat nebulous and appears to have a critical impact on the parameter and the drag force calculated. The proposed formulation for drag reduction is more consistently estimated for the range of flexibilities in this study.

Introduction

Urban hydrology, green stormwater infrastructure, river restoration and flood management all have a need for understanding how vegetation interacts with flow. Vegetated conveyances also provide additional benefits to the environment (Wilcox and Meeker, 1992) and help achieve hydrologic mimicry. Vegetation is also becoming more common for erosion control along water bodies compared with hard armouring due to the additional ecological benefits (USDA 1996) and the potential for shoreline adaption to future climate conditions (Chapman et al. 2013). One framework for our understanding of vegetation-flow interaction is through the concept of drag forces and how these measured forces change for flexible vegetation.

Parameters have been evaluated to characterize the drag of vegetation (Nepf, 1999; Poggi et al., 2004; Nezu and Sanjou, 2008; Aberle and Järvelä, 2013) in liquid and air (Finnigan, 2000; de Langre, 2008), and comparisons between obstructions with different flexibilities have been studied (Ghisalberti and Nepf, 2006; Wunder et al., 2009; Augustin et al., 2009; Aberle and Dittrich, 2012) with the conclusion that streamlining and flexibility results in significant differences in drag. Studies have been done to characterize flow velocity and turbulence from flexible vegetation (Stephan and Gutknecht, 2002) and lodging velocities (Duan et al. 2006) as well as the influence of vegetation surface wave forces (Wallerstein et al. 2002). Studies have isolated different aspects of vegetation such as foliage impacts (Wilson et al. 2008), stem flexibility impacts to turbulence (Yang and Choi, 2010), and mechanical behaviour of vegetation (Chen et al. 2011). Models have also been proposed to characterize the flow resistance (Wilson, 2007) and total hydraulic resistance (Schonebloom et al. 2010). These studies are invaluable for the understanding they have provided, but often the data are related to specific vegetation morphology and is not easily transferred to other vegetation species or morphologies (Bouma et al., 2010).

There is still a need for parameters that are predictable based on physical attributes of the vegetation. While the aforementioned studies have looked at several of the complex aspects flexible vegetation, we have attempted to isolate the flexibility of the simple cylindrical stem and understand how changes in the flexibility of a stem affect the drag. This study has investigated single cylinders of various flexibility which can represent cylindrical stemmed vegetation without foliage. For some vegetation, such as *Schoenoplectus tabernaemontani*, this data can be an appropriate representation, while for other vegetation with leaf structure, such as *Spartina pectinata*, additional work is needed to represent their drag forces. We have investigated the drag from flexible elements and developed a parameter to predict their drag based on the Cauchy Number (C_Y).

Drag Parameters

Vegetation has been represented using simply shaped rigid elements in many studies (Nepf, 1999), but other studies have also demonstrated that rigid elements may not represent flexible elements well (Aberle and Järvelä, 2013). Studies on networks of vegetation have investigated bulk impacts and wake interactions, but our study is interested in simplifying this and will focus on isolated elements, specifically to evaluate the calibration terms of flexible element drag and attempt to relate these terms to a physical meaning.

Rigid bluff bodies

Rigid bluff bodies have been used to simulate vegetation in many experiments, expanding on early investigations of drag from rigid cylinders by Lindsey (1938) and others (Prandtl and Tietjens, 1934). More recent studies have simulated vegetation with networks of emergent and submerged rigid cylinders (Nepf, 1999). The drag forces (F_d) from rigid elements are often represented by Eq.(3.1) (Robertson and Crowe, 1993),

$$F_d = \int \frac{1}{2} C_D \rho a u^2 dz \approx \sum \frac{1}{2} C_D \rho a u^2 \Delta z \qquad (3.1)$$

where F_d is the drag force, C_D is a drag coefficient, ρ is the fluid density, a is the obstruction width, u is the temporal mean flow velocity at height z acting normal to the cylinder, and z is the vertical position above the bed.

Studies on rigid bluff bodies have provided valuable insight on the impact of spacing and arrangement of obstructions on wake patterns and corresponding changes in the resulting drag on downstream obstructions. Drag has been formulated using the sum of individual forces for each element, or as a collective bulk coefficient that is a function of the geometry of the element array. Some contradictions in the literature have been noted between these concepts of bulk drag, where the bulk drag decreases (Nepf 1999, Tanino and Nepf 2008, Kothyari et al. 2009) or increases with Reynolds' Number (Re) (Schoneboom et al. 2011). The Reynolds' Number was calculated in these studies using

the obstruction width as the characteristic length (l), the fluid kinematic viscosity (ν), and the bulk flow velocity (U) in the flume such that Re = Ul/ν.

Flexible bluff bodies

Flexible bodies are understood to behave differently from rigid bodies because of deformation and interactions with turbulence and require additional consideration. Vogel (1989) proposed that the ratio of drag to velocity squared was proportional the velocity with an exponential variable term specific to the plant as seen in Eq. (3.2), where the exponent b, also referred to as the Vogel exponent, is the calibrated parameter to account for element flexibility effects on drag,

$$F_{db} \propto U^{2+b} \tag{3.2}$$

This idea has been further developed for emergent vegetation by Järvelä (2004) in Eq. (3.3) where the Leaf Area Index (LAI) is used in place of projected obstruction area, $a\Delta z$:

$$F_{d\chi} = \frac{1}{2}\left(\frac{1}{u_{\chi}^{\chi}}\right) C_{D\chi} \rho LAI U_m^{(2+\chi)} \tag{3.3}$$

where $F_{d\chi}$ is the drag force from flexible elements as a function of a calibration parameter χ , u_{χ} is a reference velocity, $C_{D\chi}$ is the form drag coefficient which is a function of Re, ρ is the density of fluid, and U_m is the bulk flow velocity. The impact of element flexibility on drag is captured by two parameters: χ and u_{χ} .

An algebraic alternative form of drag force can be derived below where the U_m and u_{χ} terms are gathered so the impact of flexibility is seen as a component of the drag coefficient.

$$F_{d\chi} = \frac{1}{2}\left(\frac{U_m^{\chi}}{u_{\chi}^{\chi}}\right) C_{D\chi} \rho LAI U_m^2 \tag{3.4}$$

Additionally, if we assume the vegetation is a uniform emergent cylinder, the LAI can be replaced by the vertical projected area (ad) where *d* is the flow depth

$$F_f = \frac{1}{2} C_{Df} \rho a d U_m^2, \tag{3.5}$$

where,

$$C_{Df} = C_D (U_m / u_b)^b = C_D \alpha_b \tag{3.6}$$

and C_{Df} is the drag coefficient for a flexible element. Since we are using a different area index than Järvelä, we have replaced the reference velocity u_{χ} with u_b and the exponent χ with b. Equation (5) is consistent with Eq. (3) with the exception of using the obstruction projected area instead of *LAI*. This also defines $\alpha_b = (U_m/u_b)^b$ which is a general modifier, representing drag reduction throughout this text, to account for how drag is affected by flexibility or reorganization and deformation.

This creates a two component drag coefficient; The first component is the form drag coefficient of a rigid body (C_D) which is dependent on shape and Re; The second component is a drag coefficient modifier for flexibility (α_b). This modifier is a function of flow velocity and Järvelä's reference velocity as well as an empirical Vogel exponent. While previous studies have determined the empirical exponent for various species (Aberle and Järvelä, 2013), our interest lies primarily on exploring the usefulness of the relative velocity term and proposing a new drag coefficient modifier for flexibility.

Characterization of flexibility

Characterizing the deformation and flexibility of an object can be achieved with parameters such as the modulus of elasticity, also known as Young's Modulus, E

(Hibbler, 1991). This parameter represents the deformation under loading that is independent of the object shape or size. Applying this technique to plants can be done with some simplifying assumptions (Niklas, 1992).

The ratio of dynamic pressure to the modulus of elasticity, also known as the Cauchy Number (C_Y), given in Eq. (3.7), is also useful in evaluating resistance and drag in flexible elements,

$$C_Y = \rho U_m^2 / E \tag{3.7}$$

where E is the Young's Modulus of the material. Researchers (de Langre, 2008;) have found the need to scale C_Y for vegetation using a slenderness number (S) equal to the ratio of the maximum to minimum cross section lengths of the obstruction. Niklas (1992) suggests that transverse loadings on slender beams is proportional to S^3, resulting in the C_{YS} shown in Eq. (3.8),

$$C_{YS} = (\rho U_m^2 / E) S^3 \tag{3.8}$$

where S is the slenderness number of the obstruction.

Experiments with fabricated obstructions can create a length to with ratio such that S of the object is consistent in all experiments. The slenderness, S, should be a property of the material and not the flow, but with emergent vegetation the height above the flow should have little influence on the drag. It is more appropriate to consider the submerged element length, which in effect makes the slenderness a function of flow depth, and is used as such in this chapter.

Flume experiments

Measuring basal torque from simply shaped rigid and flexible elements in direct flow in a laboratory flume we have been able to back calculate the b value for an assumed u_b,

which Järvelä holds as a constant reference velocity. New calibration parameters are also proposed which relate to the physical processes that influence drag in flexible vegetation.

Experimental setup

A 7.25 meter long flume on the University of Minnesota St. Paul campus was instrumented with a submersible torque sensor below the flume floor, with a port in the flume floor allowing for different elements to extend from the sensor up into the flow (Figure 3.1). The flume interior width was 0.38 meters and flume depth was 0.38 meters. The flume has a wet well extending 0.2 meters below the flume over a 2.1 meter section to allow for submersible sensors below the flume. The flume was primarily constructed out of PVC with steel reinforcement and the flume bottom was lined 0.001 meter diameter sand adhered to metal sheets. The slope of the flume could be adjusted using screw jack supports. An alternating current induction motor was used to power a 57 litre per second centrifugal pump in a small reservoir at the tail water of the flume to recirculate flow through the flume by a series of 0.15 meter diameter pipes. The discharge to the flume was measured using orifice weirs in the recirculation pipes. A series of 0.025 meter diameter pipes were used as flow straighteners from the upstream reservoir.

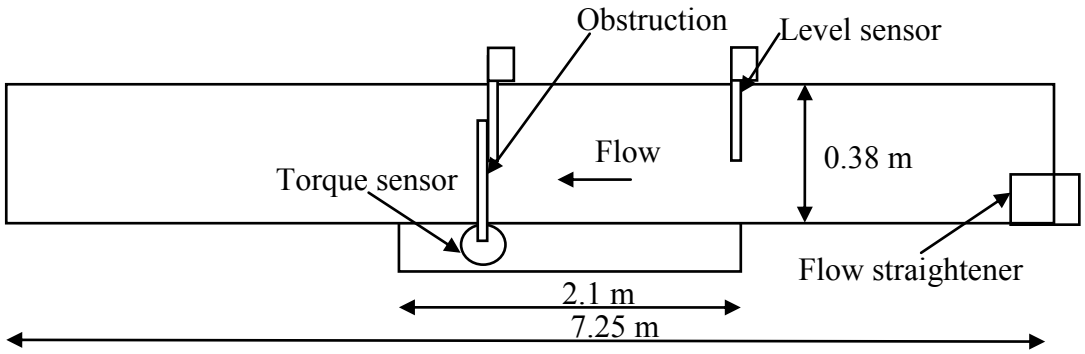

Figure 3.1. Flume schematic.

The loadings on the obstruction elements were measured using a FUTEK TFF425 submersible torque sensor mounted below the flume. The obstruction element were attached to the sensor flange with a spring flange and passed up through the floor of the flume into the flow. The torque sensor has a 0.047 N-m maximum capacity and suitable to measure small loadings such as those occurring from a single small diameter obstruction. FUTEK SensIT Test and Measurement v2.1.4 software and FUTEK USB210 interface were used to read and calibrate the data from the sensor. Additional details on the experimental setup can be found in Chapman et al. (2014).

Torque measurements were made on three cylindrical elements with different flexibilities, all tall enough to emerge from the flow in velocities from 0.216 ms^{-1} to 0.395ms^{-1}. Emergent cylindrical elements were used so that no change in projected area occurs with deflection. The least flexible element was rigid aluminium and the most flexible element was polyurethane foam cylinder. A polyethylene straw element had an intermediate flexibility compared to the other two. The elastic modulus (E) reported in Table 1 has been determined by the obstruction deflection as a cantilevered beam under load (Hibbler, 1991). This E is not a true elastic modulus of the material, but an effective E that assumes a homogeneous solid cross section, which not all of the obstructions have. Similar simplifications which do not account for internal cell wall structure or heterogeneous materials have been made for comparisons of vegetation in other studies (Niklas, 1992). All of the elements were of the same order of magnitude in diameter (Table 3.1).

While we used vegetation elements of similar size and were able to give them the same slenderness, the submerged length, related to the flow depth is more appropriate to consider when calculating C_{YS}. Table 3.2 lists the flow depths and slenderness values along with other parameters for the experiments performed.

Table 3.1 Properties of Cylindrical Obstructions

Element	*Diameter* (m)	*Elastic Modulus* (Pa)
Aluminium	0.0066	7e10
Straw	0.0055	1.23e8
Foam	0.0090	3.19e5

Table 3.2 Experimental Parameters

Element	Um (m/s)	Depth (m)	Re	*S*	C_{YS}	α
Aluminium	0.216	0.159	1704	24.04	9.27e-6	1
Aluminium	0.292	0.171	2216	25.98	2.14e-5	1
Aluminium	0.304	0.178	2303	26.95	2.59e-5	1
Aluminium	0.326	0.184	2453	27.91	3.31e-5	1
Aluminium	0.354	0.191	2643	28.87	4.31e-5	1
Aluminium	0.387	0.203	2873	30.80	6.27e-5	1
Straw	0.394	0.198	2430	36.03	5.29e-2	0.932
Straw	0.357	0.191	2221	34.65	4.32e-2	0.845
Straw	0.326	0.184	2044	33.49	3.25e-2	0.891
Straw	0.306	0.171	1926	31.18	2.31e-2	0.905
Straw	0.259	0.165	1664	30.03	1.48e-2	0.895
Foam	0.382	0.197	3868	21.88	4.81	0.472
Foam	0.357	0.191	3634	21.17	3.80	0.444
Foam	0.326	0.184	3345	20.47	2.86	0.542
Foam	0.290	0.175	3012	19.48	1.95	0.619
Foam	0.253	0.165	2670	18.35	1.25	0.712

Drag Reduction

Taking the aluminium element data as representative of a rigid element, we used Eq. (3.5) and (3.6), with α_b assumed as 1 so that b = 0, to solve for the form drag

coefficient (C_D) by knowing the drag force occurring on the element from our torque measurements, and the obstruction dimensions for the projected area. The determined C_D in relation to Re is shown in Fig. (3.2). A natural logarithmic relationship (Eq. 3.9) of C_D, fit to our experimental data ($R^2 = 0.8113$) was applied to the data for foam and straw elements of the same shape and approximate size. This allowed for the determination of the remaining drag coefficient flexibility modifier using the experimental data.

$$C_D = -0.648LN(\mathrm{Re}) + 6.212 \tag{3.9}$$

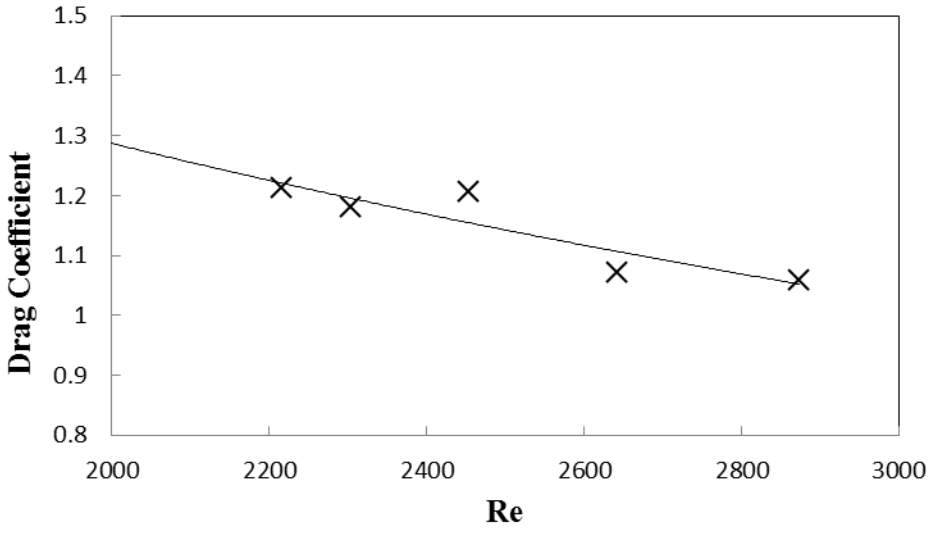

Figure 3.2. Calculated form drag coefficient for rigid element (aluminum).

The calculation of form drag approximates other cylindrical reported values (Prandtl and Tietjens, 1934; Wallerstein et al. 2002), although our values are slightly higher than observed on the Wieselsberger diagram for some Re values. These previous studies were investigating cylinders in a horizontal orientation, while our cylinder is in a vertical orientation which could account for some of the differences.

Calibration Parameters

Several different coefficients (Vogel, 1989) and calibration parameters (Järvelä , 2004) have been proposed in the literature and can be back calculated from the data collected here. Järvelä has proposed using LAI in place of the projected obstruction area since LAI is more easily obtained for field applications. Using LAI can be a challenge when leaf deformation occurs under environmental conditions such as flow and turgor pressure, which could influence the area measured. The simple morphology used in our experimental cylinders allows us to easily use the projected area in place of LAI, but our parameters cannot be directly compared to χ from other field studies.

According to Aberle and Järvelä (2013), the u_χ value for reference velocity should be the lowest velocity used in the determination of the exponent calibration parameter, χ, to achieve the proper scale. Aberle and Järvelä (2013) noted the value of b is sensitive to the ub value used, and we observed the same phenomenon. The experimental set up used here is able to determine all the values in Eq. (3.5) and Eq. (3.6) to back calculate b, provided we assume a value for u_b . For this study, the lowest velocity used for the determination of these parameters was 0.216 ms^{-1}, and so this is the best value according to the literature. We have also calculated values for b, using a slightly higher and lower value for u_b for a sensitivity analysis. These values of 0.1 ms^{-1} and 0.3 ms^{-1} were not the lowest velocities used in the experiments but provide a bracket of sensitivity. Figure 3.3 shows the sensitivity of b values for this range of u_b and indicates a relationship to Re. The calculated b values also appear more sensitive to the u_b value at larger CYS values, as seen in Fig. (3.4).

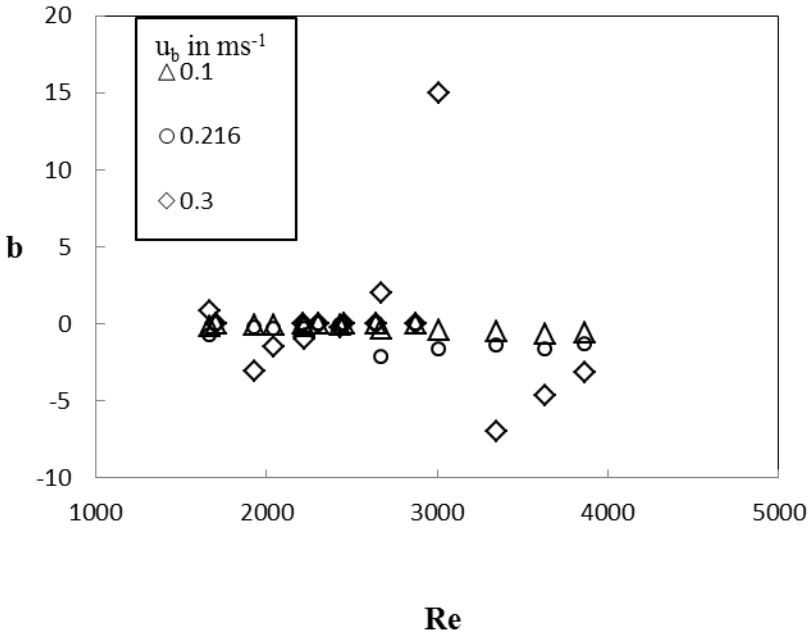

Figure 3.4. Drag parameter b calculated using reference velocity, u_b, of 0.1 ms^{-1}, 0.216 ms^{-1}, and 0.3 ms^{-1} plotted against the Reynolds' Number.

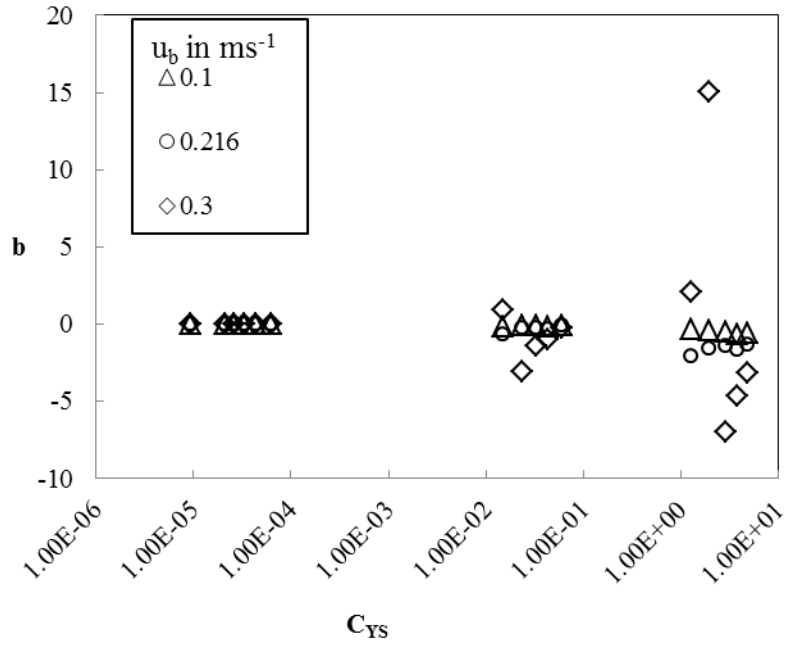

Figure 3.4. Drag parameter b calculated using reference velocity, u_b, of 0.1 ms^{-1}, 0.216 ms^{-1}, and 0.3 ms^{-1} plotted against the Cauchy Number.

Drag Reduction as a Function of Elastic Modulus

We propose to calculate the drag reduction α_b caused by flexibility by holding the exponential term fixed at 1, such that the reference velocity constant, u_b, is now a variable and the only calibrated parameter, which we shall call φ (Eq. 3.10). Use of Eq. (3.10) in place of α_b removes the noted sensitivity of b to u_b discussed in the previous section.

$$\alpha_{\varphi} = (U_m / \varphi) \tag{3.10}$$

The effects on drag reduction reported in the literature can be described with Eq. (3.10), such as when φ = U_m there is no drag reduction, or b = 0, and φ = 1 creates the same impact on drag as b = 1. Provided the calibration parameter is determined by empirical data, α_{φ} is simpler than α_b and still provides the same possible range of values without using a second parameter such as u_b. Interestingly, if we assume the drag is dependent on the flow velocity normal to the cylinder, φ would then have the physical relationship to U_m and the vegetation deflection angle provided in Eq. (3.11), where θ is the angle of deflection of the cylinder. Combining Eq.(3.10) and Eq. (3.11) results in Eq. (3.12) showing that the drag reduction is dependent on the deflection angle of the vegetation.

$$\varphi = (U_m / \cos^2 \theta) \tag{3.11}$$

$$\alpha_\varphi = \cos^2 \theta \tag{3.12}$$

Observational data on vegetation deflection under a known flow velocity could be used to estimate the drag reduction using this concept. The observed deflections simplify a continuous arc of the deformed cantilevered cylinder into an average deflection angle determined from the displacement of the tip compared to the base. The experimental observations presented here support Eq. (3.12), in that the drag reduction measured for the straw cylinder, resulted in θ of 15 degrees, while observed deflections seen in the recorded video were on the order of 10 degrees for a flow velocity of 0.39 ms^{-1} and the drag reduction measured for the foam cylinder, resulted in both a calculated and observed deflection on the order of 32 degrees for a flow velocity of 0.25 ms^{-1}.

Drag reduction occurring in relation to C_{YS} has also been reported in the literature (de Langre, 2008). Since both drag reduction and C_{YS} are calculated using U_m these plots could show spurious correlations. To investigate spurious correlations, our data for drag reduction resulting from flexibility is presented as 1/ φ, without the U_m term, plotted against the C_{YS} with S computed from the flow depth over diameter of the obstruction in Fig (3.5). A regression analysis results in an exponential trend shown in Eq. (3.13) with $R^2 = 0.737$.

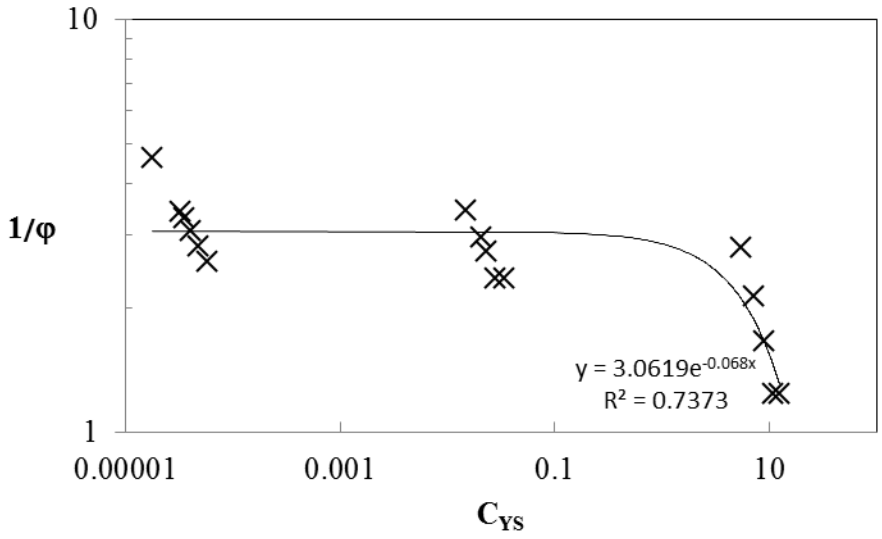

Figure 3.5. Drag reduction as 1/φ due to element flexibility vs. Cauchy Number, C_{YS}.

$$\frac{1}{\varphi} = 3.0619\exp(-0.068C_Y) \qquad (3.13)$$

Figure 3.6 plots the drag reduction, α_φ against C_{YS} for the data collected here along with reported trends of various vegetation in wind flow and a theoretical cylinder on an elastic spring (de Langre, 2008). These plots are sensitive to the S value, and additional variation is expected given the morphology differences between the flexible obstructions. The basic drag reduction relationship to C_{YS} (Fig. 3.6) is well supported by the data collected here and in other studies. An exponential function captures the trends best over wider ranges of C_{YS}. The flexible cylinder morphology studied here has α_φ related to C_{YS} by the exponential function shown in Eq. (3.14) with $R^2 = 0.955$.

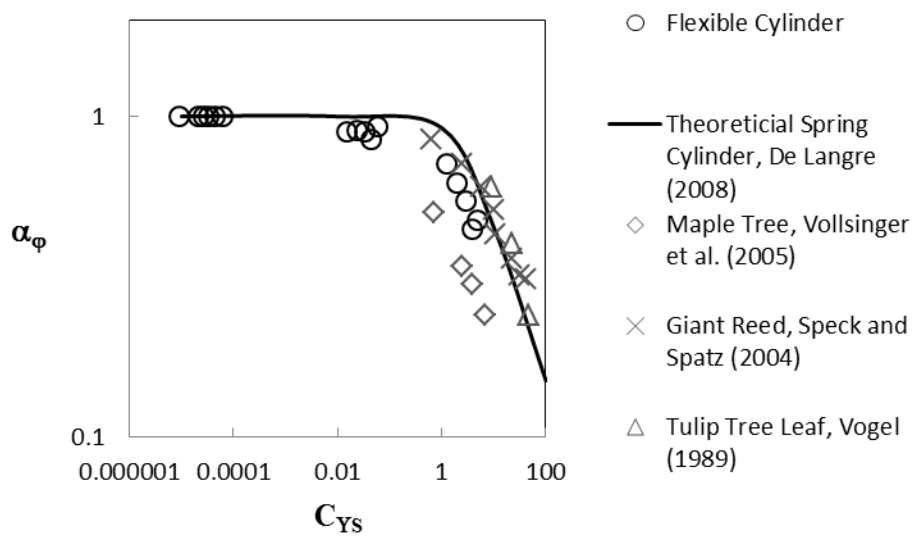

Figure 3.6. Drag reduction α_φ due to element flexibility as Cauchy Number, C_{YS}. The triangles represent the data collected in this study; The line represents a theoretical rigid cylinder mounted on a spring (de Langre, 2008); The diamonds represent maple tree crowns (Vollsinger et al., 2005); The crosses represent Giant reed (Speck and Spatz, 2004); and the circles represent tulip tree leaves (Vogel, 1989).

While Eq. (3.14) has a better fit than seen in Eq. (3.13), they both have a similar trend and the influence of spurious correlations is believed to be small due to the magnitude of the φ value.

$$\alpha_\varphi = 0.941\exp(-0.175C_{YS}) \tag{3.14}$$

Setting the intercept equal to 1 as a theoretical limit, the calibrated coefficient for our data becomes -0.192 instead of -0.175, as seen in Eq. (3.15).

$$\alpha_\varphi = \exp(-0.192C_{YS}) \tag{3.15}$$

For the theoretical cylinder on a spring, the calibrated coefficient of -0.052 is appropriate for an intercept equal to 1. To better visualize how α_φ is a function of the object elastic modulus, Eq. (3.8) and Eq. (3.15) can be combined into Eq. (3.16).

$$\alpha_\varphi = \exp[-0.192(\rho U_m^2 / E)S^3] \tag{3.16}$$

Discussion

The experimental set up implemented in this paper does appear capable of being used to determine the fitting parameters proposed by others (Vogel, 1989; Aberle and Järvelä, 2013), reducing the need for large beds of vegetation in experiments although this has not been verified by experiments on morphologies other than cylinders. The sensitivity of b to u_b creates concern regarding use of Eq. (3.6). Aberle and Järvelä (2013) reported several χ values ranging from -0.38 to -1.03 for species determined using *LAI*. The modified method used here with a known obstruction area instead of *LAI* has resulted in a similar range of b values (Fig. 3.3) for u_b on the order of 0.216 ms^{-1}, but they are not entirely comparable due to the different methodology in the area determination. Figure (3.3) and Fig. (3.4) suggest smaller reference velocity values will provide more constant b parameters, and larger reference velocity values result in calculations of b as much as 25 times larger than what has been reported in the literature (Aberle and Järvelä, 2013).

Vogel (1989) proposed the drag is not proportional to the square of velocity for vegetation because of deformation in the vegetation which is also influenced by the velocity. The data presented here supports the drag coefficient is influenced by flow, but suggests a physical relationship to the deflection angle of the vegetation (Eq. 3.10). Use of Eq. (3.10) removes the need for reference velocity values to keep drag coefficients non-dimensional.

Equation (3.12) suggests that field observations of vegetation deflection will provide insight to the flexibility modifier of drag coefficients, and it would be advisable to include deflection measurements in field studies. While this is of interest, it may not be practical due to confounding factors, such as submerged cylinders will likely show a lower drag coefficient than expected due to the flow around the terminal end (Wallerstein et al. 2002) in addition to variations in area. Equation (3.12) does provide insight to the physical principals governing the drag reduction.

Use of Eq. (3.16) appears to provide a less variable drag coefficient modifier applied to flexible elements and provides greater confidence in interpolating between tested elements than use of fitting parameter b and reference velocity u_b. Equation (3.16) is dimensionless without the need for a reference velocity and it behaves according to using physical parameters of velocity and elastic modulus.

The ability to estimate E for vegetation or other materials remains as a challenge for this technique. It is possible to estimate E for vegetation by assuming a homogeneously solid material and measuring the deflection under load, but there is

significant variability in natural vegetation (de Langre, 2011), partially due to internal structure and variation caused by turgor pressure (Niklas,1991; 1992).

For comparison to other literature, additional exponential relationships of the form presented in Eq. (3.15) have been determined for other morphologies of maple tree crowns (Vollsinger et al., 2005), giant reed (Speck and Spatz, 2004), and tuliptree (Vogel, 1989) as shown in Table 3.3 with the Normalized Mean Square Error (NMSE) (Gershenfeld and Wiegrend, 1993) as an indicator of the regression fit. The smaller NMSE values indicate the regression fits the data well and values greater than one indicate that the mean by itself represents the data better than the regression equation. The exponents that result when the intercept is forced through 1 are also shown in Table 3.3 with NMSE values.

Table 3.3 Function coefficients for $\alpha = \alpha_1 \exp(\alpha_2 C_{YS})$

Element	α_1	α_2	*NMSE*	α_2*	*NMSE**
Theoretical Cylinder	1	-0.052	-	-0.052	-
Flexible Cylinder	0.9414	-0.175	0.066	-0.192	0.101
Giant Reed	0.688	-0.023	0.17	-0.037	0.672
Maple Tree	0.4912	-0.114	0.091	-0.259	2.214
Tuliptree	0.7137	-0.024	0.013	-0.033	0.231

* Regression values where the α_1 term is held at 1.0.

The giant reed and flexible cylinder have similar morphology and have the closest match to the theoretical spring cylinder condition. The maple data deviate from the cylindrical morphology trend much more than the tuliptree, but both of these species have mulit-lobe leaf morphology. Forcing a common intercept collapses much of the data around the theoretical trend except for the Vollsinger et al. (2005) data on maple tree crowns, suggesting further study to isolate the physical properties influencing the maple tree morphology is needed. It should be noted these other studies are not entirely relevant for emergent flow since they were tree canopy wind tunnel studies.

The coefficients shown in Table 3.3 can be refined as more data is collected. Since Eq. (3.16) was developed by isolation of the vegetation stem flexibility, it is also possible that additional drag coefficient modifiers for leaf area, leaf shape, or leaf flexibility could be developed that are used in combination with α_{φ}. These additional modifiers could have a relationship to C_{YS}, but would also likely include dependant variables related to the leaf area or other morphology descriptors.

Conclusions

The drag forces occurring on flexible bluff bodies are different from the drag occurring on rigid bluff bodies due to deformation and reorganization and better characterization of flexible bluff bodies is needed. Use of a Vogel exponent or the χ in Järvelä's method appears feasible, but use of Eq. (3.10) presented here provides a more predicable alternative since it does not rely on a reference velocity that is defined in the experiments. Alternatively, Eq. (3.16) relies on a mechanical property of the obstruction,

the elastic modulus, where the drag reduction is caused by the reorganization of the elements to be other than normal to the flow velocity. Unfortunately, the mechanical properties of vegetation are not often readily available for this to be of immediate practical use. Equation (3.5) and (3.6) also preserves the traditional exponent of the Eq. (3.1) drag relationship, but places a modifier onto the drag coefficient for flexible elements, rather than a Vogel exponent arrangement applied to the flow velocity. Equation (3.6) also has the benefit of keeping C_D as a dimensionless value without the need for a reference velocity. The data presented here has developed a drag coefficient modifier primarily for flexible stems, but additional modifiers are possible for other morphologies determined through a similar process of isolation and testing.

Chapter Acknowledgements

The author would like to thank Brad Hansen, Stephanie Nappa, Mary Blickenderfer, and the St. Anthony Fall Laboratory staff for their hard work and assistance with this study. The author is also grateful to the anonymous reviewers for suggestions that greatly helped improve this manuscript. Contact the author for access to data used in this study.

This work was made possible through funding by the Minnesota Pollution Control Agency and United States Environmental Protection Agency 319 grants under the Clean Water Act.

Chapter Notation

a = Projected obstruction width (m)

b = Vogel exponent for flexible elements (-)

c = Drag coefficient fitting parameter (-)

C_D = Form Drag Coefficient (-)

C_{Df} = Flexible Element Drag Coefficient (-)

$C_{D\chi}$= Drag Coefficient (-)

C_Y = Cauchy Number (-)

C_{YS} = Cauchy Number with Slenderness modification (-)

d = flow depth (m)

E = Modulus of Elasticity (Pa)

F_d = Drag force (N)

F_{db} = Drag force calculated with b parameter (N)

F_f = Drag force calculated with α_b parameter (N)

$F_{d\chi}$ = Drag force calculated with χ parameter (N)

l = characteristic length (m)

LAI = Leaf Area Index (-)

NMSE = Normalized Mean Square Error

Re = Reynolds Number (-)

S = Slenderness number (-)

U = flow velocity (ms-1)

U_m= Mean flow velocity (m s-1)

u_b = Reference flow velocity (m s-1)

u_χ = Reference flow velocity (m s-1)

z = vertical position (m)

α_b = drag reduction due to flexibility with b

α_φ = drag reduction due to flexibility with φ

α_1 = drag reduction function coefficient

α_2 = drag reduction function coefficient

φ = drag reduction function coefficient

θ = vegetation deflection angle

χ= Drag coefficient fitting parameter (-)

ρ = density of fluid (kg m^{-3})

ν = kinematic fluid viscosity ($m^2 s^{-1}$)

Chapter 4
Flexible Vegetation Drag in Waves

Summary

Understanding energy dissipation by vegetation is critical for the effective management of shoreline erosion. Current methods for estimating energy dissipation require plant specific parameters that are difficult to estimate for the large variety of plant morphologies used in shoreline protection, requiring testing on each species of interest. A simple and fast method to characterize drag in terms of wave interaction and obstruction natural frequency is needed to fully explore drag forces on vegetation. Our method directly measures hydrodynamic forces on individual plant shoots using a torque sensor mounted beneath the bed of a flume. This sensor allows data to be collected simply and inexpensively with high temporal accuracy that provides insight into drag forces and torque frequency from a variety of flexible elements when coupled with wave monitoring. The technique can evaluate of several types of obstructions quickly without the need to set up an entire obstruction field. The data collected also suggests that more flexible objects result in less drag force on each element and suggests that frequency response is related to the frequencies existing in the driving wave and the natural frequency of the obstruction element, although harmonic synchronization appears to occur in some cases doubling the expected drag force magnitude.

Introduction

Although our knowledge of the mechanism of how vegetation dissipates wave energy and contributes to shoreline protection by damping waves continues to increase, large areas of off-shore vegetation and wetlands continue to be degraded and destroyed each year (USEPA, 2007), and vegetation benefits, which also include aesthetics, habitat, and biodiversity, are lost with their removal. Vegetation has been shown to effectively attenuate flow (Fonseca, et al. 1982; Peterson et al. 2004) and wave energy (Dean 1978; Fonseca and Cahalan, 1992; Kobayashi et al., 1993; Mendez et al. 1999; Möller et al., 1999; Dean and Bender, 2006; Augustin et al., 2009). Several models for predicting wave dissipation through vegetation have been proposed based on conservation of energy (Dalrymple et al., 1984; Mendez and Losada, 2004) and conservation of momentum (Kobayashi et al., 1993) for linear waves and these have subsequently been expanded and new models proposed (Dubi and Torum, 1995; Mendez et. al 1999; Chen and Zhao, 2012). Additional models investigating wave attenuation under the combination of wave flow and current flow (Ota et al, 2005; Li and Yan, 2007) have also been proposed.

As these models have grown in complexity they are better able to address conditions found in the field, but to predict these conditions they require input parameters that are species specific. Bulk drag characterization from the wave height decay through a field of plant elements in a test flume or site is often used as a standard of practice (USACE, 2006). The bulk drag characterization requires the establishment of an obstruction field. This method can be cumbersome and the results cannot be translated over to other species easily (Bouma et al., 2010), and needs to be performed on each species or plant morphology (USACE, 2006). Even within a single species, the seasonal

changes in plant foliage influence the bulk canopy drag (Schoneboom and Aberle, 2009) so testing at several different stages of growth is needed to fully characterize some species (Paul and Amos, 2011).

We have instrumented a single plant element instead of evaluating the flow conditions before and after the obstruction network, eliminating the time and expense needed for establishing an entire vegetation field. We feel this is advantageous as experiments can be run more efficiently on a larger number of species. This is similar to an approach used by Wunder et al. (2009) and Schoneboom and Aberle (2009). While Wunder et al. (2009) used a frame to mount elements and transmit forces to a load cell and Schoneboom and Arberle (2009) used a load cell mounted below the flume, we used a torque sensor mounted below the flume to simplify these arrangements further and provide a high frequency temporal response. While torque sensors have been used in previous studies (Flocard and Finnigan, 2009; Pasternack et al. 2007) they have not previously been mounted with vegetation or vegetation surrogates.

The lack of information on species limits the usefulness of the models developed and generalizations of plant behavior have not proved to be robust enough for practice (Mendez and Losada, 2004). While some species, such as *Cabomba caroliana, Nympheae rubra,* and *Eichinodorus grandifloru* (Pennings et al. 2009), *Laminaria hyperborea* (Dubi and Torum, 1995; Mork, 1996), *Macrocystis pyrifera* (Elwany et al., 1995; Elwany and Flick, 1996), *Posidonia oceanica* (Gacia and Duarte, 2001; Stratigaki, et al. 2009), *Spartina alterniflora* (Möller et al.,1996, 1999), *Zostera marina* (Fonseca and Cahalan, 1992; Ifuku and Hayashi, 1998), have been characterized for energy

dissipation parameters, many more species have no information available. Establishing relationships of drag to the Reynolds number (Re), using the orbital velocity and vegetation diameter as the characteristic length, and Keulegan-Carpenter number (KC), using the orbital velocity and vegetation diameter as the characteristic length, have also been attempted with some success (Mendez and Losada, 2004; Augustin et al., 2009), but there has not been strong evidence which one of these non-dimensional parameters is better suited to represent drag for plants (USACE, 2006). Sarpkaya and Isaacson (1981) extensively look at the inter-relation of drag and momentum of obstructions in waves to Re and KC, along with other non-dimensional parameters, but do not unite these parameters in one relation. Use of a non-dimensional drag coefficient is advantageous as it is independent of plant area, which may change seasonally, but is dependent on the morphology and hydrodynamics. For *Thalassia testudinum* (Bradley and Houser, 2009), *Zostera noltti* (Paul and Amos, 2011), and artificial kelp (Kobayashi et al., 1993; Mendez et al., 1999) exponential functions of Reynolds number were determined for estimation of drag coefficients with reasonable accuracy.

Procedures have been developed to translate individual obstruction drag elements into a canopy drag (Dalrymple et al.,1984; Kobayashi et al., 1993; Mendez et al., 1999). These methods based on fundamental principles of energy and momentum conservation and superposition have been used to reasonably model canopies, but the drag parameters for the bulk system are often modified from the drag parameters associated with individual elements.

Many previous studies have incorporated rigid elements to simulate vegetation fields in directional fluid flow (Nepf, 1999; Poggi et al. 2004; Nezu and Sanjou, 2008), directional atmospheric flow (Finnigan, 2000) and in wave fluid flow (Dalrymple et al., 1984), but there have been fewer studies that have incorporated flexible elements into the experimental design in either direct flow (Ghisalberti and Nepf, 2006; Wunder et al., 2009) or in wave conditions (Augustin et al., 2009). Some research has looked at simpler properties such as wet biomass (Pennings et al., 2009) for defining the parameters of vegetation, but a more efficient characterization method is still needed.

Studies focusing on characterization of turbulence through laser and Doppler techniques (Finnigan, 2000; Poggi et al., 2004; Nezu and Sanjou, 2008) have provided insight to the wake effects and eddy structures that develop in canopies. While this is fundamental to deeper understanding of the interactions within the canopy, there is also a need for breaking the complexities down into simpler components such as the basic characterization of drag force differences occurring due to the flexibility of vegetation.

Our goal is to characterize and predict vegetation drag forces by collecting data on a single vegetation element in a flume, as opposed to establishing a full network of vegetation and monitoring wave decay affects. We have used the torque sensor instrumentation arrangement to measure the forces on artificial vegetation under wave conditions. We have used both rigid and flexible artificial vegetation and also with a single element and with a single element located within a field of artificial vegetation, although the methodology is applicable for a great variety of vegetation morphologies. The experimental setup can be used to study directional flow and wave conditions;

however, wave conditions are of greater importance in shoreline protection and are the focus of the data in this paper.

While use of a torque sensor cannot separate force components of form drag, skin friction drag, and others, it does provide a total drag reaction occurring at the base of the artificial vegetation which is suitable for this study. Wake interactions are not monitored directly with this instrument, but can be inferred by comparing reactions when upstream artificial vegetation is present or not. Additionally, by using fully emergent artificial vegetation, we have limited the scope of this work to consider flow within the vegetation canopy.

Background

The form drag force on artificial vegetation can be estimated, assuming an unsteady, non-uniform flow of a viscous fluid and neglecting inertial forces of the vegetation, and can also be interpreted as a torque at the base of the vegetation, as seen in Equation 4.1,

$$F_d = \int_o^d \frac{1}{2} C_D \rho \, w \, u^2 \, dz = \int_o^d \frac{1}{z} \left(\frac{dT_d}{dl}\right) dz \tag{4.1}$$

where F_D = drag force, u = flow velocity, w = projected vegetation width, C_D = drag coefficient of vegetation, and ρ = fluid density, T_d = the torque on the vegetation at z, l = moment arm for vegetation at z, d = flow depth, T is the total torque and z = vertical

position up from the bed. For the limit as z approaches the bottom of the channel, we assume that (T_d/l) approaches zero by linear wave theory.

The velocity profile for can be determined using linear wave theory and the measured wave height (Sorenson, 2006) and will be used with determined moment arm estimates to convert the torque data into resultant forces.

By using a constant, representative drag coefficient, Equation 1 can be simplified using $\Delta z = d/n$ to create Equation 4.2,

$$F_d = \frac{1}{2} C_D \rho \Delta z \sum_{i=1}^{n} w_i u_i^2 = \frac{T}{l} \tag{4.2}$$

where n is the number of vertical grid points. The spatially averaged drag coefficient for a measured total torque acting on the vegetation over a known mean water depth can be determined using Equation 4.3.

$$C_D = \frac{(\frac{T}{l})}{(\frac{1}{2})\rho \Delta z \sum_{i=1}^{n} w_i u_i^2} \tag{4.3}$$

The moment arm was estimated using the sum of the wave amplitude and mean water depth, and the velocity was determined from the calculated orbital velocity within the wave. The drag force calculation can be further simplified by assuming the mean water depth as the moment arm as in Equation 4.4, where T is the total sum of torque on the vegetation.

$$\tilde{F}_d = T/\dot{l} \tag{4.4}$$

Equation 4.4 is a useful simplification when the torque and drag forces vary with time as they do in wave conditions. Under wave conditions, the torque response will vary with each wave period and while translation of this signal into a single representative value can be done using an RMS average, it can also be translated into a single value by integrating over time. Combining equation 4.1 and 4.4 and using the integration limits of time gives Equation 4.5, which is an expression for the time-averaged drag coefficient.

$$\tilde{C}_D = \frac{\int_0^T T \, dt}{\int_0^t \frac{1}{2} \rho A u^2 \, dt} \tag{4.5}$$

Where A is the vegetation projected area and t is time in data series. A correction for the simplified moment arm based on the orbital velocity profile can be applied to Equation 4.5, to have a more accurate value as shown in Equation 4.6, where β is the reduction of the moment arm estimated using the resultant depth averaged velocity equivalent to the calculated orbital velocity profile using the wave period determined from the spectral density plot.

$$C_D = \tilde{C}_D * \beta \tag{4.6}$$

Where C_D is the drag coefficient, $\tilde{C}_D$ is the time averaged drag coefficient, and β is the reduction factor based on wave period.

Method

An indoor experimental flume in the Biosystems and Agricultural Engineering Building on the St. Paul campus of the University of Minnesota was used in this study. It was retrofitted to include a submersible torque sensor below the flume floor, to which artificial vegetation could be attached and subjected to either directional flow or wave conditions. The submersible torque sensor allowed for direct measurement of the torque on the vegetation from the flow, and back calculation of the drag forces occurring on the vegetation.

A schematic of the experimental flume is shown in Figure 4.1. The flume has a total length of 7.25 meters, an interior flow width of 0.38 meters, and total depth of 0.38 meters. This flume has an additional wet well extending 0.2 meters below the flume over a 2.1 meter test section. This allows for elements to be placed below the flume floor, such as submersible sensors. The flume is primarily constructed out of PVC with steel reinforcement. The flume bottom is lined with 1 mm diameter sand adhered to metal sheets. The slope of the flume can be adjusted using screw jack supports.

When operated for wave simulation, an artificial beach is placed in the last 1 meter of the flume. A hinged paddle is used to generate waves using a 12 volt DC motor stepped down to a paddle arm through a belt and pulleys. The flume wet well allows for a FUTEK TFF425 submersible torque sensor to be mounted below the flume, with a single vegetation element attached to the sensor passing up through the floor of the flume into the flow, 0.62 meters behind the start of the obstruction canopy when used. The torque sensor has a 0.047 N-m maximum capacity, suitable to measure small loadings such as

those occurring from a single small diameter vegetation stem. The FUTEK SensIT Test and Measurement v2.1.4 software and FUTEK USB210 interface were used to read and calibrate the data from the sensor. This model of torque sensor has a flange end, and a PVC plate was mounted onto the flange with springs, to allow obstruction elements and vegetation to be mounted to the sensor through compression.

(a)

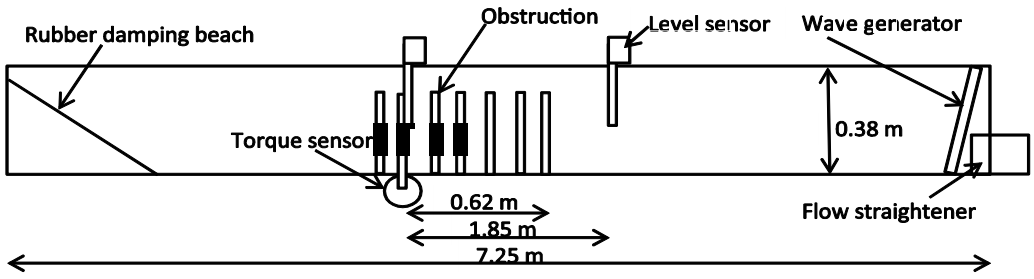

(b)

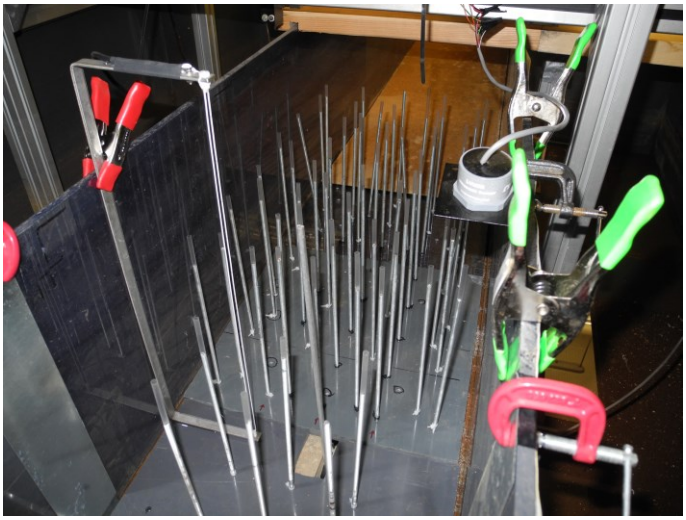

(c)

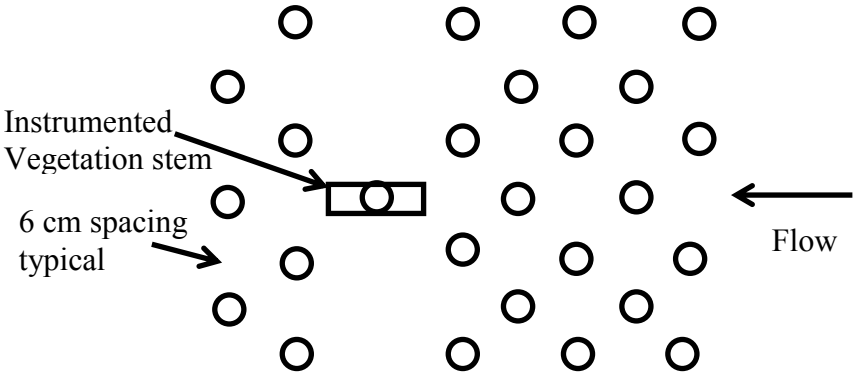

Figure 4.1. Flume schematic, vegetation layout, and photograph of test section.

Water surfaces are measured using RBR WG-55 capacitance level sensors. One WG-55 sensor is placed adjacent to the vegetation to measure the wave conditions near the vegetation torque data. A second WG-55 sensor is placed 1.85 meters upstream of the vegetation element to characterize the wave conditions prior to any vegetation. The WG-55 sensor data was collected using a DATAQ DI-149 voltage data logger. A submersible digital video camera placed in the wet well was also used to film the vegetation through the clear flume wall marked with grid lines at 5 mm spacing for data verification. The statistical software program R (RDCT 2011) was used for spectral signal analysis using packages of stats (Venables and Ripley, 2002), car (Fox and Weisberg, 2011), and pastecs (Ibanez et. al, 2013).

Three different artificial vegetation stems covering a range of flexibilities were used in these experiments, made of aluminum, polyurethane foam, and a thin walled polyethylene straw. These will be referred to as aluminum, foam, and straw vegetation for simplification. We attempted to use artificial vegetation with similar size, shape, and surface texture. The vegetation diameters and other physical properties are reported in Table 4.1.

Table 4.1. Artificial vegetation physical properties

	Dia. (mm)	Eff. Specific Gravity	Specific Gravity	m*	m* eff.	M. of Elasticity (Pa) +	Freq. f_o (Hz)	Damp-ing α
Alum.	6.6	2.575	2.575	2.022	2.022	7e10	4.464	0.007
Straw	5.5	1.095	1.904	0.158	0.860	1.23e8	6.49	0.089
Foam	9.0	0.020	0.020	0.016	0.016	3.19e5	10	0.002

+This value was determined assuming the element was a solid homogenous body

Table 4.1 lists the artificial vegetation and their Young's Modulus, or moduli of elasticity as determined by loading the vegetation as a cantilevered beam. The moduli were determined as if the element was a solid homogeneous cylindrical mass, which is not the case for all artificial vegetation tested or for live vegetation, but this technique allows for a comparison of flexibility.

Table 4.1 also includes the artificial vegetation specific gravity. While specific gravity is a property of the material, some of the artificial vegetation has voids filled with air or water, depending on saturation. An effective specific gravity can be calculated for the composite artificial vegetation assuming the voids are filled with water during the experiment. The two m* properties in Table 4.1 are used to quantify the damping due to the mass of an oscillating object. Gabbai and Benaroya (2005) represented this damping using m* defined as the mass of the obstruction divided by the fluid density and by

square of the vegetation diameter. Due to the saturated void space, an m* effective can also be calculated assuming all the open voids are saturated with water.

The experimental setup can be used for the measurement of the natural frequency of the vegetation tested. When vegetation is located in the torque sensor, it is possible to apply a single temporary force and monitor the response after the force is released. The torque signal decay (Figure 4.2) can be used to measure the natural frequency (f_o) and the damping coefficient (α), as reported in Table 4.1. The natural frequency is the inverse of the difference between torque peak values. The damping ratio is the natural log of the ratio of peak torque for two consecutive cycles divided by 2π. Due to the low mass of the foam vegetation, the frequency and slow decay response shown for the foam vegetation is mostly generated by the mass of the torque sensor itself. The natural frequency of the torque sensor without mounted vegetation is the same as the frequency response with the foam vegetation. The spatial distribution of vegetation mass along the vegetation length is believed to cause the differences in the rate of signal decay or damping seen in the straw and aluminum vegetation.

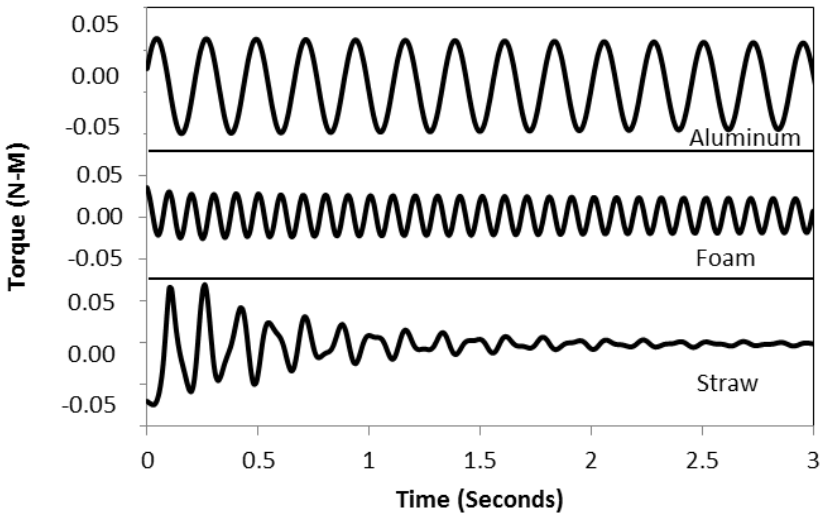

Figure 4.2. Natural vibration response of the aluminum, foam and straw artificial vegetation in the experimental setup.

Experiments were performed with networks of artificial vegetation arranged upstream from the test element. The networks included rows of additional vegetation downstream of the test vegetation stem. These artificial vegetation canopies were mounted using threaded studs in panels on the floor of the flume. The canopy vegetation were arranged in a staggered pattern at different densities corresponding to flow vegetation fractional volumes of flow domain ranging from 0.003 to 0.025 (Table 4.2) where a fractional volume of the flow domain is defined as the ratio of vegetation diameter squared to mean vegetation spacing distance squared (Nepf, 1999).

Table 4.2. Artificial vegetation network (canopy) spacing

Vegetation	Dense		Medium		Thin	
	Elements per m^2	Fractional Volume	Elements per m^2	Fractional Volume	Elements per m^2	Fractional Volume
Aluminum	310	0.0135	142	0.0062	86	0.0037
Straw	310	0.0094	155	0.0047	86	0.0026
Foam	310	0.0251	155	0.0125	86	0.0069

Five different wave conditions were generated for each vegetation arrangement and were varied by altering the wave period through the frequency of the wave paddle motion. Wave periods generated ranged from 0.7 to 1.1 seconds (Table 4.3) and the water depth in the flume was 0.22 ± 0.02 m, as limited by the flume and wave generator construction. The vegetation size and wave heights correspond to full scale for some shallow inland lakes with emergent vegetation.

Table 4.3. Wave parameters

Wave Condition	Period (s)	Height (m)
1	1.009 ± 0.043	0.022 ± 0.0045
2	0.908 ± 0.027	0.022 ± 0.0061
3	0.846 ± 0.016	0.031 ± 0.0046
4	0.806 ± 0.009	0.030 ± 0.0058
5	0.758 ± 0.028	0.0282 ± 0.0029

Results and Discussion

The instrumentation system is able to provide quick useful analysis of drag forces from a variety of obstruction types in wave conditions as tested. The water surface displacement can be coupled with our torque response to provide insight into drag forces. The output values from the torque sensor did not require any additional manipulation or adjustment with the experimental set up, as would be necessary using load cells with mounting arms (Wunder et al. 2009). The technique also allowed for evaluation of several types of vegetation quickly without the need to set up entire vegetation fields.

The torque response contained in it dominant frequencies that were directly related to the major driving wave frequency of the experiment (Figures 4.3, 4.4, and 4.5). In addition to the dominant frequency related to the wave period, the torque response had additional frequencies for different artificial vegetation. The number of these frequencies varied with the type of artificial vegetation. The less flexible aluminum vegetation had fewer frequencies (Figure 4.3) compared to the straw (Figure 4.4) and foam (Figure 4.5). Foam had the most additional frequencies, which the authors speculate is due to the greater flexibility and subsequent greater motion.

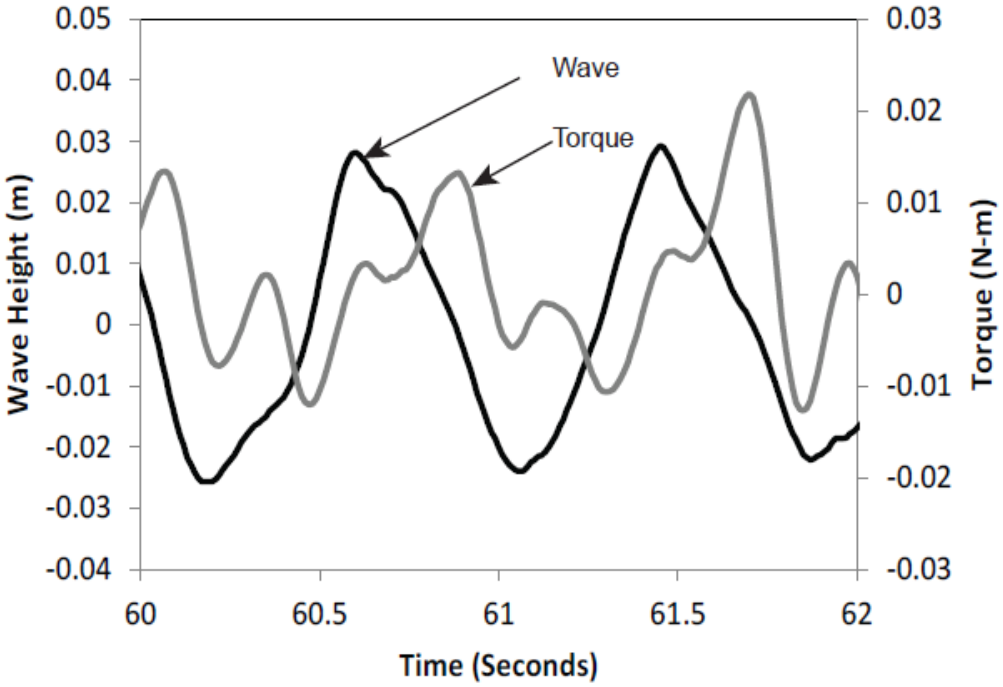

Figure 4.3. Two seconds of aluminium artificial vegetation torque response in waves. The wave height at the instrumented vegetation is on the left axis, and the vegetation torque is shown on the secondary axis.

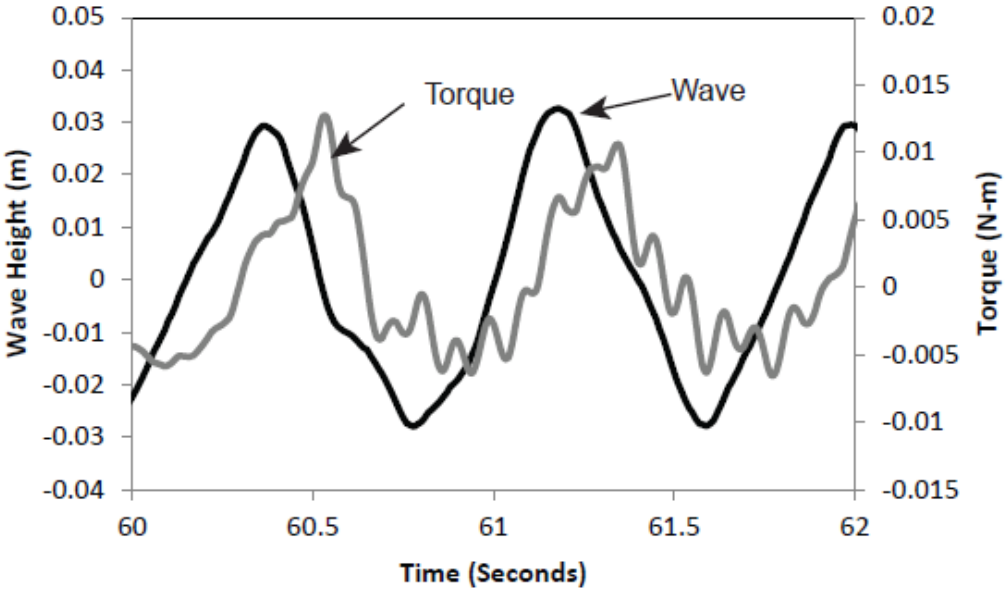

Figure 4.4. Two seconds of straw artificial vegetation torque response in waves. The wave height at the instrumented vegetation in on the left axis, and the vegetation torque is shown on the secondary axis.

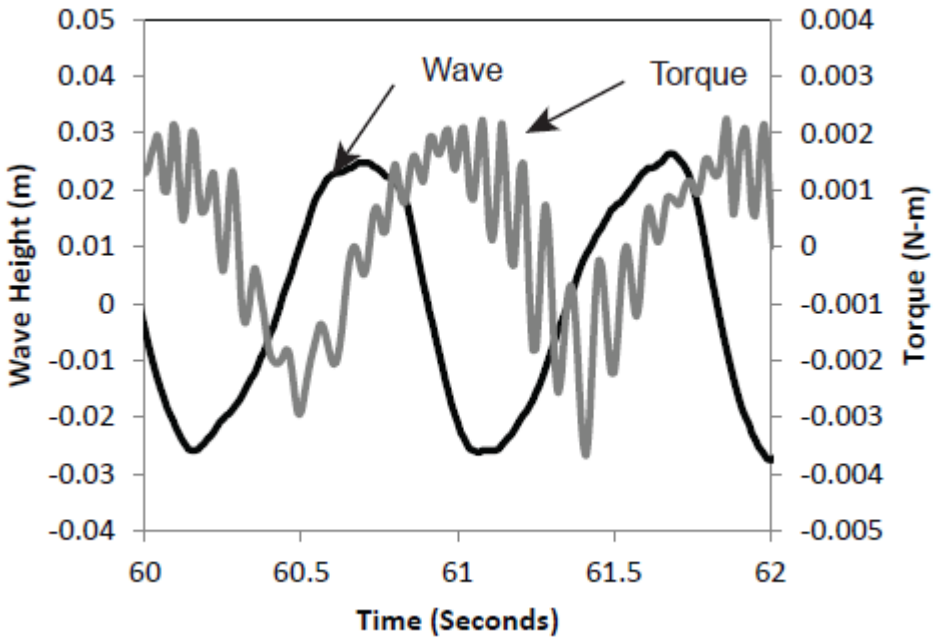

Figure 4.5. Two seconds of foam artificial vegetation torque response in waves. The wave height at the instrumented vegetation in on the left axis, and the vegetation torque is shown on the secondary axis.

The magnitude of the torque response is also stronger in the less flexible aluminum, on the order of 0.02 N-m peak values, compared to the more flexible straw element, on the order of 0.01 N-m peak values, or the most flexible foam vegetation having peak torque values of 0.002 N-m peak values. The more rigid vegetation will either transfer more forces to the base where they are observed by the torque sensor, while the more flexible vegetation will not transfer all of the force to the base and

distribute energy by greater motion, or receive more drag force than the flexible vegetation due to their reduced deformation compared to the flexible vegetation.

Since the flow depths are approximately equal in Figures 4.3 through 4.5, drag forces are directly related to the magnitude of the torque readings for these tests. More flexible vegetation in our tests resulted in smaller drag forces and drag coefficients. This outcome is similar to that obtained by Mullarney and Henderson (2010) for their investigations of *Schoenoplectus americanus*. They found that wave dissipation, which can be estimated from the drag (Dalrymple et al., 1984), for flexible stems was only 30% of that predicted for rigid stems. This effect was frequency dependent with a maximum reduction around 1Hz. However, the trends in Figures 4.3 through 4.5 are different than those obtained by Wunder et al. (2009). Flexibility increased drag forces in their study of what was referred to as a willow branch. The topology, natural frequency, and damping coefficient of the willow branch might account for the different response.

A fast Fourier transform was used to develop spectral density plots of the torque response using Program R (RDCT 2011) and associated packages. Torque values and wave height values are also correlated with time (Devore, 2001) using the same software. Results are summarized in Figures 4.6, 4.7, and 4.8 and are discussed below. The spectral density is highly periodic, and as expected the largest spectral density occurs at a frequency value that correlates with the driving water wave frequency, but additional frequencies also have large spectral density values.

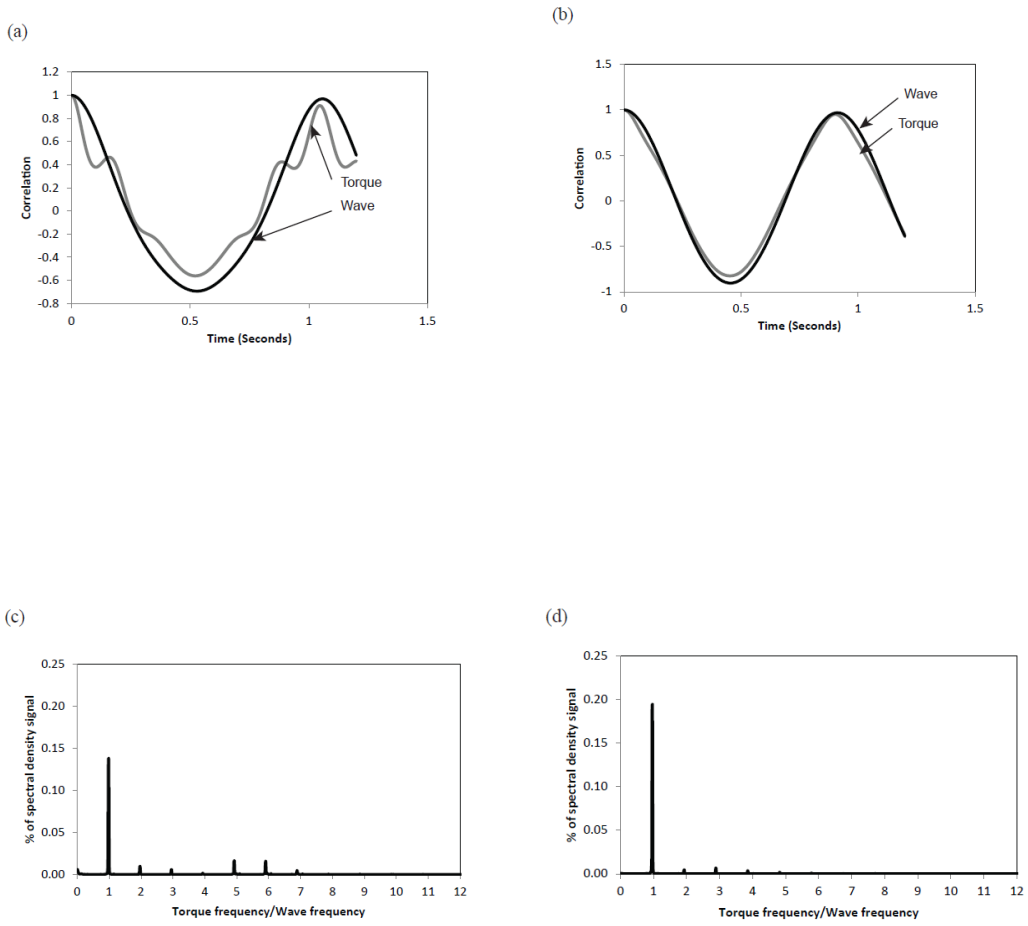

Figure 4.6. Comparison of two torque correlation and torque spectral density plots of the aluminium artificial vegetation with a natural frequency of 4.46 Hz. Figures 6a and 6c are from the same experiment that had a vegetation drag force of 0.009879 N, wave height of 0.022 m, wave period of 1.03 s, and mean water depth of 0.218 m. Figures 6b and 6d are from the same experiment that had a vegetation drag force of 0.02361 N, wave height of 0.022 m, wave period of 0.91 s, and mean water depth of 0.23m.

Figure 4.6a combines the torque and wave data into a single correlation plot and while Figure 4.6c shows the spectral density results an experiment with aluminium vegetation. Figure 4.6b and 4.6d show a similar correlation plot and spectral density information for another experiment with aluminium vegetation under slightly different wave frequencies. The vegetation Re are nearly the same for the two runs, the wave heights are both 0.022m, the same dense network density is used, the mean water depth is 0.218 and 0.23, but the wave period is 1.03 seconds for Figures 4.6a and 4.6c and 0.87 seconds for Figures and 4.6b and 4.6d. We calculated Re using the maximum orbital velocity in the wave and the vegetation diameter for the length scale. The drag force corresponding to Figure 4.6c is approximately 2.4 times larger than that corresponding to Figure 4.6d. Insight into this difference can be obtained by considering the power spectral densities for the two runs. The power spectral density is proportional to the modulus squared of the Fourier amplitude at each frequency and is the power distributed over the observed frequency range. To simplify interpretation, the power spectral density results are presented in Figures 4.6c and 4.6d as a percentage of total spectral density with respect to a normalized frequency, defined as the torque frequency divided by the dominant fluid wave frequency. The influence of the driving fluid wave frequency in the response of the torque may be seen in Figures 4.6c and 4.6d where the strongest signal matches the wave frequency. However, Figure 4.6c has a greater number of subsequent frequencies, which appear to be resonant frequencies, in the torque response compared to Figure 4.6d.

Figures 4.7 and 4.8 for the straw and foam vegetation show similar a response as seen in Figure 4.6. The flow conditions for Figure 4.7 have Re of 725 and 614, wave heights of 0.022 and 0.013 m, Periods of 0.96 and 0.91 seconds, and depths of 0.206 and 0.208 m for the Figure 4.7a and 4.7c paired plots and Figure 4.7b and 4.7d paired plots respectively. For the straw, the drag forces are again smaller for the conditions of Figure 4.7a than those of Figure 4.7b as they were with the aluminum vegetation. However for the foam vegetation, we do not have two runs that can be compared having similar character in the spectral density. The flow conditions for Figure 4.8 have Re of 1020 and 932, wave heights of 0.014 and 0.017 m, Periods of 0.9 and 1.04 seconds, and depths of 0.198 and 0.24 m for the Figure 4.8a and 4.8c paired plots and Figure 4.8b and 4.8d paired plots respectively. There was not a reduction of drag force to the strength of the spectral density at the secondary frequency (Figure 4.8) so little can be concluded from this. The secondary frequencies in the foam vegetation did correspond to a 10Hz signal, which is possibly due to the torque sensor mass which was not damped by the vegetation mass.

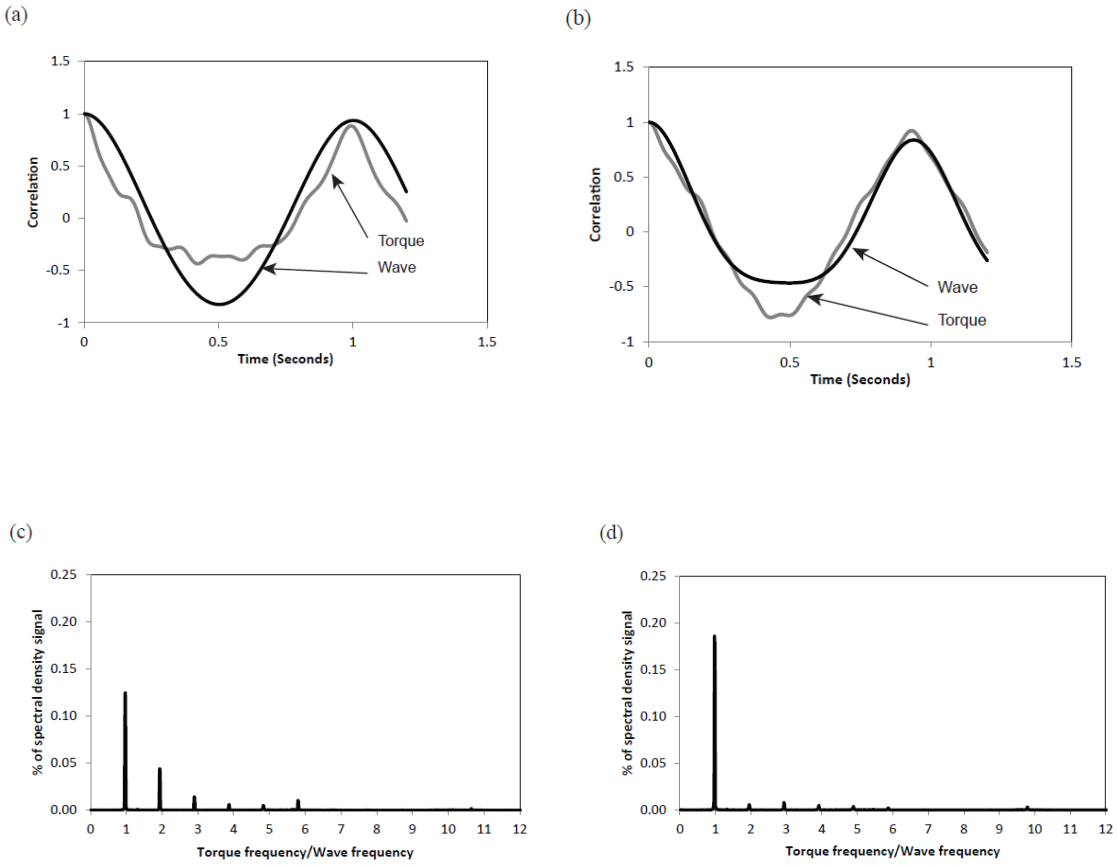

Figure 4.7. Comparison of two torque correlation and torque spectral density plots of the straw artificial vegetation with a natural frequency of 6.49Hz. Figures 7a and 7c are from the same experiment that had a vegetation drag force of 0.0111 N, wave height of 0.023 m, wave period of 0.96s, and mean water depth of 0.206m. Figures 7b and 7d are from the same experiment that had a vegetation drag force of 0.0212 N, wave height of 0.014m, wave period of 0.91 s, and mean water depth of 0.208.

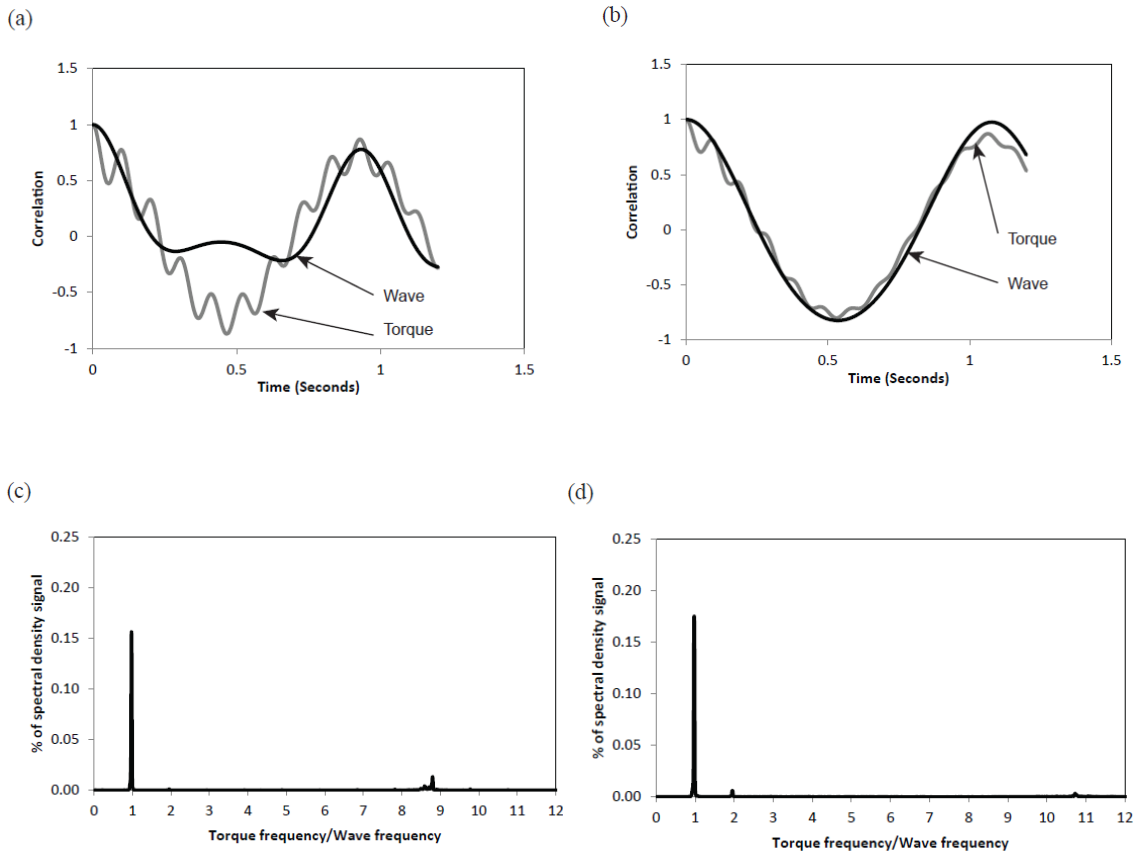

Figure 4.8. Comparison of two torque correlation and torque spectral density plots of the foam artificial vegetation with a natural frequency of 10 Hz. Figures 8a and 8c are from the same experiment that had a vegetation drag force of 0.01883 N, wave height of 0.0146 m, wave period of 0.9 s, and mean water depth of 0.198 m. Figures 8b and 8d are from the same experiment that had a vegetation drag force of 0.009694 N, wave height of 0.0191m, wave period of 1.04 s, and mean water depth of 0.24 m.

The largest spectral density in the torque frequencies matches the wave frequency as forced by the wave generator, as seen in Figures 4.6, 4.7, and 4.8 where the largest signal is at a frequency ratio of 1. Subsequent frequency values are harmonic values of the torque frequency. We have compared the amount of spectral density occurring at this wave frequency to the total spectral density plot in order to index this phenomenon. Figure 6d has 85% of the energy density concentrated into the fundamental frequency and Figure 4.6c has 60% of the energy density concentrated into the fundamental frequency. A lower percentage of the energy density occurring at the driving wave frequency suggests there are more competing significant frequencies in the signal. Figure 4.9a shows the drag force estimated from torque compared to the percentage of spectral energy density occurring in the driving wave fundamental frequency for the dense vegetation network. Figure 4.9b shows data for the intermediate density networks, and Figure 4.9c shows only data collected using the thinnest network of vegetation having a flow obstruction fractional volume of 0.002 to 0.007 upstream of the test vegetation stem. Greater spectral density occurring in a fundamental frequency, which the authors attribute to evidence of synchronization where frequencies interact to create larger amplitudes, tends to result in higher drag forces (Figure 4.9a), which is more apparent when comparing vegetation tested under thinner network densities (Figure 4.9b and 4.9c). High percentages of signal concentration tend to occur when the wave frequency is at a harmonic synchronization with the natural frequency of the element. The wake effects generated by the networks of vegetation located prior to the test element appear to reduce the occurrence of synchronization and are another difference between individual drag and

bulk drag effects, but larger drag forces occur for vegetation with fewer resonant frequencies in the spectral density.

(a)

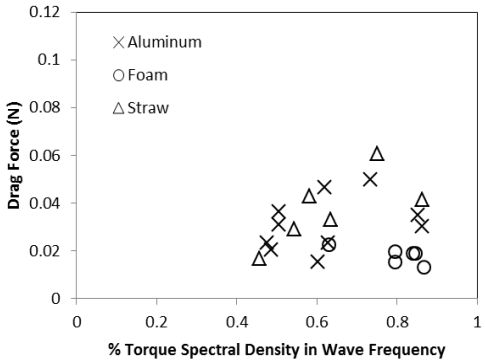

(b)

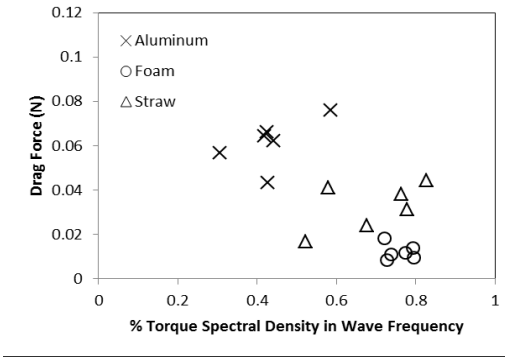

(c)

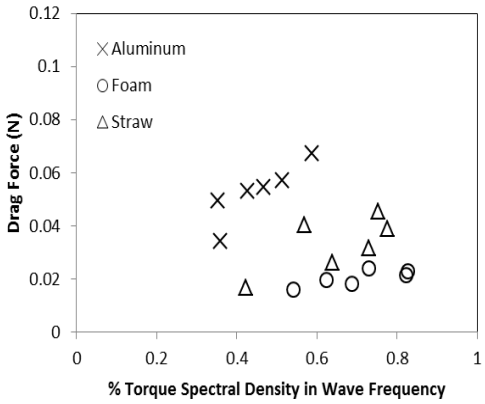

Figure 4.9. The percentage of torque spectral density signal occurring at the wave frequency compared to the drag force on the element for aluminium (X marker), Straw (triangle marker), and foam (circle marker). Figure 4.9a is for a dense canopy of vegetation, 4.9b is the medium canopy, and 4.9c is the thinnest of vegetation canopies upstream of the torque sensor.

We estimate the artificial vegetation natural frequency as a harmonic value wave frequency when the quotient of these two values is an integer value. A plot of the harmonic integer vs. the percentage of torque spectral density at the wave frequency suggests that higher percentages occur at harmonic integers in the less flexible vegetation (Figure 4.10), but there is not a strongly defensible trend. The three groupings of data by vegetation type in Figure 4.10 result from the three vegetation types tested having different natural frequencies. The more flexible foam vegetation shows less harmonic influence than the more rigid vegetation having high percentages of spectral density at harmonic values, possibly due to increased deformation of the vegetation. The smaller foam mass may also result in more influence by the sensor natural frequency.

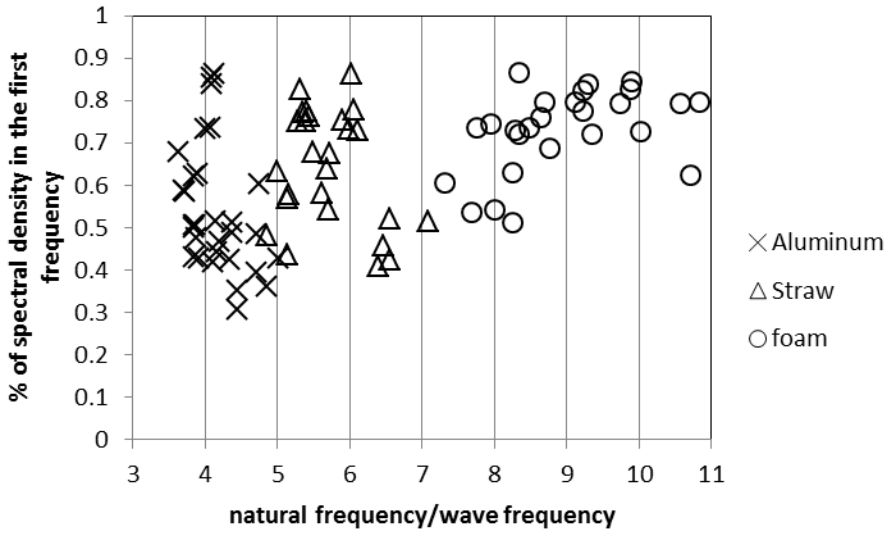

Figure 4.10. The artificial vegetation natural frequency divided by the water wave frequency is along the horizontal axis and the percentage of the spectral density signal occurring in the wave frequency.

The harmonic values and synchronization of vegetation movement with the wave period does appear to result in higher drag for the less flexible vegetation. The drag appears to be more substantially influenced by the flexibility of the vegetation, and the synchronization results in higher scatter in the data. Variations in the drag appear related to the oscillation frequency spectrum of the vegetation and in turn the hydroelastic behaviors and related vortex shedding frequencies. The drag differences can be explained if the higher harmonics of the wave frequencies and the natural frequencies of the vegetation resonate to reinforce the torque amplitude (Gabbai and Benaroya, 2005).

These observations suggest that higher drag forces are possible when the driving wave frequency is close to the natural frequency of the system, as more energy can be transferred into the vegetation by constructive interference at these certain frequency bands. This phenomenon of synchronization occurs in many other systems and appears to be influential in the drag forces of vegetal elements as well. The natural frequency of the vegetation appears to be a key factor as to whether synchronization will occur, as well as the wake effects of other obstructions.

While it is possible to estimate a drag coefficient by taking a root mean square average of the time series data collected by assuming it has the form of a sine wave (Sorenson, 2006), the experimental arrangement used herein allows for more direct analysis of the wave data. It does not appear possible to compare analyze the torque values collected at each time step however and some averaging over longer time intervals of the drag coefficient is needed (Sarpkaya and Isaacson, 1981). The observed wave height for each discrete time interval allows calculation of the wave velocity from linear wave theory and comparison to the torque value measured for an instantaneous drag coefficient calculated from Equation 4.6. This procedure results in extreme value singularity points due to the slight lag in the element torque response compared to the wave forces, so a torque is occurring for a null velocity, or a null torque value occurs when a velocity value is present.

A representative drag coefficient can be determined by integration of the torque and velocity data using Equation 4.5 over longer time intervals. The integrated drag

coefficient value becomes stable when integration time intervals greater than a wave period are used, as shown in Figure 4.11.

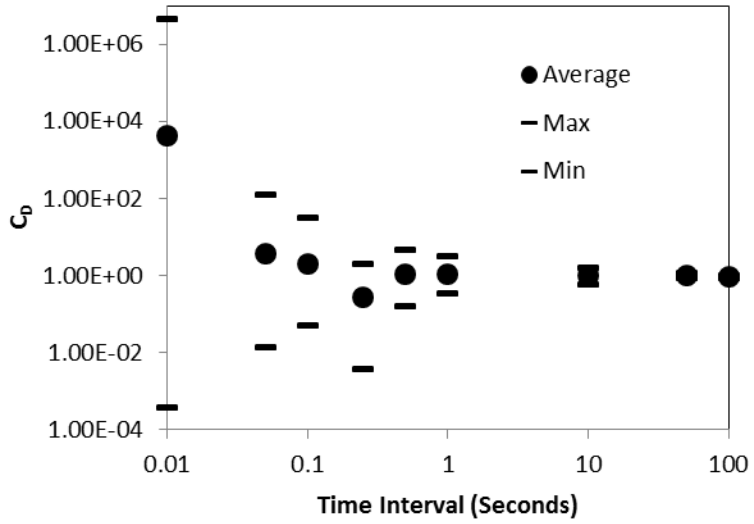

Figure 4.11. The integrated $\tilde{C}_D$ average, maximum, and minimum values for different integration time durations. The driving wave had a period of 1 second.

Drag coefficients are commonly related to either the Re or KC (USACE, 2006), using the orbital velocity and the vegetation diameter as the characteristic length. We calculated KC using the maximum orbital velocity, the wave period from the spectral analysis, and the vegetation diameter for the length scale. We have chosen to include a flexibility parameter consisting of the natural log of the modulus of elasticity of the vegetation divided by the natural log of a reference modulus of elasticity, taken as 100,000 Pa. The use of the reference elasticity does not significantly change the drag

coefficient relationships, but does maintain the non-dimensionality of Re and KC in Figure 4.12 and Figure 4.13. Larger drag coefficients are noted at low Re and KC values. While low Re values suggest this is an area where inertial forces are more dominant, it is likely that inertial forces are dominating in the areas of low KC values as well. Additional experiments using materials with different mass but similar flexibility could further our understanding of this trend.

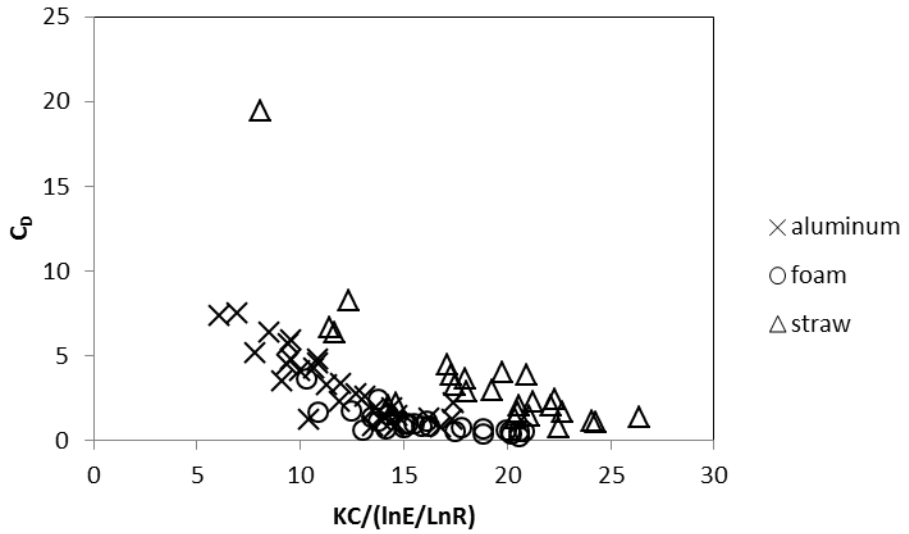

Figure 4.12. Drag Coefficient, C_D , as a function of KC, adjusted for the modulus of elasticity of the vegetation.

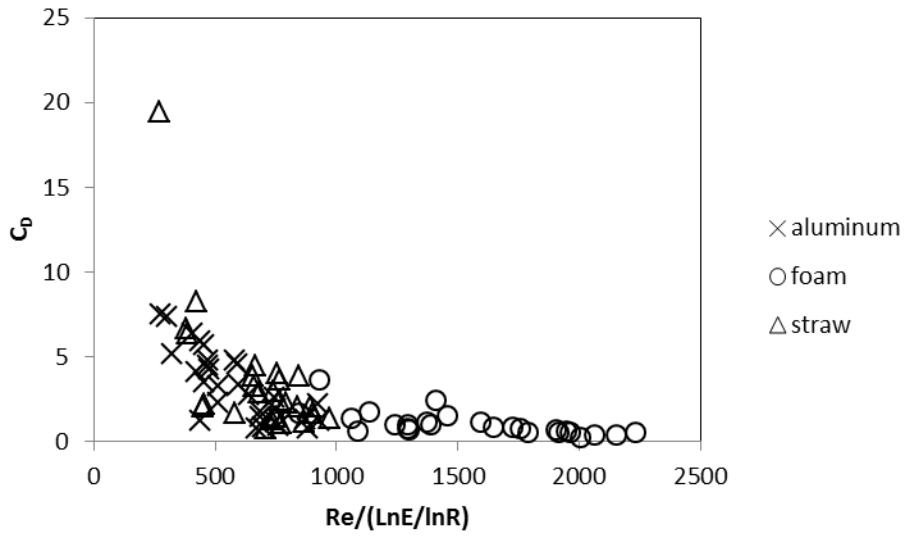

Figure 4.13. Drag Coefficient, C_D , as a function of Re, adjusted for the modulus of elasticity of the vegetation.

Increases in drag of 60% and greater have been reported (Sarpkaya, 1979) due to hydroelastic behavior and a similar effect appears to be occurring in some of the experiments of this study. The wave periods in our study ranged from 3 to 10 times greater than the Strouhal vortex shedding periods estimated for the vegetation, and so our experiments were likely to have cycles of vortex shedding in the lee side of the vegetation with oscillatory forces acting normal to flow (Sorensen, 2006). The natural frequency divided by the Strouhal vortex shedding frequency was in the range of 1 to 1.4 for the experiments on aluminum and straws, which is a range found to result in synchronization (Sarpkaya, 1979). The experiments with foam were unlikely to have synchronization according to the natural frequency divided by the Strouhal vortex shedding frequency ratios were much greater than 1.4. The correlation plots for foam

demonstrated complex signals, but due to the frequency value of 10 Hz, we believe this is influenced by the natural frequency of the sensor and not the vegetation.

While the torque response data provides insight into how the flexibility of vegetation can influence the drag, this experimental technique can also be used to calculate drag coefficients of the vegetation for use in wave dissipation applications. The analysis technique required is significantly more complex due with the time varying flow velocities estimated through linear wave theory compared to the averaging needed for analysis when this instrumentation is used for unidirectional flow.

While this experiment did not include the larger wave periods and wave lengths sometimes found in nature, the vegetation scales well with field conditions. Larger wave periods and wave lengths will likely result in a greater intensity of vortex shedding and disturbances related to frequency.

Chapter Conclusion

The technique of attaching vegetation, or any obstruction, to a torque sensor is a simple and convenient way to gather data on force reactions in flow. These measurements allow us to efficiently measure the drag coefficient of different flexible obstructions or vegetation species and vegetation species at many stages of development without the need to establish an entire field of vegetation. When an entire field of vegetation is established, this technique can be used to understand the differences between individual drag and bulk drag. This technique also provides the frequency of loadings on the vegetation. The drag appears to be influenced by driving wave

frequencies interacting with the vegetation, but the magnitude of the effect on drag appears to be also influenced by other factors such as flexibility of the vegetation. The more flexible vegetation result in less drag, indicating that use of rigid obstruction data may not appropriate for understanding flexible vegetation. The drag and wave frequency interaction is also likely influenced by vegetation morphology, flexibility, and dampening characteristics. Generalized relationships of drag coefficients to Re and KC can be improved by incorporating a non-dimensional modulus of elasticity factor for flexible vegetation. The torque sensor represents a useful tool to more precisely measure the response of flexible vegetation to waves.

Chapter Acknowledgements

This work was funded in part by the Minnesota Pollution Control Agency and the U.S. Environmental Protection Agency through the Clean Water Act Section 319 Grant funding. This work was also possible through the help of Brad Hansen, Mary Blickenderfer and Stephanie Nappa.

Chapter 5
Case Study of Shoreline Erosion Evaluation

Site Information

The following chapter provides an example demonstrating the use of the novel information described in the previous chapters. This does not provide new methodology, but uses techniques previously described in the literature and this thesis.

The site location used for this example is on Bass Lake in Itasca County, Minnesota, coordinate location N47.17.406 w093.36.862 (Figure 5.1). Since wave data is not available for the site, the wave conditions have been estimated using the methods outlined by Young and Verhagen (1996) and are shown in Table 5.1. Figure 5.2 defines the general parameter values and the "0" subscript denotes deep water wave parameters. The "rms" subscript denotes the root mean square value. The depth of water at wave breaking is noted as *db* and the wave period in seconds is noted as *T*. The information needed for this estimate include the longest fetch distance of 1854 meters which occurs at approximately 310 degrees or WNW; the average depth along the fetch which is 3.23 meters; and the U10 peak wind gust of 29.9m/s, according to the November 1998 International Falls Airport data for August available through the NOAA National Climatic Data Center.

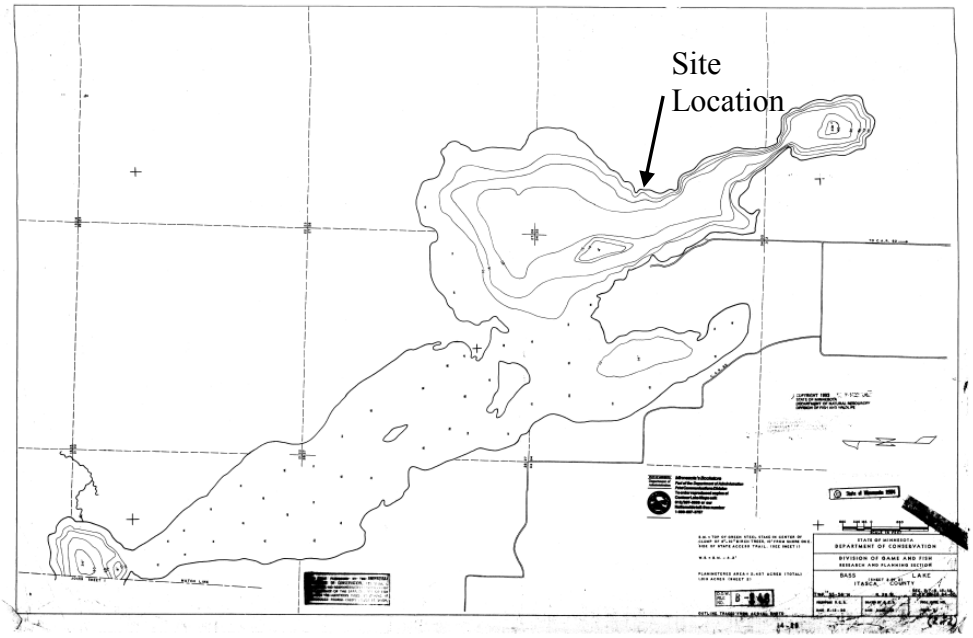

Figure 5.1 Case study location on Bass Lake.

Table 5.1 Estimated Incoming Wave Parameters

Wave Parameter	Value
H_0	0.6149 m
L_0	45.152 m
T	5.377 s
H_{rms}	0.434 m
db	0.738 meter

Additional wave parameters (Table 5.2) can be estimated using the Coastal Engineering Manual (USACE, 2002) and the values presented in Table 5.1. The maximum orbital velocity (U) and fluid shear stress (τ) at the wave bottom are also diagramed in Figure 5.2.

Table 5.2 Additional estimates of wave parameters estimated from Coastal Engineering Manual (USACE, 2002)

Wave Parameter	Value	Reference section
U_{bottom}	0.536 m/s	II-1-9
$\tau_{Maximum\ bottom}$	0.0173 N/ m2	III-6-53

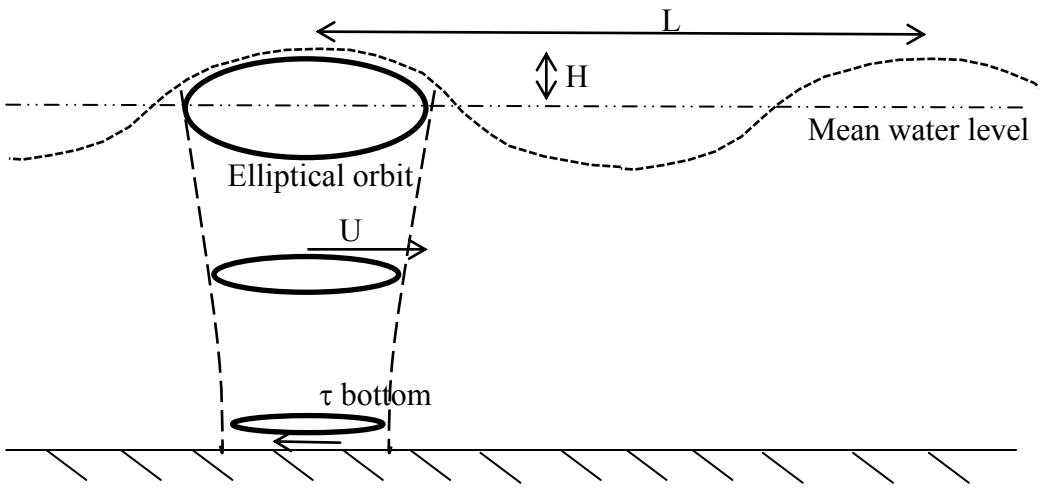

Figure 5.2 Wave particle profile

Wave Assessment

The Shields Criterion (Shields, 1936) can be used to assess if erosion will occur due to the orbital fluid motion of the wave. The Shields Criterion is a ratio of the fluid shear force to the weight of the soil particle. In this case, the maximum bottom shear value is used for the calculation of the shear velocity (U*). The near shore bottom material is assumed to have a D_{50} grain size of 0.003 meters based on field observations. Assuming a soil specific gravity of 2.65 and a water viscosity of $1x10^{-6}$, the Shields

Criterion can be used to estimate if particle movement is likely to occur from the wave parameters presented above. Equations 5.1 to 5.4 demonstrate the calculations needed to meet the Shields criteria of motion, with summary values presented in Table 5.3.

$$U^* = (\tau_{Maximum\ bottom} / \rho_{fluid})^{0.5} = (0.01733/1)^{0.5} = 0.13167 \quad (5.1)$$

$$\tau^* = U^{*2}/(g^*(\rho_{soil}-1)*D_{50}) = (0.13167)^2/(9.81*(2.65-1)*0.003) = 0.357 \quad (5.2)$$

$$Rep^* = (g^*(\rho_{soil}-1)*D_{50})^{0.5} * D_{50}/ \upsilon = (9.81*(2.65-1)*0.003)^{0.5} * 0.003/ 1x10^{-6}$$
$$= 6.61x10^2 \quad (5.3)$$

$$\tau^*critical = 0.22*Rep^{*-6}+0.06*10^{(-7.7(Rep^*-0.6))} = 0.046322 \quad (5.4)$$

Since τ^*critical calculated using Equation 5.4 is smaller than τ^* calculated using Equation 5.2, particle motion and erosion will likely occur. These equations can adjust force components acting on slopes and beaches as well resulting in smaller τ^*critical values. Based on these calculations, peak wind gusts occurring in August will result in shoreline erosion at this location.

Table 5.3 Shields Criterion values

Condition	τ^*critical	τ^*	Motion
Hrms = 0.434 m	0.0463	0.357	Yes
Hrms = 0.3 m	0.0463	0.1865	Yes
Hrms = 0.16 m	0.0463	0.0404	No
Hrms = 0.16 m, beach	0.0423	0.0404	No

The energy dissipation and resulting reduction of wave height can be estimated using methodologies proposed by Mendez and Losada (2004). The wave parameters presented in Table 5.1 and near shore bathymetry determined through field surveys are evaluated through a stepwise integration to calculate the energy decay as the wave approaches the shoreline. This method calculates the energy loss (ε_b) from the wave interaction with the lake bottom and the energy loss (ε_v) from the wave interaction with any vegetation obstructions, where wave height is estimated using a steady state energy balance (equation 5.5)

$$(\partial EC_g)/\partial x = -\delta = -\varepsilon_b - \varepsilon_v \quad (5.5)$$

$$\varepsilon_b = (3\sqrt{\pi})/16\rho g[(B^3 f_p)/(\gamma_b^4 h^3)]Hrms^7 \quad (5.6)$$

$$\varepsilon_v = 1/(2\sqrt{\pi})\rho C_D bv\, N(kg/2\sigma)^3 [(\sinh^3(k\alpha h)+3\sinh(k\alpha h))/(3k\cosh^3(kh))]Hrms^3 \quad (5.7)$$

Where E is the wave energy density, C_g is the group celerity, ρ is the fluid density, g is the acceleration of gravity, B and γ_b are adjustment parameters for wave breaking, fp is the peak frequency, Hrms is the root mean squared wave height, C_D is the drag coefficient, bv is the vegetation area per unit height, N is the vegetation density, k is the wave number, σ is the angular wave frequency, α is a fraction of vegetation height to water depth, and h is water depth.

This calculation has been done using visual basic code presented in Appendix G. The resulting wave height decay as the wave interacts with the lake bed causes a RMS wave height of 0.3 meters at station 215, where the mean water depth is 0.6 meters. Shields criteria suggests that soil particles will be in motion, even after the reduction in wave height from the bottom interaction. The water depth at station 215 is approximately 0.63 meters, which is nominally the same as the wave breaking depth of 0.738 meters.

Figure 5.3 shows the RMS wave height values at each station approaching the shore. Stations closer in than 215 meters are more difficult to predict due to wave set up and wave breaking, but it is possible to superimpose wave set up using the USACE Coastal Engineering Manual (USACE, 2002).

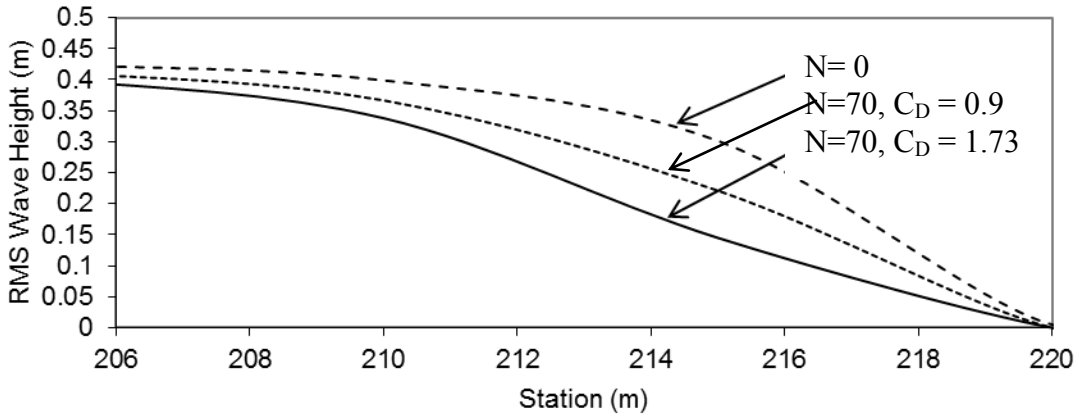

Figure 5.3 RMS wave height demonstrating decay as the waves approach shore through vegetation. N is the number of plants per square meter and C_D is the drag coefficient of plant elements.

Vegetation Assessment

From this analysis so far we conclude that soil particle motion will likely occur. We also can plot the wave height as a function of distance from the shore zone. The next step is to evaluate the wave heights and bottom shear occurring if vegetation is established in the system. This condition corresponds to the N = 70 curves in Figure 5.3.

Information given in Chapter 2 can be used to select the vegetation and its design parameters. Several species can likely be established in the near shore zone. Some species appear aggressive and more likely to result in monocultures, such as *Sparganium eurycarpum* or *Bolboschoenus fluviatilis*, while others do not appear to establish well such as *Carex lacustris*. While these results provide insight into plant response, care should be taken as other responses are possible. These studies were only conducted for one growing season, and other research has found the first season of growth is not a good indicator of biomass production in species such as *Carex* (Budelsky and Galatowitsch, 2000).

One species our research shows establishes well in deeper water, is not seen as aggressive or leading to monocultures but has reasonable biomass production is softstem bulrush (*Schoenoplectus tabernaemontani*), so we will plan our design with this species.

The data collected for Chapter 2 report the softstem bulrush diameter ranges from 0.0063m and 0.00224 meter. We will use the average value of 0.0042m. The modulus of elasticity of the softstem bulrush can be estimated from the data collected for Chapter 2 (Figure 5.4). We will use a value of $5x10^8$ Pa for this species.

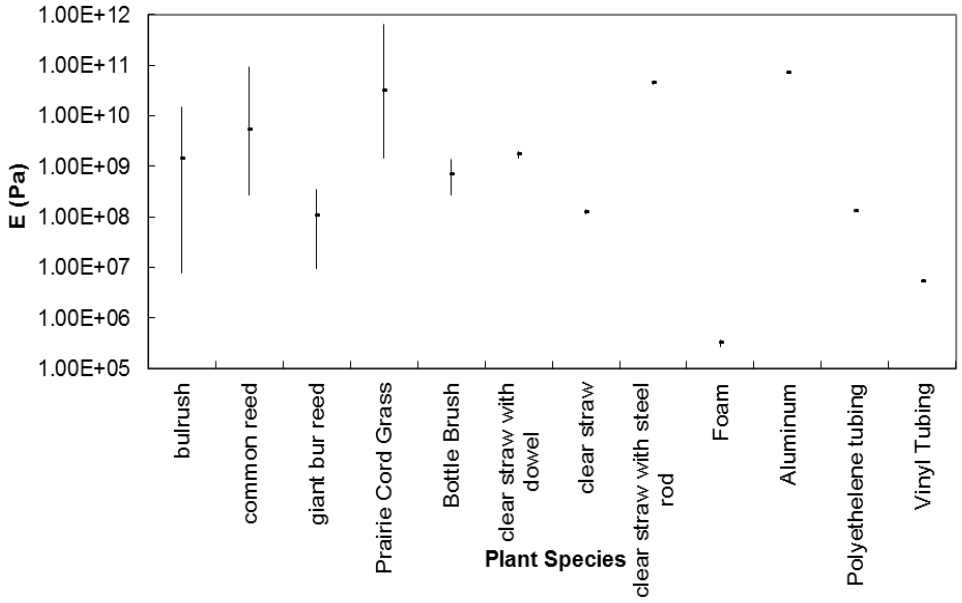

Figure 5.4 Modulus of Elasticity for select materials and vegetation

The drag coefficient for a rigid cylinder in directional flow can be estimated using function of Re (Lindsey, 1938). Using this relationship the Cd would be 0.9. If this shore experienced directional flow, the evaluation of drag coefficient provided in Chapter 3 would be appropriate for refining this form drag value to account for the flexibility of the obstruction.

Since we are evaluating wave action, we will use the drag coefficient relationships established in Chapter 4. The KC value exceeds the maximum value used in the flume study, so we will calculate C_D using the Re relationship (Eq. 5.8) as discussed in chapter 4.

Re = (0.5358)(0.0042)/1e-6 = 2250

$$Re/Ln(E)/Ln(100000) = 2250/ln(5x10^8)/ln(100000) = 1293.25 \quad (5.8)$$

Equation 5.9 provides an exponential regression ($R^2 = 0.6288$) from the data used in Figure 4.13.

$$C_D = 6.3087e^{-0.001(Re/Ln(E)/Ln(100,000))} = 1.73 \quad (5.9)$$

The Mendez and Losada (2004) energy dissipation calculations discussed above can again be used to determine the wave height reduction resulting from the vegetation. Applying an individual C_D value to a network is consistent with the Mendez methodology, as network effects are considered to be additive. By using a C_D of 1.73 and N = 70, the wave height as a function of station can be obtained, as shown in Figure 5.3. A range of vegetation density values can be evaluated with this methodology along with the size of the vegetation field to determine the optimal vegetation planting. In this case, values of N = 50, N = 70, N = 100, N=200 were all evaluated and N = 70 stems per square meter were found to have an optimal impact on wave height. The RMS wave height is approximately 0.16 m at station 215. As shown in Table 5.3, the Shield's dimensionless bed shear is now less than the critical value. From Shields Criterion, we therefore conclude that soil particles are stable under these conditions, even when accounting for the sloping beach face. The vegetation is assumed to be established over a 20 meter field, starting 6 meters out from shore and extending into the lake.

To illustrate the difference between our and traditional design approaches, the wave heights as a function of station were also computed using the N = 70 and the drag coefficient for a rigid cylinder of $C_D = 0.9$. These wave heights are also shown in Figure 5.3. The RMS wave height is 0.22 m at station 215. Based on Shields Criterion, particle movement would occur for this condition. More vegetation would then be required for beach protection.

As discussed in chapter 4, the data suggests that larger drag coefficients occur at smaller Re values likely due to inertia effects. In this situation, this would result in the use of a "rigid cylinder" approximation to create a conservative design. In a situation where Re values exceed 3400, the rigid cylinder approximation would result in a non-conservative design and additional factors of safety would need to be incorporated to assure a stable shoreline.

This simple analysis does not consider wave reflections or refractions that may occur due the shoreline shape or bathymetric details. Other design tools are available that could be used initially to estimate wave conditions that may be occurring at a specific site. In addition, this analysis does not consider installation quality or other environmental factors that could affect the success of vegetation for erosion control, such as calm water plant establishment conditions, protection from consumption or disturbance from animals, adequate soil nutrients, or protection from ice damage.

These calculations demonstrate the evaluation of shoreline erosion using the information provided in this thesis. Additional data could be collected to refine our understanding and provide better parameters for shoreline erosion control designs.

Chapter 6
Conclusion

This thesis has advanced the understanding of shoreline erosion control using vegetation for inland lakes. While the vegetation species and experimental parameters were primarily focused on those found in Minnesota, many of the findings are relevant to other locations and scenarios.

Significant progress was made using a submergible torque sensor to measure drag response in an experimental flume. This sensor allowed for higher frequency data on single elements, which allowed for the determination of wave frequency and vegetal natural frequency influence on the drag occurring on the element. This sensor also allowed for the data needed to create a relationship between the modulus of elasticity and the drag occurring on the element in wave conditions. Using the torque sensor in a directional flow condition, we confirmed that the modulus of elasticity and Cauchy Number have an exponential relationship with the drag reduction and developed improved estimates of the parameters in these relationships. Keulegan-Carpenter and Reynolds numbers have been used in functional relationships for estimating drag coefficients in the literature previously. This thesis finds estimating drag coefficients is improved when the modulus of elasticity or Cauchy Number are incorporated into the relationship.

The vegetation plots provided new observations on how water level changes affect plant communities. While some data has been collected for individual species,

there are no studies looking at the plant communities using these species and these changes. These findings have shown us that *Bolboshoenus fluviatilis* and *Sparganuim eurycarpum* are capable of producing large amounts of biomass when subjected to water level changes and potentially could be good species for projects that need reliable erosion control. It is possible these same species could limit the biodiversity of the plant community due to their aggressive nature, so other species should be also used and possibly planted in greater frequency. Species that appear to not be well suited to establishing diversity in these plant communities with changing water levels include *Carex vulpinoidea* and *Carex lacustris*.

Vegetation responses observed in this research have also been seen in other studies with fewer species. These include inundation depth frequency and duration influence plant biomass production, placement of plants in restoration influence plant biomass production, *Carex* species are affected by inundation levels in a wet regime, *Carex lacustris* is sensitive to competition from other species, and wetter regimes result in lower diversity.

There is research in the literature that attempts to relate the element flexibility to an exponential modifier on the velocity, or Vogel exponent. This formulation requires the use of a reference velocity that also serves to keep the equation non-dimensional. While this thesis demonstrates that it is possible to use this formulation, it found that exponent value can be sensitive to the reference velocity. This thesis shows that it is more reliable to combine the calibration parameters into one reference velocity term, or

more simply to recognize that the drag modification occurs as an exponential function of the Cauchy Number, which is a function of the elastic modulus of the vegetation.

The examples presented demonstrate how the information provided in this thesis can be used to better mitigate shoreline erosion using vegetation. More information is now available to aid in the selection of vegetation species, with considerations for future climate, biomass competition, and diversity. A better understanding of the hydrodynamic forces acting on vegetation in currents and wave flow is also presented. Much of the previous work on vegetation used rigid surrogates for vegetation, and work with flexible obstructions demonstrates that flexibility plays a role in the value of hydrodynamic forces. Some simplified regressions and relationships have also been provided here to aid in the selection the drag coefficient with considerations for obstruction flexibility and wave frequency.

Future Research

Further research into two topics is needed. The experimental set up appears sound and able to accommodate many types of obstructions, and additional work with a variety of plant species would expand the understanding of the flexibility in species. Experiments using different networks of flexible obstructions could also provide further understanding of the wake effects of flexible vegetation and how it is different from rigid elements.

Creating a reliable engineered design with vegetation also requires an understanding of how the established vegetation may change throughout the growing

season. A vegetative growth model with parameters for water inundation stressors would help provide a predictive tool to better assess erosion on shorelines.

References

Chapter 1 References

Intergovernental Panel on Climate Change (IPCC). (2007) Synthesis Report, Fourth Assessment Report, IPCC Plenary XXVII, Valencia Spain, November 2007.

Komar, P.D., (1998) *Beach Processes and Sedimentation*, 2nd ed., 544 pp., Simon and Schuster, Upper Saddle River, N.J.

NOAA, (2014) http://oceanservice.noaa.gov/facts/shorelength.html

NOAA, (2013a) http://stateofthecoast.noaa.gov/population/welcome.html

NOAA, (2013b) http://oceanservice.noaa.gov/facts/oceanfacts.php/oceanorsea.html

U.S. Army Corps of Engineers. (2002) Coastal Engineering Manual. Engineering Manual 1110-2-1100, U.S.Army Corps of Engineers, Washington, D.C. (in 6 volumes).

Wilcox, D.A., and J.C. Meeker. (1992) Implications for faunal habitat related to altered macrophyte structure in regulated lakes in northern Minnesota. Wetlands 12:192-203

Chapter 2 References

Bailey-Serres, J., and L.Voesenek. (2008) Flooding Stress: Acclimations and Genetic Diversity. *Annual Review of Plant Biology*. 59:313-339.

Blom, K., and L. Voesenek. (1996) Flooding: the survival strategies of plants. *TREE* Vol. 11, no. 7, July.

Budelsky, R., and S. Galatowitsch. (2000) Effects of water regime and competition on the establishment of a native sedge in restored wetlands. *Journal of Applied Ecology*, 37:971-985.

Bunn, S.E., and A.H. Arthington. (2002) Basic Principles and Ecological Consequences of Altered Flow Regimes for Aquatic Biodiversity. *Environmental Management* Vol. 30, No. 4, pp. 402-507.

Casanova, M.T., and M.A. Brock. (2000) How do depth, duration and frequency of flooding influence the establishment of wetland plant communities? *Plant Ecology* 147: 237-250.

Flora of North America: http://fna.huh.harvard.edu/

Galatowitsch, S.M., N.O.Anderson, and P.D. Ascher. (1999) Invasiveness in Wetland Plants in Temperate North America. *Wetlands*, Vol.19, No. 4, pp. 733-755.

Henderson, C.L., C.J. Dindorf, and F.J. Rozumalski. (1999) *Lakescaping for wildlife and water quality*, Minnesota Department of Natural Resources, Nongame Wildlife Program, Section of Wildlife, St. Paul.

Intergovernmental Panel on Climate Change (IPCC). (2007) Synthesis Report, Forth Assessment Report, IPCC Plenary XXVII, Valencia Spain, November 2007.

Kent, M. and P. Corker.(1992) *Vegetation description and analyses: a practical approach*. CRC Press.

Kirkman, L.K., and R.R. Sharitz. (1992) Growth in controlled water regimes of three grasses common in freshwater wetlands of the southeastern USA. *Aquatic Botany*, 44:345-359.

Liukkonen, B. (2012) Adapting Minnesota Shoreland Best Management Practices for Climate Change. Minnesota Pollution Control Agency Clean Water Act 319 Grant Final Report, April 13, 2012.

Montgomery. (1997) *Design and Analysis of Experiments*. John Wiley and Sons, New York.

Nielsen, D.L., and A.J. Chick. (1997) Flood-mediated changes in aquatic macrophyte community structure *Marine Freshwater Research* Vol. 48 153-157.

Miller, R.C., and J.B. Zedler. (2003) Responses of native and invasive wetland plants to hydroperiod and water depth. *Plant Ecology* vol. 167 1:57-69.

Minnesota Department of Transportation. (2005) Standard Specifications for Construction.

Seabloom, E.W., A.G. Van der Valk, and K.A. Moloney. (1998) The role of water depth and soil temperature in determining initial composition of wetland coenoclines. Plant Ecology, 138, 203-216.

Squires, L., and A.G. van der Valk. (1992) Water-depth tolerances of the dominant emergent macrophytes of the Delta Marsh, Manitoba. *Can. J. Bot*. 70:1860-1867.

United States Department of Agriculture (USDA). (1996) Chapter 16: Streambank and Shoreline Protection, Engineering Field Handbook Part 650.

Vanderbosch, D.A., and S.M. Galatowitsch. (2010) An assessment of lakeshore restorations in the Minneapolis/St.Paul Metropolitan Area. Ecol Restor 28:71-80.

Vanderbosch, D.A., and S.M. Galatowitsch. (2011) Factors affecting the establishment of Schoenoplectus tabernaemontani (C.C.Gmel.) Palla in urban lakeshore restorations. *Wetlands Ecol Management*, 19:35-45.

Visser, E., K. Blom, and L. Voesenek. (1996) Flooding-induced adventitious rooting in Rumex: Morphology and development in an ecological perspective ACTA BOTANICA NEERLANDICA Vol. 45 1:17-28, March.

Webb, J.A., E.M. Wallis, and M.J. Stweardson. (2012) A systematic review of published evidence linking wetland plants to water regime components. *Aquatic Botany* article in press.

Wilcox, D.A., and J.C. Meeker. (1992) Implications for faunal habitat related to altered macrophyte structure in regulated lakes in northern Minnesota. Wetlands 12:192-203.

Wilson, S.D., and P.A. Keddy. (1988) Species Richness, Survivorship, and Biomass Accumulation along an Environmental Gradient. *Oikos*, Vol. 53 No. 3: 375-380.

Yetka, L.A., and S.M. Galatowitsch. (1999) Factors Affecting Regevation of Carex lacustris nad Carex stricta from Rhizomes. *Restoration Ecology* Vol.7 No.2:162-171.

Chapter 3 References

Aberle, J., and A. Dittrich, (2012), An experimental study of drag forces acting on flexible plants, Proc. Int. Conf. River Flow 2012, San Jose, Costa Rica, 193-200, R.E. Murillo Munoz, ed. Taylor & Francis, London, UK.

Aberle, J., and J. Järvelä (2013), Flow resistance of emergent rigid and flexible floodplain vegetation, J. of Hyd. Res. 51:1, 33-45.

Augustin, L.N., J.L. Irish, and P. Lynett, (2009), Laboratory and Numerical Studies of Wave Damping by Emergent and Near-Emergent Wetland Vegetation, Coastal Engineering, 56, 332-340

Bouma, T.J., M.B. DeVries, and P.M.J. Herman, (2010), Comparing ecosystem engineering efficiency of two plant species with contrasting growth strategies, Ecology, 91(9) pp.2696-2704

Chapman, J.A., M.M. Blickenderfer, B.N. Wilson, J.S. Gulliver, and S.S. Missaghi, (2013), Competition and Growth of Eight Shoreline Restoration Species in Changing Water Level Environments, Ecological Restoration, Vol. 31, No.4.

Chapman, J.A., J.S. Gulliver, B.N. Wilson, (2014), Flume Instrumentation for Measurement of Drag on Flexible Elements in Wave Flow, Experiments in Fluids, 55:1715 DOI 10.1007/s00348-014-1715-7

Chen, L., M. Stone, K. Acharya, K.A. Steinhaus, (2011), Mechanical analysis for emergent vegetation in flowing fluids, J. of Hydraulic Research, 49:6, 766-774, DOI: 10.1080/00221686.2011.621359

de Langre, E., (2008), Effects of Wind on Plants, Annu. Rev. of Fluid Mechanics 40:141-68

de Langre, E., (2011), Methodological advances in predicting flow-induced dynamics of plants using mechanical-engineering theory, J. of Experimental Biology 215,914-921

Duan, J.G., B. Barkdoll, R. French, (2006), Lodging Velocity for an Emergent Aquatic Plant in Open Channels, J. of Hydraulic Engineering, Vol 132, No. 10, DOI:10.1061/(ASCE)0733-9429(2006)132:10(1015)

Finnigan, J., (2000), Turbulence in Plant Canopies, Annu. Rev. Fluid Mech. 32:519-571

Ghisalberti, M., and H. Nepf , (2006), The structure of the shear layer in flows over rigid and flexible canopies, Env. Fluid Mech., 6:277-301

Gosselin, F.P., and E. de Langre, (2011), Drag reduction by reconfiguration of a poroelastic system, J. of Fluids and Structures.

Gerchenfeld, N.A. and A.S. Weigend, (1993), The future of time series: Learning and understanding. In Time Series Prediction: Forecasting the Future and Understanding the Past. Eds. Weigend and Gershenfeld, SFI Studies in the Sciences of Complexity, Proc Vol XV, Addison-Wesley.

Hibbler, R.C., (1991), Mechanics of materials, Macmillan Publishing, New York.

Järvelä, J. (2004), Determination of flow resistance caused by non-submerged woody vegetation, Int. J. River Basin Manag. 2:1, 61-70.

Kothyari, U.C., K. Hayashi, and H. Hashimoto, (2009), Drag coefficient of unsubmerged rigid vegetation stems in open channel flows, J. Hydraulic Res. 47(6), 691-699.

Lindsey, W.F., (1938), Drag of Cylinders of Simple Shapes, NACA Report*, 619*

Nepf, H.M., (1999), Drag, Turbulence, and Diffusion in Flow Through Emergent Vegetation, Water Resources Research, Vol. 35, No. 2, P 479-489.

Nezu, I., and M. Sanjou, (2008), Turbulence structure and coherent motion in vegetated canopy open-channel flows, J. of Hydro-environment Res., 2:62-90

Niklas, K.J., (1991), The elastic moduli and mechanics of populous tremuloides (salicaceae) petioles in bending and torsion, Amer. J. of Bot. 78(7): 989-996

Niklas, K. J. (1992), Plant Biomechanics: An Engineering Approach to Plant Form and Function, University of Chicago Press.

Poggi, D., A. Porporato, L. Ridolfi, J.D. Albertson, and G.G. Katul, (2004), The effect of vegetation density on canopy sub-layer turbulence, Boundary-Layer Meteogology, 111: 565-587

Prandtl, L., and O. Tietjens, (1934), Applied Hydro-&Aeromechanics, J. P. den hartog, Dover New York Vol. II.

Robertson, J.A., and C.T. Crowe, (1993), Engineering Fluid Mechanics 5th ed. Houghton Mifflin

Schoneboom, T., J. Aberle, and A. Dittrich, (2010), Hydraulic resistance of vegetated flows: Contribution of bed shear stress and vegetative drag to total hydraulic resistance, River Flow Dittrich, Koll, Aberle and Geisenhainer (ed.) ISBN 978-3-939230-00-7

Schoneboom, T., J. Aberle, and A. Dittrich, (2011), Spatial variability, mean drag forces, and drag coefficients in an array of rigid cylinders, Experimental methods in hydraulic research, geoplanet: earth and planetary sciences. Vol. 1, 255-265, P. Rowinski, ed. Springer, Berlin.

Speck, O., and H. Spatz, (2004), Damped oscillations of the giant reed *Arundo donax* (Poaceae), Am. J. Bot. 91:789-796.

Stephan, U., D. Gutknecht, (2002), Hydraulic resistance of submerged flexible vegetation, Journal of Hydrology, 269 27-43

Tanino, Y., and H.M. Nepf, (2008), Laboratory investigation of mean drag in a random array of rigid emergent cylinders, J. Hydraulic Eng. 134(1), 34-41.

United States Department of Agriculture (USDA) (1996), Engineering Field Handbook Part 650, Chapter 16: Streambank and Shoreline Protection.

Vogel, S. (1989), Drag and Reconfiguration of Broad Leaves in High Winds, J. of Experimental Botany, Vol.40, No. 217, 941-948.

Vollsinger, S., S.J. Mitchell, K.E. Byrne, M.D. Novak, and M. Rudnicki, (2005), Wind tunnel measurements of crown streamlining and drag relationships for several hardwood species, Can. J. Forest Res., 35:1238-1249.

Wallerstein, N.P., C.V.Alonso, S.J. Bennett, C.R.Thorne, (2002), Surface Wave Forces Acting on Submerged Logs, J. of Hydraulic Engineering, Vol. 128, No. 3, DOI:10.1061/(ASCE)0733-9429(2002)128:3(349)

Wilcox, D.A., and J.C. Meeker, (1992), Implications for faunal habitat related to altered macrophyte structure in regulated lakes in northern Minnesota, Wetlands 12:192-203.

Wilson, C.A.M.E., (2007), Flow resistance models for flexible submerged vegetation, J. of Hydrology, 342, 213-222

Wilson, C.A.M.E., J.Hoyt, I. Schnauder, (2008), Impact of Foliage on the Drag Force of Vegetation in Aquatic Flows, J. of Hydraulic Engineering, Vol. 134, No. 7, DOI: 10.1061/(ASCE)0733-9429(2008)134:7(885)

Wunder, S., B. Lehmann, and F. Nestmann, (2009), Measuring drag force of flexible vegetation directly: Development of an experimental methodology, 33rd International Association of Hydraulic Engineering & Research Congress: Water Engineering for a Sustainable Environment

Yang, W., S. Choi, (2010), Impact of stem flexibility on mean flow and turbulence structure in depth-limited open channel flows with submerged vegetation, J. of Hydraulic Research, 47:4, 445-454, DOI: 10.1080/00221686.2009.9522020

Chapter 4 References

Augustin LN, Irish JL, Lynett P, (2009) Laboratory and Numerical Studies of Wave Damping by Emergent and Near-Emergent Wetland Vegetation. Coastal Engineering, 56, 332-340

Bouma TJ, DeVries MB, Herman PMJ, (2010) Comparing ecosystem engineering efficiency of two plant species with contrasting growth strategies. Ecology, 91(9) pp.2696-2704

Bradley K, Houser C, (2009) Relative velocity of seagrass blades: Implications for wave attenuation in low-energy environments. J. of Geophys. Res. 114

Chapman JA, Blickenderfer MM, Wilson BN, Gulliver JS, Missaghi SS, (2013) Competition and Growth of Eight Shoreline Restoration Species in Changing Water Level Environments. Ecological Restoration, Vol. 31, No.4

Chen Q, Zhao H, (2012) Theoretical Models for Wave Energy Dissipation Caused by Vegetation. ASCE J. of Engineering Mechanics, 138:2221-229

Dalrymple RA, Kirby JT, Hwang PA, (1984) Wave Diffraction Due to Areas of Energy Dissipation. J. of Waterways, Port, Coastal, and Ocean Engineering, Vol. 110, No. 1, February

Dean RG, (1978) Effects of vegetation on shoreline erosional processes. Wetland functions and values: The state of our understanding. Proc., National Symp. on Wetlands, P. E. Greeson, J. R. Clark, and J. E. E. Clark, eds., American Water Resources Association, Lake Buena Vista, FL, 415–426

Dean RG, Bender CJ, (2006) Static wave setup with emphasis on damping effects by vegetation and bottom friction. Coastal Eng., 53(2–3), 149–156

Devore JL, (2001) Probability and Statistics for Engineering and Sciences. Duxbury Press, New York.

Dubi A, Torum A, (1995) Wave damping by kelp vegetation. Proceedings of the 24th Coastal Engineering Conference. ASCE, B.L.Edge editor, New York, pp. 142-156

Elwany MHS, Flick RE, (1996) Relationship between kelp beds and beach width in Southern California. J. of Waterways Ports Coastal Engineering, 122(1) 34-37

Elwany MHS, O'Reilly WC, Guza RT, Flick RE, (1995) Effects of Southern California kelp beds on waves. J. of Waterways Ports Coastal Engineering, 121(2) 143-150

Finnigan J, (2000) Turbulence in Plant Canopies, Annu. Rev. Fluid Mech. 32:519-571

Flocard F, Finnigan TD, (2009) Experimental investigation of power capture from pitching point absorbers. Proceedings 8th European Wave and Tidal Energy Conference, Uppsala, Sweden

Fonseca MS, Cahalan JA, (1992) A preliminary evaluation of wave attenuation for four species of seagrass. Estuarine Coastal Shelf Sci., 35(6), 565–576

Fonseca MS, Fisher JS, Zieman JC, Thayer GW, (1982) Influence of the seagrass, Zostera marina, on current flow. Estuarine Coastal Shelf Sci., 15(4), 351–364

Fox J, Weisberg S, (2011) An R Companion to Applied Regression, Second Edition, Sage. https://r-force.r-project.org/projects/car/

Gabbi RD, Benaroya H, (2005) An overview of modeling and experiments of vortex-induced vibration of circular cylinders. Journal of Sound and Vibration 282: 575-616

Gacia E, Duarte CM, (2001) Sediment retention by a Mediterranean Posidonia oceanica meadow: the balance between deposition and resuspension. Estuar. Coast. Shelf Sci. 52,505-514

Ghisalberti M, Nepf H, (2006) The structure of the shear layer in flows over rigid and flexible canopies. Env. Fluid Mech., 6:277-301

Hibbler RC, (1991) Mechanics and Materials, Macmillan Publishing ISBN 0-02-354451-1

Ibanez F, Grosjean P, Etienne M, (2013) Regulation, decomposition and analysis of space-time series. http://www.sciviews.org/pastecs

Ifuku M, Hayashi H, (1998) Development of eelgrass Zostera marina bed utilizing sand drift control mats, Coast. Eng. J. 40(3) 223-239

Kobayashi N, Raichle AW, Asano T, (1993) Wave attenuation by vegetation. J. Waterw. Port Coastal Ocean Eng., 119(1), 30–48

Li CW, Yan K, (2007) Numerical Investigation of Wave-Current-Vegetation Interaction. ASCE Journal of Hydraulic Engineering, 133:794-803

Lindsey WF, (1938) Drag of Cylinders of Simple Shapes. NACA Report, 619

Mendez FJ, Losada IJ, Losada MA, (1999) Hydrodynamics induced by wind waves in a vegetation field. J. Geophys. Res., 104(C8), 18383–18396

Mendez FJ, Losada IJ, (2004) An Empirical Model to Estimate the Propagation of Random Breaking and Nonbreaking Waves Over Vegetation Fields. Coastal Engineering 51 103-118

Möller I, Spencer T, French JR, (1996) Wind wave attenuation over saltmarsh surfaces: preliminary results from Norfolk England. J. Coast. Res. 12(4), 1009-1016

Möller I, Spencer T, French JR, Leggett D, Dixon M, (1999) Wave transformation over salt marshes: A field and numerical modeling study from North Norfolk, England. Estuarine Coastal Shelf Sci., 49(3), 411–426

Morison JR, Johnson JW, O'Brien MP, Schaaf SA, (1950) The Forces Exerted by Surface Waves on Piles. Petroleum Transactions, American Institute of Mining Engineers, Vol. 189, pp.145-154

Mork M, (1996) Wave attenuation due to bottom vegetation. Waves and Nonlinear Processes in Hydrodynamics, Kluwer Academic Publishing, Oslo, Norway, pp. 371-382

Mullarney JC, Henderson SM, (2010) Wave-forced motion of submerged single-stem vegetation. J. Geophys. Res., 115

Nepf HM, (1999) Drag, Turbulence, and Diffusion in Flow Through Emergent Vegetation. Water Resources Research, Vol. 35, No. 2, P 479-489

Nezu I, and Sanjou M, (2008) Turbulence structure and coherent motion in vegetated canopy open-channel flows. J. of Hydro-environment Res., 2:62-90

Niklas KJ, (1991) The elastic moduli and mechanics of populous tremuloides (salicaceae) petioles in bending and torsion. Amer. J. of Bot. 78(7): 989-996

Niklas KJ, (1992) Plant Biomechanics: An Engineering Approach to Plant Form and Function. University of Chicago Press.

Ota T, Kobayashi N, Kirby JT, (2005) Wave and current interactions with vegetation. Proc,. 29th Int. Conf. Coastal Engineering 2004, ASCE, Reston, Va., 508–520.

Pasternack GB, Ellis CR, Marr JD, (2007) Jet and hydraulic jump near-bed stresses below a horseshoe waterfall. Water Resources Research, 43, W07449, doi:10.1029/2006WR005774

Paul M, Amos CL, (2011) Spatial and seasonal variation in wave attenuation over Zostera noltii. J. Geophys. Res., 116, C08019, doi:10.1029/2010JC006797.

Peterson C H, Luettich R A Jr., Michelli F, Skilleter GA, (2004) Attenuation of water flow inside seagrass canopies of differing structure. Mar. Ecol. Prog. Ser., 268, 81–92.

Penning WE, Raghuraj R, Mynett AE, (2009) The Effects of Macrophyte Morphology and Patch Density on Wave Attenuation. Proceedings of the 7th ISE and 8th HIC, Concepcion, Chile.

Poggi D, Porporato A, Ridolfi L, Albertson JD, Katul GG, (2004) The effect of vegetation density on canopy sub-layer turbulence. Boundary-Layer Meteogology, 111: 565-587

Pope SB, (2000) Turbulent Flows, Cambridge University Press.

RDCT (R Development Core Team). (2011) R: A language and environment for statistical computing, v. 2.14.1, R Foundation for Statistical Computing, Vienna, Austria. https://r-force.r-project.org

Sarpaka T, (1979) Vortex induced oscillations: a selective review. Journal of Applied Mechanics 46(2) 241-258

Sarpaka T, and Isaacson M, (1981) Mechanics of Wave Forces on Offshore Structures. Van Nostrand Reinhold Company, New York.

Schoneboom T, and Aberle J, (2009) Influence of foliage on drag force of flexible vegetation. 33rd IAHR Congress Proceedings: Water Engineering for a Sustainable Environment

Sorensen RM, (2006) Basic Coastal Engineering. Springer

Stratigaki V, Manca E, Prinos P, Losada I, Lara J, Sclavo M, Caceres I, Sanchez-Arcilla A, (2009) Large Scale experiments on wave propagation over Posidonia oceanica. Proceedings 33rd IAHR Congress: Water Engineering for a Sustainable Environment

United States Army Corps of Engineers (USACE), (2006) Waves in Seagrass Systems: Review and Technical Recommendations. ERDC TR-06-15

U.S. Environmental Protection Agency, America's Wetlands, July 2007

Venables WN, and Ripley BD, (2002) Modern Applied Statistics with S. Springer, New York, New York, fourth edition.

Wunder S, Lehmann B, Nestmann F, (2009) Measuring drag force of flexible vegetation directly: Development of an experimental methodology. 33rd International Association of Hydraulic Engineering & Research Congress: Water Engineering for a Sustainable Environment

Chapter 5 References

Lindsey, W.F., (1938) Drag of Cylinders of Simple Shapes, NACA Report, 619

Mendez, F.J., and I.J. Losada, (2004) An Empirical Model to Estimate the Propafation of Random Breaking and Non-Breaking Waves over Vegetation Fields. Coastal Engineering 51 103-118.

Shields, A., (1936) Anwendung der Aehnlichkeitsmechanik und der Turbulenzforschung auf die Geschiebebewegung [Application of similarity mechanics and turbulence research

on shear flow]. Mitteilungen der Preußischen Versuchsanstalt für Wasserbau (in German) 26. Berlin: Preußische Versuchsanstalt für Wasserbau.

U.S. Army Corps of Engineers. (2002) Coastal Engineering Manual. Engineering Manual 1110-2-1100, U.S.Army Corps of Engineers, Washington, D.C. (in 6 volumes).

Young, I.R., and L.A. Verhagen, (1996) The Growth of fetch limited waves in water of finite depth. Part 1. Total energy and peak frequency, Coastal Engineering 29, 47-48

Appendix A

Vegetation Growth Data

Explanation of Data

The following data was collected in 2010 in outdoor basins planted at the University of Minnesota St. Anthony Falls Laboratory. Four basins were used, labeled as A, B, C, and D. Water regimes for each basin were:

A = wet,
B = Dry,
C = Fluctuating or Climate change, and
D = normal.

Plants were placed according to a grid system, with rows 1 to 14 running across the sloping bed with row 1 being the wettest and row 14 being the driest and columns A to P running down the sloping bed. The species planted are indicated by two letter abbreviations where:

RB = *Bolboschoenus fluviatilis* (River bulrush)
GB = *Sparganium eurycarpum* (Giant bur-reed)
SB = *Schoenoplectus tabernaemontani* (Softstem bulrush)
LS = *Carex lacustris* (Lake sedge)
FS = *Carex vulpinoidea* (Fox sedge)
BB = *Carex comosa* (Bottlebrush sedge)
PC = *Spartina pectinata* (Prairie cordgrass)
CR = *Juncus effusus* (Common rush)

Biomass harvested is reported in grams, plant height is reported in cm, and plant diameter extremes (large and small) are reported in cm.

						2010 All Biomass values in g									All measurements in CM							
						Bioma	Bioma	Bioma	Bioma	Bioma	Bioma	Bioma	Bioma	Biomass								
Row	Column Letter	Trial	Column	Basin	Species	RB	GB	SB	LS	FS	BB	PC	CR	sum	June Leaf Height	July Leaf Height	August Leaf Height	September Leaf Height	July, Bulrush D (L)	July, Bulrush D (S)	August, Bulrush D (L)	August, Bulrush D (S)
1	A	1	1	A	RB	138								138	49	119	133	153				
1	B	1	2	A	SB			39						39	56	144	171	203	0.9	0.2	0.9	0.3
1	C	1	3	A	GB		232							232	49	98	167	186				
1	D	1	4	A	LS				0					0	46	81	115					
1	E	2	5	A	LS				10					10	64	81	103	122				
1	F	2	6	A	RB	73								73	40	90	114	153				
1	G	2	7	A	SB			30						30	42	112	141	163	0.4	0.2	0.6	0.3
1	H	2	8	A	GB		115							115	45	87	153	174				
1	I	3	9	A	SB			25						25	41	106	166	176	0.4	0.2	0.5	0.2
1	J	3	10	A	LS				0					0	61	95	0	58				
1	K	3	11	A	RB	75								75	37	93	126	145				
1	L	3	12	A	GB		135							135	47	107	154	196				
1	M	4	13	A	RB	49								49	34	97	136	142				
1	N	4	14	A	GB		55							55	44	81	126	156				
1	O	4	15	A	SB			28						28	42	113	135	165	0.4	0.3	0.6	0.2
1	P	4	16	A	LS				9					9	54	98	128	100				
2	A	1	1	A	SB			21						21	58	107	154	158	0.6	0.2	0.6	0.2
2	B	1	2	A	GB		307							307	48	100	163	188				
2	C	1	3	A	LS				8					8	56	83	119	148				
2	D	1	4	A	RB	130								130	37	88	150	120				
2	E	2	5	A	GB		127							127	42	85	164	180				
2	F	2	6	A	SB			7						7	24	82	160	180	0.3	0.2	0.9	0.3
2	G	2	7	A	RB	132								132	46	102	152	135				
2	H	2	8	A	LS				0					0	67	79	0					
2	I	3	9	A	RB	41								41	39	80	129	117				
2	J	3	10	A	SB			11						11	22	86	123	184	0.3	0.2	0.6	0.5
2	K	3	11	A	LS				0					0	58	85	0					
2	L	3	12	A	GB		97							97	26	87	147	197				
2	M	4	13	A	GB		146							146	54	117	143	199				
2	N	4	14	A	SB			26						26	47	107	126	188	0.4	0.1	0.4	0.2
2	O	4	15	A	RB	49								49	33	91	134	130				
2	P	4	16	A	LS				0					0	59	92	0	10*				
3	A	1	1	A	LS				19					19	57	100	138	144				
3	B	1	2	A	SB			40						40	37	98	159	172	0.5	0.2	0.8	0.4
3	C	1	3	A	RB	139								139	44	91	155	151				
3	D	1	4	A	GB		254							254	51	103	168	190				
3	E	2	5	A	RB	148								148	26	80	135	171				
3	F	2	6	A	SB			36						36	45	112	160	205	0.6	0.2	0.7	0.4
3	G	2	7	A	LS				5					5	58	77	115	134*				
3	H	2	8	A	GB		252							252	51	104	161	208				
3	I	3	9	A	SB			27						27	44	96	127	172			0.6	0.2
3	J	3	10	A	RB	34								34	34	83	140	129	0.6	0.1		
3	K	3	11	A	GB		231							231	55	98	155	191				
3	L	3	12	A	LS				8					8	51	79	137	140*				
3	M	4	13	A	RB	66								66	52	99	143	189				
3	N	4	14	A	GB		221							221	48	96	149	184				
3	O	4	15	A	LS				9					9	51	89	113	145*				
3	P	4	16	A	SB			30						30	35	105	137	163	0.5	0.2	0.6	0.4
4	A	1	1	A	SB			33						33	37	121	169	174	0.8	0.2	0.8	0.4
4	B	1	2	A	RB	81								81	40	97	141	142				
4	C	1	3	A	GB		155							155	49	92	153	191				
4	D	1	4	A	LS				0					0	18	0	0					
4	E	2	5	A	SB			24						24	45	101	153	130			0.7	0.3
4	F	2	6	A	GB		259							259	48	93	173	204	0.6	0.2		
4	G	2	7	A	LS				13					13	68	85	143	148				
4	H	2	8	A	RB	139								139	37	89	157	174				
4	I	3	9	A	RB	102								102	34	89	132	160				

						2010	All Biomass values in g									All measurements in CM							
						Bioma	Bioma	Bioma	Bioma	Bioma	Bioma	Bioma	Bioma	Biomass									
Row	Column Letter	Trial	Column	Basin	Species	RB	GB	SB	LS	FS	BB	PC	CR	sum	June Leaf Height	July Leaf Height	August Leaf Height	September Leaf Height	July, Bulrush D (L)	July, Bulrush D (S)	August, Bulrush D (L)	August, Bulrush D (S)
4	J	3	10	A	LS				0					0	55	69	0					
4	K	3	11	A	SB			11						11	41	92	130	148	0.5	0.1	0.6	0.3
4	L	3	12	A	GB		147							147	42	93	145	170				
4	M	4	13	A	GB		103							103	51	94	164	185				
4	N	4	14	A	SB			12						12	43	98	130	150	0.6	0.2	0.7	0.2
4	O	4	15	A	LS				7					7	66	88	115	83				
4	P	4	16	A	RB	113								113	35	87	127	92				
5	A	1	1	A	RB	127								127	42	101	130	119				
5	B	1	2	A	LS				21					21	76	91	129	151				
5	C	1	3	A	SB			16						16	40	90	147	200	0.5	0.2	0.6	0.3
5	D	1	4	A	GB		207							207	46	90	160	201				
5	E	2	5	A	LS				10					10	53	60	103	110*				
5	F	2	6	A	SB			20						20	37	101	153	189	0.6	0.1	0.7	0.3
5	G	2	7	A	RB	104								104	41	88	134	140				
5	H	2	8	A	GB		114							114	50	93	157	200				
5	I	3	9	A	SB			30						30	51	109	160	198	0.6	0.2	0.7	0.2
5	J	3	10	A	GB		248							248	43	92	157	197				
5	K	3	11	A	RB	63								63	23	72	128	135				
5	L	3	12	A	LS				0					0	59	62	101					
5	M	4	13	A	RB	111								111	32	88	130	123				
5	N	4	14	A	LS				5					5	58	69	0					
5	O	4	15	A	GB		149							149	51	80	137	154				
5	P	4	16	A	SB			26						26	27	87	138	147	0.4	0.2	0.6	0.2
6	A	1	1	A	LS				8					8	36	83	137	135				
6	B	1	2	A	SB			49						49	44	93	158	185	0.8	0.1	0.8	0.4
6	C	1	3	A	GB		213							213	61	94	160	184				
6	D	1	4	A	RB	88								88	46	77	125	120				
6	E	2	5	A	LS				2					2	55	70	105	122				
6	F	2	6	A	GB		122							122	50	82	144	177				
6	G	2	7	A	SB			6						6	8	84	124	140			0.6	0.2
6	H	2	8	A	RB	84								84	46	85	142	128				
6	I	3	9	A	RB	54								54	47	98	150	155				
6	J	3	10	A	SB			30						30	49	96	140	130	0.5	0.2	0.4	0.3
6	K	3	11	A	GB		259							259	52	90	151	185				
6	L	3	12	A	LS				4					4	36	64	118	123				
6	M	4	13	A	LS				0					0	43	45	0					
6	N	4	14	A	GB		134							134	50	83	127	163				
6	O	4	15	A	RB	49								49	33	76	121	130				
6	P	4	16	A	SB			28						28	59	104	140	144	0.5	0.2	0.6	0.3
7	A	1	1	A	RB	129								129	42	89	109	123				
7	B	1	2	A	GB		212							212	39	83	142	178				
7	C	1	3	A	SB			86						86	46	97	138	177	0.9	0.1	0.8	0.2
7	D	1	4	A	LS				20					20	53	72	118	134				
7	E	2	5	A	RB	109								109	35	84	113	136				
7	F	2	6	A	GB		164							164	50	83	143	162				
7	G	2	7	A	LS				23					23	64	60	110	125				
7	H	2	8	A	SB			64						64	49	109	139	175	0.9	0.2	0.9	0.4
7	I	3	9	A	GB		158							158	57	83	149	163				
7	J	3	10	A	RB	68								68	35	70	138	148				
7	K	3	11	A	LS				17					17	76	70	123	127				
7	L	3	12	A	SB			74						74	34	96	144	184			0.7	0.3
7	M	4	13	A	GB		163							163	43	89	147	164				
7	N	4	14	A	RB	39								39	48	76	107	111				
7	O	4	15	A	SB			55						55	50	83	134	149	0.5	0.2	0.8	0.2
7	P	4	16	A	LS				16					16	66	91	115	115				
8	A	1	1	A	FS	63	87			0				150	47	41	0					
8	B	1	2	A	BB						43			43	50	50	88	100				
8	C	1	3	A	PC							12		12	33	70	101					
8	D	1	4	A	CR								19	19	53	49	76	92	0.2	0.1	0.2	0.1
8	E	2	5	A	CR	51	21	7					33	112	45	56	78	85	0.2	0.1	0.2	0.1

						2010	All Biomass values in g									All measurements in CM							
						Bioma	Bioma	Bioma	Bioma	Bioma	Bioma	Bioma	Bioma	Biomass									
Row	Column Letter	Trial	Column	Basin	Species	RB	GB	SB	LS	FS	BB	PC	CR	sum	June Leaf Height	July Leaf Height	August Leaf Height	September Leaf Height	July, Bulrush D (L)	July, Bulrush D (S)	August, Bulrush D (L)	August, Bulrush D (S)
8	F	2	6	A	BB						0			0	31	40	0					
8	G	2	7	A	FS					0				0	25	21	0					
8	H	2	8	A	PC							6		6	36	52	99	100				
8	I	3	9	A	PC	65	91					0		156	36	40	60	93				
8	J	3	10	A	CR								59	59	61	61	86	88	0.2	0.1	0.2	0.1
8	K	3	11	A	FS					0				0	28	35	0					
8	L	3	12	A	BB						11			11	45	50	78	90				
8	M	4	13	A	FS	29				0				29	25	21	0					
8	N	4	14	A	PC							4		4	47	41	66	64				
8	O	4	15	A	CR								6	6	48	56	0	142	0.2	0.1		
8	P	4	16	A	BB						18			18	60	59	92	101				
9	A	1	1	A	CR	47	96						37	180	54	66	81	98	0.2	0.1	0.2	0.1
9	B	1	2	A	FS					0				0	43	42	0					
9	C	1	3	A	BB						0			0	42	28	0					
9	D	1	4	A	PC							6		6	22	47	95	100				
9	E	2	5	A	PC	72						12		84	23	63	102	100				
9	F	2	6	A	CR								41	41	59	61	80	99	0.2	0.1	0.2	0.1
9	G	2	7	A	FS					0				0	24	26	0					
9	H	2	8	A	BB						9			9	41	46	76	89				
9	I	3	9	A	FS	20	21			0				41	33	42	0					
9	J	3	10	A	BB						0			0	47	44	77	76				
9	K	3	11	A	CR								19	19	44	49	75	79	0.2	0.1	0.3	0.1
9	L	3	12	A	PC							11		11	52	76	117	123				
9	M	4	13	A	PC	5						3		8	34	40	90	103				
9	N	4	14	A	BB						11			11	59	47	75	76				
9	O	4	15	A	FS					0				0	30	24	0					
9	P	4	16	A	CR								14	14	54	66	64	72	0.2	0.1	0.2	0.1
10	A	1	1	A	BB	27	18				82			127	51	59	94	112				
10	B	1	2	A	CR								52	52	52	52	81	88	0.2	0.1	0.3	0.1
10	C	1	3	A	PC							8		8	26	57	103	114				
10	D	1	4	A	FS					0				0	19	27	0					
10	E	2	5	A	FS	12				0				12	29	41	0					
10	F	2	6	A	BB						59			59	62	50	83	99				
10	G	2	7	A	CR								73	73	48	59	79	103	0.2	0.1	0.3	0.1
10	H	2	8	A	PC							7		7	23	53	103	101				
10	I	3	9	A	CR	6							62	68	54	54	75	86	0.2	0.1	0.3	0.1
10	J	3	10	A	FS					0				0	26	38	0					
10	K	3	11	A	BB						0			0	46	43	0	35				
10	L	3	12	A	PC							5		5	54	64	72	84				
10	M	4	13	A	CR								18	18	52	52	70	81	0.2	0.1	0.2	0.1
10	N	4	14	A	PC							8		8	35	44	78	110				
10	O	4	15	A	FS					0				0	27	30	0					
10	P	4	16	A	BB						58			58	65	60	91	99				
11	A	1	1	A	PC	14	3					12		29	30	64	99	100				
11	B	1	2	A	FS					0				0	32	44	0					
11	C	1	3	A	BB						0			0	33	21	0					
11	D	1	4	A	CR								76	76	52	56	75	85	0.3	0.1	0.3	0.1
11	E	2	5	A	BB						15			15	53	34	80	85				
11	F	2	6	A	CR								73	73	52	58	74	85	0.3	0.1	0.3	0.1
11	G	2	7	A	PC							7		7	32	50	92	102				
11	H	2	8	A	FS					0				0	31	41	0					
11	I	3	9	A	FS					0				0	33	37	0					
11	J	3	10	A	BB						44			44	60	52	79	94				
11	K	3	11	A	PC							5		5	16	33	86	91				
11	L	3	12	A	CR								36	36	52	47	69	85	0.2	0.1	0.2	0.1
11	M	4	13	A	BB						24			24	60	44	76	91				
11	N	4	14	A	CR								38	38	45	44	68	82	0.2	0.1	0.3	0.1
11	O	4	15	A	FS					0				0	19	19	0					
11	P	4	16	A	PC							1		1	17	20	0					
12	A	1	1	A	FS					0				0	23	44	0					

						2010	All Biomass values in g									All measurements in CM							
						Bioma	Bioma	Bioma	Bioma	Bioma	Bioma	Bioma	Bioma	Biomass									
Row	Column Letter	Trial	Column	Basin	Species	RB	GB	SB	LS	FS	BB	PC	CR	sum	June Leaf Height	July Leaf Height	August Leaf Height	September Leaf Height	July, Bulrush D (L)	July, Bulrush D (S)	August, Bulrush D (L)	August, Bulrush D (S)
12	B	1	2	A	BB						71			71	46	46	85	105				
12	C	1	3	A	CR								71	71	59	58	74	82	0.3	0.1	0.2	0.1
12	D	1	4	A	PC							8		8	25	37	79	88				
12	E	2	5	A	CR								84	84	48	55	80	84	0.3	0.1	0.3	0.1
12	F	2	6	A	FS					10				10	37	39	64	69				
12	G	2	7	A	BB						46			46	56	50	67	89				
12	H	2	8	A	PC							9		9	26	43	96	105				
12	I	3	9	A	CR								145	145	57	61	79	93	0.3	0.1	0.3	0.1
12	J	3	10	A	FS					8				8	38	42	69	88				
12	K	3	11	A	PC							1		1	20	24	78	85				
12	L	3	12	A	BB						47			47	45	31	70	82			0.3	0.1
12	M	4	13	A	CR								50	50	52	54	73	77	0.3	0.1		
12	N	4	14	A	BB						27			27	45	39	78	85				
12	O	4	15	A	PC									0	30	24	0	34				
12	P	4	16	A	FS					0				0	13	10	0					
13	A	1	1	A	BB	10					105			115	58	54	86	104				
13	B	1	2	A	FS					0				0	34	46	78					
13	C	1	3	A	PC							13		13	20	56	101	115				
13	D	1	4	A	CR								105	105	50	55	76	84	0.3	0.1	0.3	0.1
13	E	2	5	A	FS					13				13	27	29	67	79				
13	F	2	6	A	PC							21		21	27	43	83	97				
13	G	2	7	A	CR								98	98	54	55	71	84	0.3	0.1	0.3	0.1
13	H	2	8	A	BB						39			39	46	25	63	84				
13	I	3	9	A	BB						61			61	55	51	73	95				
13	J	3	10	A	CR								93	93	61	60	64	88	0.3	0.1	0.3	0.1
13	K	3	11	A	FS					0				0	25	32	0	20*				
13	L	3	12	A	PC							12		12	30	49	99	117				
13	M	4	13	A	FS					0				0	23	30	0	25				
13	N	4	14	A	PC							14		14	36	36	92	103				
13	O	4	15	A	BB						66			66	62	46	70	89				
13	P	4	16	A	CR								67	67	59	63	67	76	0.3	0.1	0.2	0.1
14	A	1	1	A	CR								64	64	48	69	79	79	0.3	0.1	0.3	0.1
14	B	1	2	A	PC							28		28	27	59	99	107				
14	C	1	3	A	FS					7				7	27	45	62	63				
14	D	1	4	A	BB						59			59	49	42	68	86				
14	E	2	5	A	BB						50			50	59	40	62	81				
14	F	2	6	A	PC							12		12	13	41	85	110				
14	G	2	7	A	CR								112	112	50	59	71	77	0.3	0.1	0.4	0.1
14	H	2	8	A	FS					20				20	33	42	88	73				
14	I	3	9	A	FS					18				18	22	32	58	68				
14	J	3	10	A	BB						55			55	47	36	67	82				
14	K	3	11	A	PC							25		25	40	53	92	104				
14	L	3	12	A	CR								116	116	46	54	78	80	0.4	0.1	0.4	0.1
14	M	4	13	A	BB						105			105	65	47	76	100				
14	N	4	14	A	CR								98	98	44	56	70	89	0.3	0.1	0.3	0.1
14	O	4	15	A	FS					8				8	24	46	62	30				
14	P	4	16	A	PC							10		10	15	56	86	100				
1	A	1	1	B	RB	201								201	32	95	141	160	1.1	0.3	1.2	0.3
1	B	1	2	B	SB			94						94	39	138	195	202				
1	C	1	3	B	GB		170							170	60	98	165	172				
1	D	1	4	B	LS				0					0	69	97	124	0				
1	E	2	5	B	LS				2					2	59	80	111	0				
1	F	2	6	B	RB	219								219	40	118	167	180	0.9	0.2	1.2	0.4
1	G	2	7	B	SB			32						32	51	124	201	218				
1	H	2	8	B	GB		207							207	58	131	202	208	1	0.3	0.9	0.5
1	I	3	9	B	SB			14						14	39	122	180	176				
1	J	3	10	B	LS				4					4	57	80	131	120				
1	K	3	11	B	RB	252								252	36	110	164	172				
1	L	3	12	B	GB		137							137	47	110	186	190				
1	M	4	13	B	RB	216								216	34	108	165	168				

						2010	All Biomass values in g									All measurements in CM							
						Bioma	Bioma	Bioma	Bioma	Bioma	Bioma	Bioma	Bioma	Biomass									
Row	Column Letter	Trial	Column	Basin	Species	RB	GB	SB	LS	FS	BB	PC	CR	sum	June Leaf Height	July Leaf Height	August Leaf Height	September Leaf Height	July, Bulrush D (L)	July, Bulrush D (S)	August, Bulrush D (L)	August, Bulrush D (S)
1	N	4	14	B	GB		263							263	59	122	173	193	1	0.2	1.2	0.4
1	O	4	15	B	SB			42						42	43	121	187	164				
1	P	4	16	B	LS				20					20	55	98	119	128	1.2	0.2	1.2	0.3
2	A	1	1	B	SB			61						61	45	132	177	197				
2	B	1	2	B	GB		99							99	46	95	156	164				
2	C	1	3	B	LS				4					4	51	85	135	121				
2	D	1	4	B	RB	117								117	42	119	172	168				
2	E	2	5	B	GB		202							202	61	122	172	184	1	0.2	0.9	0.4
2	F	2	6	B	SB			5						5	29	119	170	152				
2	G	2	7	B	RB	171								171	36	108	167	125				
2	H	2	8	B	LS				12					12	55	90	152	146				
2	I	3	9	B	RB	82								82	48	123	170	122	1.1	0.2	0.9	0.5
2	J	3	10	B	SB			3						3	48	128	198	140				
2	K	3	11	B	LS				12					12	72	92	135	155				
2	L	3	12	B	GB		68							68	61	118	176	186				
2	M	4	13	B	GB		144							144	52	115	184	190	1	0.2	1.4	0.2
2	N	4	14	B	SB			35						35	59	128	199	192				
2	O	4	15	B	RB	187								187	50	122	169	180				
2	P	4	16	B	LS				10					10	62	94	139	131				
3	A	1	1	B	LS				17					17	59	101	144	161	1	0.2	0.8	0.4
3	B	1	2	B	SB			14						14	44	130	159	169				
3	C	1	3	B	RB	130								130	37	118	156	125				
3	D	1	4	B	GB		120							120	45	121	187	185				
3	E	2	5	B	RB	100								100	36	114	157	151	1	0.3	0.5	0.4
3	F	2	6	B	SB			10						10	59	123	111	130				
3	G	2	7	B	LS				3					3	52	95	131	107				
3	H	2	8	B	GB		113							113	43	103	183	153	1.1	0.3	0.8	0.3
3	I	3	9	B	SB			0						0	35	119	166					
3	J	3	10	B	RB	79								79	35	125	181	127				
3	K	3	11	B	GB		87							87	58	120	194	165				
3	L	3	12	B	LS				20					20	74	118	156	144				
3	M	4	13	B	RB	136								136	48	122	145	132				
3	N	4	14	B	GB		122							122	52	121	201	187				
3	O	4	15	B	LS				2					2	71	102	155	164	1.2	0.3	1	0.4
3	P	4	16	B	SB			30						30	59	125	150	177	0.9	0.4	0.9	0.3
4	A	1	1	B	SB			25						25	46	113	154	166				
4	B	1	2	B	RB	146								146	33	102	163	167				
4	C	1	3	B	GB		144							144	51	113	198	161				
4	D	1	4	B	LS				1					1	41	66	120	40			1	0.2
4	E	2	5	B	SB			0						0	42	111	154	149	1	0.4		
4	F	2	6	B	GB		164							164	47	114	165	181				
4	G	2	7	B	LS				0					0	48	75	92					
4	H	2	8	B	RB	157								157	52	126	173	182				
4	I	3	9	B	RB	100								100	34	121	184	137				
4	J	3	10	B	LS				3					3	66	80	131	69	1	0.4	0.8	0.4
4	K	3	11	B	SB			4						4	30	111	180	107				
4	L	3	12	B	GB		91							91	48	120	181	161				
4	M	4	13	B	GB		239							239	43	111	160	174	1.2	0.3	0.9	0.4
4	N	4	14	B	SB			51						51	34	139	204	201				
4	O	4	15	B	LS				30					30	79	108	155	164				
4	P	4	16	B	RB	167								167	45	104	150	182				
5	A	1	1	B	RB	184								184	31	109	141	149				
5	B	1	2	B	LS				14					14	65	88	122	145	1.2	0.2	1.2	0.3
5	C	1	3	B	SB			86						86	43	132	181	195				
5	D	1	4	B	GB		58							58	42	103	168	159				
5	E	2	5	B	LS				8					8	56	99	149	137	1	0.3	1	0.3
5	F	2	6	B	SB			31						31	49	116	164	161				
5	G	2	7	B	RB	91								91	40	124	178	176				
5	H	2	8	B	GB		119							119	54	111	185	179	1.1	0.3	1	0.6
5	I	3	9	B	SB			10						10	32	115	137	152				

						2010	All Biomass values in g									All measurements in CM							
						Bioma	Bioma	Bioma	Bioma	Bioma	Bioma	Bioma	Bioma	Biomass									
Row	Column Letter	Trial	Column	Basin	Species	RB	GB	SB	LS	FS	BB	PC	CR	sum	June Leaf Height	July Leaf Height	August Leaf Height	September Leaf Height	July, Bulrush D (L)	July, Bulrush D (S)	August, Bulrush D (L)	August, Bulrush D (S)
5	J	3	10	B	GB		108							108	48	113	159	195				
5	K	3	11	B	RB	124								124	36	113	165	146				
5	L	3	12	B	LS				3					3	71	88	133	82				
5	M	4	13	B	RB	125								125	40	101	190	200				
5	N	4	14	B	LS				13					13	58	84	140	166				
5	O	4	15	B	GB		181							181	45	110	171	170	0.7	0.1	0.9	0.4
5	P	4	16	B	SB			0						0	37	104	164	173				
6	A	1	1	B	LS				11					11	49	79	134	124	1.5	0.2	1.5	0.4
6	B	1	2	B	SB			124						124	59	117	183	173				
6	C	1	3	B	GB		76							76	48	99	184	143				
6	D	1	4	B	RB	196								196	33	85	128	170				
6	E	2	5	B	LS				22					22	65	109	155	156				
6	F	2	6	B	GB		162							162	50	98	195	114	1	0.3	0.9	0.4
6	G	2	7	B	SB			6						6	21	120	182	116				
6	H	2	8	B	RB	189								189	40	112	180	121				
6	I	3	9	B	RB	213								213	39	123	189	163	0.8	0.1	0.8	0.3
6	J	3	10	B	SB			20						20	33	107	160	159				
6	K	3	11	B	GB		133							133	32	94	180	170				
6	L	3	12	B	LS				11					11	66	93	122	126				
6	M	4	13	B	LS				14					14	70	98	130	187				
6	N	4	14	B	GB		182							182	51	94	170	179				
6	O	4	15	B	RB	272								272	26	98	169	167	0.5	0.1	1	0.4
6	P	4	16	B	SB			18						18	34	98	172	165				
7	A	1	1	B	RB	182								182	45	93	140	115				
7	B	1	2	B	GB		50							50	51	70	150	130	1.1	0.2	0.8	0.4
7	C	1	3	B	SB			59						59	32	109	170	165				
7	D	1	4	B	LS				12					12	51	83	126	130				
7	E	2	5	B	RB	173								173	46	118	162	158				
7	F	2	6	B	GB		70							70	61	105	191	161				
7	G	2	7	B	LS				10					10	61	79	133	130	1	0.3	0.8	0.4
7	H	2	8	B	SB			6						6	45	115	160	159				
7	I	3	9	B	GB		139							139	53	97	162	173				
7	J	3	10	B	RB	107								107	45	109	151	161				
7	K	3	11	B	LS				23					23	77	94	146	152	1.1	0.1	1	0.4
7	L	3	12	B	SB			38						38	36	106	163	163				
7	M	4	13	B	GB		128							128	51	98	172	182				
7	N	4	14	B	RB	238								238	35	108	174	171	1	0.1	1	0.3
7	O	4	15	B	SB			88						88	45	118	169	170				
7	P	4	16	B	LS				45					45	67	118	145	165				
8	A	1	1	B	FS	184	35			6				225	36	37	56	67				
8	B	1	2	B	BB						54			54	51	56	103	125				
8	C	1	3	B	PC							13		13	34	69	146	158	0.4	0.1	0.4	0.1
8	D	1	4	B	CR								93	93	56	66	98	112	0.3	0.1	0.3	0.1
8	E	2	5	B	CR	88	66						34	188	58	67	91	113				
8	F	2	6	B	BB						50			50	66	63	113	113				
8	G	2	7	B	FS					16				16	38	50	94	105				
8	H	2	8	B	PC							37		37	42	101	199	193				
8	I	3	9	B	PC	133	42					26		201	23	88	173	170	0.3	0.1	0.3	0.1
8	J	3	10	B	CR								31	31	51	65	103	91				
8	K	3	11	B	FS					4				4	23	34	69	68				
8	L	3	12	B	BB						0			0	30	27	64	63				
8	M	4	13	B	FS	162	85			16				263	33	44	79	109				
8	N	4	14	B	PC							28		28	22	74	128	132	0.3	0.1	0.3	0.1
8	O	4	15	B	CR								37	37	59	65	76	99				
8	P	4	16	B	BB						53			53	67	66	89	128	0.4	0.1	0.5	0.1
9	A	1	1	B	CR	143	5						79	227	61	76	98	112				
9	B	1	2	B	FS					10				10	40	26	67	92				
9	C	1	3	B	BB						37			37	48	46	74	111				
9	D	1	4	B	PC							43		43	36	76	142	157				
9	E	2	5	B	PC	189	57					18		264	26	57	95	140	0.4	0.1	0.4	0.1

						2010	All Biomass values in g									All measurements in CM							
						Bioma	Bioma	Bioma	Bioma	Bioma	Bioma	Bioma	Bioma	Biomass									
Row	Column Letter	Trial	Column	Basin	Species	RB	GB	SB	LS	FS	BB	PC	CR	sum	June Leaf Height	July Leaf Height	August Leaf Height	September Leaf Height	July, Bulrush D (L)	July, Bulrush D (S)	August, Bulrush D (L)	August, Bulrush D (S)
9	F	2	6	B	CR								84	84	60	68	100	120				
9	G	2	7	B	FS					25				25	32	51	102	132				
9	H	2	8	B	BB						60			60	47	55	89	120				
9	I	3	9	B	FS	110	27			10				147	28	35	79	100				
9	J	3	10	B	BB						3			3	20	17	55	56	0.3	0.1	0.4	0.1
9	K	3	11	B	CR								36	36	53	54	84	126				
9	L	3	12	B	PC							29		29	42	101	142	142				
9	M	4	13	B	PC	137	62					31		230	37	69	134	175				
9	N	4	14	B	BB						9			9	38	32	62	96				
9	O	4	15	B	FS					14				14	40	46	75	104	0.4	0.1	0.4	0.1
9	P	4	16	B	CR								67	67	48	72	84	94				
10	A	1	1	B	BB	194					68			262	53	59	77	89	0.3	0.1	0.5	0.1
10	B	1	2	B	CR								61	61	52	58	69	102				
10	C	1	3	B	PC							60		60	54	72	130	134				
10	D	1	4	B	FS					33				33	43	57	94	119				
10	E	2	5	B	FS	148	16			12				176	28	51	93	102				
10	F	2	6	B	BB						75			75	73	51	82	111	0.4	0.1	0.4	0.1
10	G	2	7	B	CR								43	43	55	64	80	120				
10	H	2	8	B	PC							62		62	43	91	151	156	0.4	0.1	0.4	0.1
10	I	3	9	B	CR	171	29						59	259	63	64	74	85				
10	J	3	10	B	FS					27				27	39	58	90	122				
10	K	3	11	B	BB						30			30	52	47	81	95				
10	L	3	12	B	PC							26		26	36	88	124	137	0.3	0.1	0.4	0.1
10	M	4	13	B	CR	138	16						37	191	62	62	71	96				
10	N	4	14	B	PC							33		33	27	63	145	141				
10	O	4	15	B	FS					47				47	39	58	93	123				
10	P	4	16	B	BB						38			38	42	45	90	95				
11	A	1	1	B	PC	105						55		160	28	83	122	121				
11	B	1	2	B	FS					18				18	39	45	62	97				
11	C	1	3	B	BB						21			21	55	43	55	67	0.3	0.1	0.3	0.1
11	D	1	4	B	CR								34	34	53	51	55	68				
11	E	2	5	B	BB	156					66			222	62	52	81	102	0.3	0.1	0.3	0.1
11	F	2	6	B	CR								28	28	56	53	66	95				
11	G	2	7	B	PC							53		53	36	76	121	155				
11	H	2	8	B	FS					23				23	37	42	64	104				
11	I	3	9	B	FS	81				10				91	28	32	65	73				
11	J	3	10	B	BB						10			10	59	32	62	63				
11	K	3	11	B	PC							86		86	32	58	111	166	0.3	0.1	0.2	0.1
11	L	3	12	B	CR								25	25	56	55	61	68				
11	M	4	13	B	BB	146					26			172	41	48	80	80			0.3	0.1
11	N	4	14	B	CR								25	25	58	59	68	83				
11	O	4	15	B	FS					34				34	47	61	95	115				
11	P	4	16	B	PC							108		108	74	109	143	141				
12	A	1	1	B	FS	84				28				112	40	48	60	89				
12	B	1	2	B	BB						10			10	26	25	52	68	0.3	0.1	0.3	0.1
12	C	1	3	B	CR								27	27	57	54	66	64				
12	D	1	4	B	PC							47		47	23	48	105	118	0.3	0.1	0.3	0.1
12	E	2	5	B	CR	81							42	123	47	53	70	71				
12	F	2	6	B	FS					16				16	24	34	53	77				
12	G	2	7	B	BB						54			54	56	48	52	71				
12	H	2	8	B	PC							31		31	31	62	103	104	0.4	0.1	0.3	0.1
12	I	3	9	B	CR	36							43	79	61	64	61	70				
12	J	3	10	B	FS					39				39	47	50	62	90				
12	K	3	11	B	PC							33		33	30	51	98	121				
12	L	3	12	B	BB						18			18	45	37	55	70	0.3	0.1	0.3	0.1
12	M	4	13	B	CR	56							31	87	56	58	56	59				
12	N	4	14	B	BB						11			11	31	23	46	52				
12	O	4	15	B	PC							60		60	37	93	103	122				
12	P	4	16	B	FS					50				50	38	65	88	107				
13	A	1	1	B	BB	11					83			94	61	57	93	88				

						2010	All Biomass values in g									All measurements in CM							
						Bioma	Bioma	Bioma	Bioma	Bioma	Bioma	Bioma	Bioma	Biomass									
Row	Column Letter	Trial	Column	Basin	Species	RB	GB	SB	LS	FS	BB	PC	CR	sum	June Leaf Height	July Leaf Height	August Leaf Height	September Leaf Height	July, Bulrush D (L)	July, Bulrush D (S)	August, Bulrush D (L)	August, Bulrush D (S)
13	B	1	2	B	FS					19				19	32	43	63	66				
13	C	1	3	B	PC							93		93	42	72	110	109	0.3	0.1	0.3	0.1
13	D	1	4	B	CR								30	30	63	63	55	60				
13	E	2	5	B	FS	5				18				23	25	41	75	82				
13	F	2	6	B	PC							51		51	27	70	100	119	0.4	0.1	0.2	0.1
13	G	2	7	B	CR								46	46	61	65	60	46				
13	H	2	8	B	BB						50			50	48	48	65	75				
13	I	3	9	B	BB	8					29			37	50	38	60	71	0.3	0.1	0.2	0.1
13	J	3	10	B	CR								36	36	52	55	55	53				
13	K	3	11	B	FS					28				28	40	52	72	88				
13	L	3	12	B	PC							110		110	52	87	140	153				
13	M	4	13	B	FS	6				21				27	29	57	59	76				
13	N	4	14	B	PC							114		114	29	91	139	144				
13	O	4	15	B	BB						44			44	61	51	70	74	0.4	0.1	0.3	0.1
13	P	4	16	B	CR								41	41	49	66	68	56	0.4	0.1	0.3	0.1
14	A	1	1	B	CR								106	106	63	70	76	79				
14	B	1	2	B	PC							56		56	38	81	141	121				
14	C	1	3	B	FS					7				7	20	26	30	22				
14	D	1	4	B	BB						42			42	65	56	73	72				
14	E	2	5	B	BB						61			61	68	60	68	78				
14	F	2	6	B	PC							86		86	21	86	107	104	0.3	0.1	0.2	0.1
14	G	2	7	B	CR								46	46	55	57	45	41				
14	H	2	8	B	FS					25				25	20	51	66	68				
14	I	3	9	B	FS					39				39	31	44	60	73				
14	J	3	10	B	BB						28			28	52	44	60	70				
14	K	3	11	B	PC							99		99	32	84	104	110	0.3	0.1	0.2	0.1
14	L	3	12	B	CR								33	33	43	57	48	66				
14	M	4	13	B	BB						26			26	43	45	68	64	0.3	0.1	0.2	0.1
14	N	4	14	B	CR								38	38	54	58	50	50				
14	O	4	15	B	FS					30				30	20	48	55	73				
14	P	4	16	B	PC							149		149	54	121	140	136				
1	A	1	1	C	RB	253								253	45	127	161	160				
1	B	1	2	C	SB			45						45	39	154	174	200	1	0.3	0.9	0.4
1	C	1	3	C	GB		208							208	67	115	177	191				
1	D	1	4	C	LS				9					9	62	90	137	160				
1	E	2	5	C	LS				15					15	56	89	153	159				
1	F	2	6	C	RB	243								243	62	123	182	173				
1	G	2	7	C	SB			39						39	47	130	208	193	0.9	0.3	0.9	0.5
1	H	2	8	C	GB		121							121	59	122	179	188				
1	I	3	9	C	SB			43						43	52	141	175	194	0.8	0.3	1	0.6
1	J	3	10	C	LS				8					8	61	95	133	119				
1	K	3	11	C	RB	146								146	37	63	177	167				
1	L	3	12	C	GB		78							78	33	95	170	182				
1	M	4	13	C	RB	413								413	40	110	174	168				
1	N	4	14	C	GB		160							160	58	132	174	167				
1	O	4	15	C	SB			69						69	37	130	170	183	0.7	0.4	1.2	0.4
1	P	4	16	C	LS				31					31	79	109	124	143				
2	A	1	1	C	SB			56						56	50	122	170	192	1	0.2	1.1	0.4
2	B	1	2	C	GB		226							226	67	119	182	197				
2	C	1	3	C	LS				15					15	71	95	145	141				
2	D	1	4	C	RB	264								264	33	113	178	147				
2	E	2	5	C	GB		166							166	54	108	182	188				
2	F	2	6	C	SB			18						18	33	134	194	180	1.2	0.4	1.2	0.4
2	G	2	7	C	RB	227								227	41	125	184	182				
2	H	2	8	C	LS				0					0	44	59	169	117				
2	I	3	9	C	RB	163								163	40	117	175	184				
2	J	3	10	C	SB			11						11	48	131	183	182	0.9	0.3	0.9	0.5
2	K	3	11	C	LS				9					9	73	101	154	170				
2	L	3	12	C	GB		215							215	42	120	182	195				
2	M	4	13	C	GB		105							105	49	122	189	200				

						2010	All Biomass values in g									All measurements in CM							
						Bioma	Bioma	Bioma	Bioma	Bioma	Bioma	Bioma	Bioma	Biomass									
Row	Column Letter	Trial	Column	Basin	Species	RB	GB	SB	LS	FS	BB	PC	CR	sum	June Leaf Height	July Leaf Height	August Leaf Height	September Leaf Height	July, Bulrush D (L)	July, Bulrush D (S)	August, Bulrush D (L)	August, Bulrush D (S)
2	N	4	14	C	SB			11						11	49	130	166	166	0.9	0.3	0.9	0.4
2	O	4	15	C	RB	221								221	50	124	163	169				
2	P	4	16	C	LS				35					35	66	105	143	140				
3	A	1	1	C	LS				6					6	73	91	125	118				
3	B	1	2	C	SB			86						86	57	109	169	211	0.9	0.2	1.2	0.4
3	C	1	3	C	RB	165								165	44	105	174	133				
3	D	1	4	C	GB		84							84	45	103	156	143				
3	E	2	5	C	RB	252								252	40	118	151	174				
3	F	2	6	C	SB			49						49	53	130	185	188	1	0.3	0.9	0.5
3	G	2	7	C	LS				17					17	59	110	168	153				
3	H	2	8	C	GB		125							125	53	113	181	180				
3	I	3	9	C	SB			18						18	42	141	198	193	1.1	0.3	0.9	0.6
3	J	3	10	C	RB	158								158	47	113	169	183				
3	K	3	11	C	GB		110							110	52	111	187	192				
3	L	3	12	C	LS				5					5	57	103	161	161				
3	M	4	13	C	RB	151								151	40	85	181	173				
3	N	4	14	C	GB		61							61	50	92	179	181				
3	O	4	15	C	LS				6					6	56	102	162	131				
3	P	4	16	C	SB			47						47	39	130	155	154	1.1	0.2	1.1	0.4
4	A	1	1	C	SB			14						14	43	106	143	154	0.6	0.1	0.5	0.3
4	B	1	2	C	RB	257								257	43	112	157	180				
4	C	1	3	C	GB		160							160	55	105	184	178				
4	D	1	4	C	LS				9					9	50	85	132	151				
4	E	2	5	C	SB			40						40	49	134	204	189	0.7	0.2	1	0.5
4	F	2	6	C	GB		146							146	50	108	189	190				
4	G	2	7	C	LS				10					10	81	97	136	135				
4	H	2	8	C	RB	159								159	32	100	143	165				
4	I	3	9	C	RB	180								180	41	111	179	158				
4	J	3	10	C	LS				20					20	87	97	165	164				
4	K	3	11	C	SB			8						8	45	109	150	137	0.7	0.2	0.6	0.5
4	L	3	12	C	GB		147							147	45	109	170	185				
4	M	4	13	C	GB		78							78	18	99	162	164				
4	N	4	14	C	SB			54						54	56	127	170	174	0.6	0.3	1	0.3
4	O	4	15	C	LS				30					30	84	102	151	170				
4	P	4	16	C	RB	163								163	37	99	159	155				
5	A	1	1	C	RB	199								199	31	106	155	127				
5	B	1	2	C	LS				19					19	74	94	125	167				
5	C	1	3	C	SB			55						55	52	130	179	170	1	0.2	1.2	0.4
5	D	1	4	C	GB		121							121	57	113	174	183				
5	E	2	5	C	LS				12					12	68	86	158	170				
5	F	2	6	C	SB			54						54	43	134	181	188	0.9	0.2	1	0.4
5	G	2	7	C	RB	118								118	48	103	155	164				
5	H	2	8	C	GB		186							186	53	114	178	181				
5	I	3	9	C	SB			12						12	52	128	185	188	1.2	0.2	0.8	0.5
5	J	3	10	C	GB		104							104	33	104	171	168				
5	K	3	11	C	RB	149								149	39	87	171	159				
5	L	3	12	C	LS				5					5	58	80	145	145				
5	M	4	13	C	RB	160								160	34	107	157	161				
5	N	4	14	C	LS				1					1	57	86	137	76				
5	O	4	15	C	GB		148							148	53	105	159	144				
5	P	4	16	C	SB			99						99	39	124	177	189	1.4	0.2	1.5	0.3
6	A	1	1	C	LS				18					18	68	96	138	126				
6	B	1	2	C	SB			63						63	55	128	171	181	1.2	0.3	1.1	0.5
6	C	1	3	C	GB		86							86	59	111	190	153				
6	D	1	4	C	RB	210								210	47	97	156	147				
6	E	2	5	C	LS				0					0	66	86	134	97				
6	F	2	6	C	GB		112							112	39	96	161	180				
6	G	2	7	C	SB			42						42	46	112	186	95	0.9	0.3	1.3	0.4
6	H	2	8	C	RB	84								84	46	95	164	168				
6	I	3	9	C	RB	145								145	39	110	165	166				

						2010	All Biomass values in g									All measurements in CM								
						Bioma	Bioma	Bioma	Bioma	Bioma	Bioma	Bioma	Bioma	Biomass										
Row	Column Letter	Trial	Column	Basin	Species	RB	GB	SB	LS	FS	BB	PC	CR	sum	June Leaf Height	July Leaf Height	August Leaf Height	September Leaf Height	July, Bulrush D (L)	July, Bulrush D (S)	August, Bulrush D (L)	August, Bulrush D (S)
6	J	3	10	C	SB			45						45	35	106	153	166	0.7	0.2	0.9	0.2
6	K	3	11	C	GB		83							83	36	80	160	167				
6	L	3	12	C	LS				14					14	69	90	151	163				
6	M	4	13	C	LS				22					22	87	96	138	151				
6	N	4	14	C	GB		142							142	44	102	161	183				
6	O	4	15	C	RB	162								162	43	107	164	172				
6	P	4	16	C	SB			72						72	56	122	160	180	1.4	0.5	1.5	0.2
7	A	1	1	C	RB	154								154	50	112	133	139				
7	B	1	2	C	GB		131							131	61	84	139	148				
7	C	1	3	C	SB			58						58	41	120	171	190	1	0.2	1	0.3
7	D	1	4	C	LS				22					22	67	75	137	164				
7	E	2	5	C	RB	68								68	39	92	144	147				
7	F	2	6	C	GB		177							177	45	75	131	158				
7	G	2	7	C	LS				21					21	81	84	135	133				
7	H	2	8	C	SB			147						147	41	130	186	210	1.2	0.2	1.5	0.3
7	I	3	9	C	GB		91							91	52	89	145	155				
7	J	3	10	C	RB	71								71	37	83	147	155				
7	K	3	11	C	LS				24					24	63	86	143	166				
7	L	3	12	C	SB			58						58	37	101	171	193	0.8	0.2	1	0.4
7	M	4	13	C	GB		169							169	47	83	151	167				
7	N	4	14	C	RB	134								134	40	90	149	157				
7	O	4	15	C	SB			102						102	33	114	176	184	1.2	0.2	1.3	0.4
7	P	4	16	C	LS				36					36	67	90	140	155				
8	A	1	1	C	FS	122	87	27		5				241	45	45	46	61				
8	B	1	2	C	BB						94			94	71	66	92	101				
8	C	1	3	C	PC							17		17	78	102	124	85				
8	D	1	4	C	CR								42	42	55	65	95	126	0.4	0.1	0.3	0.1
8	E	2	5	C	CR	72	26	8					87	193	51	65	101	134	0.4	0.1	0.4	0.1
8	F	2	6	C	BB						135			135	74	75	117	122				
8	G	2	7	C	FS					0				0	16	25	0					
8	H	2	8	C	PC							29		29	47	84	119	125				
8	I	3	9	C	PC	72	13					37		122	48	77	133	145				
8	J	3	10	C	CR								50	50	54	65	97	116	0.4	0.1	0.4	0.1
8	K	3	11	C	FS					0				0	31	18	0					
8	L	3	12	C	BB						57			57	57	62	109	121				
8	M	4	13	C	FS	108	55	32		0				195	35	25	69	45				
8	N	4	14	C	PC							22		22	29	73	106	144				
8	O	4	15	C	CR								65	65	45	68	91	111			0.4	0.1
8	P	4	16	C	BB						79			79	44	61	99	105				
9	A	1	1	C	CR	55	106						45	206	46	69	64	103	0.3	0.1	0.3	0.1
9	B	1	2	C	FS					22				22	44	52	78	104				
9	C	1	3	C	BB						94			94	56	57	95	106				
9	D	1	4	C	PC							58		58	52	106	143	150				
9	E	2	5	C	PC	48	37					39		124	43	90	114	124				
9	F	2	6	C	CR								101	101	53	67	89	112	0.4	0.1	0.4	0.1
9	G	2	7	C	FS					4				4	44	42	39	71				
9	H	2	8	C	BB						84			84	66	56	103	100				
9	I	3	9	C	FS	85				7				92	32	52	68	80				
9	J	3	10	C	BB						106			106	60	57	104	114				
9	K	3	11	C	CR								98	98	57	67	91	116	0.4	0.1	0.4	0.1
9	L	3	12	C	PC							78		78	71	107	158	165				
9	M	4	13	C	PC	105	16					32		153	68	101	154	170				
9	N	4	14	C	BB						42			42	51	65	86	104				
9	O	4	15	C	FS					11				11	33	50	77	94				
9	P	4	16	C	CR								120	120	65	77	85	100	0.5	0.1	0.4	0.1
10	A	1	1	C	BB	37	32				75			144	46	52	92	93				
10	B	1	2	C	CR								87	87	62	59	74	97	0.4	0.1	0.3	0.1
10	C	1	3	C	PC							57		57	39	113	128	136				
10	D	1	4	C	FS					20				20	45	47	72	98				
10	E	2	5	C	FS	70	3			10				83	46	50	50	98				

						2010 All Biomass values in g									All measurements in CM							
						Bioma	Bioma	Bioma	Bioma	Bioma	Bioma	Bioma	Bioma	Biomass								
Row	Column Letter	Trial	Column	Basin	Species	RB	GB	SB	LS	FS	BB	PC	CR	sum	June Leaf Height	July Leaf Height	August Leaf Height	September Leaf Height	July, Bulrush D (L)	July, Bulrush D (S)	August, Bulrush D (L)	August, Bulrush D (S)
10	F	2	6	C	BB						53			53	39	53	70	95				
10	G	2	7	C	CR								102	102	46	60	90	107	0.4	0.1	0.5	0.1
10	H	2	8	C	PC							46		46	37	88	44	157				
10	I	3	9	C	CR	81	3						121	205	55	68	87	104	0.3	0.1	0.5	0.1
10	J	3	10	C	FS					17				17	52	50	82	107				
10	K	3	11	C	BB						38			38	42	47	77	123				
10	L	3	12	C	PC							52		52	21	97	139	150				
10	M	4	13	C	CR	143	2						71	216	57	68	87	105	0.4	0.1	0.5	0.1
10	N	4	14	C	PC							63		63	49	93	130	135				
10	O	4	15	C	FS					7				7	29	33	55	70				
10	P	4	16	C	BB						42			42	47	49	80	91				
11	A	1	1	C	PC	17	11					92		120	29	91	141	154				
11	B	1	2	C	FS					23				23	32	34	78	94				
11	C	1	3	C	BB						12			12	49	27	50	71				
11	D	1	4	C	CR								71	71	56	68	73	101	0.3	0.1	0.4	0.1
11	E	2	5	C	BB	12	7				156			175	67	65	92	110				
11	F	2	6	C	CR								90	90	56	63	83	96	0.4	0.1	0.5	0.1
11	G	2	7	C	PC							31		31	46	74	106	128				
11	H	2	8	C	FS					22				22	44	47	99	104				
11	I	3	9	C	FS	28	5			28				61	35	42	79	116				
11	J	3	10	C	BB						97			97	67	61	82	100				
11	K	3	11	C	PC							83		83	53	90	141	158				
11	L	3	12	C	CR								119	119	51	66	100	104	0.5	0.1	0.5	0.1
11	M	4	13	C	BB	68					112			180	62	64	96	100				
11	N	4	14	C	CR								57	57	54	72	94	111			0.3	0.1
11	O	4	15	C	FS					10				10	29	33	62	90				
11	P	4	16	C	PC							73		73	44	93	123	143				
12	A	1	1	C	FS	5				33				38	37	48	69	94				
12	B	1	2	C	BB						97			97	66	61	77	93				
12	C	1	3	C	CR								76	76	59	63	74	85	0.4	0.1	0.4	0.1
12	D	1	4	C	PC							19		19	46	64	95	113				
12	E	2	5	C	CR	18							73	91	66	62	70	85	0.4	0.1	0.4	0.1
12	F	2	6	C	FS					15				15	41	40	70	90				
12	G	2	7	C	BB						62			62	68	60	79	98				
12	H	2	8	C	PC							74		74	30	94	139	165				
12	I	3	9	C	CR	10							103	113	61	67	90	98	0.5	0.1	0.5	0.1
12	J	3	10	C	FS					27				27	42	46	68	103				
12	K	3	11	C	PC							41		41	22	84	110	117				
12	L	3	12	C	BB						80			80	66	50	107	94				
12	M	4	13	C	CR	95							67	162	51	56	80	71	0.4	0.1	0.3	0.1
12	N	4	14	C	BB						63			63	51	53	70	86				
12	O	4	15	C	PC							48		48	34	68	119	115				
12	P	4	16	C	FS					61				61	31	49	80	105				
13	A	1	1	C	BB						39			39	45	44	60	78				
13	B	1	2	C	FS					18				18	27	44	55	74				
13	C	1	3	C	PC							65		65	64	95	114	127				
13	D	1	4	C	CR								45	45	64	64	65	82	0.5	0.1	0.3	0.1
13	E	2	5	C	FS					24				24	43	47	73	97				
13	F	2	6	C	PC							26		26	53	87	106	99				
13	G	2	7	C	CR								80	80	52	61	77	89	0.4	0.1	0.4	0.1
13	H	2	8	C	BB						57			57	53	56	77	91				
13	I	3	9	C	BB						57			57	53	53	72	98				
13	J	3	10	C	CR	23							59	82	47	65	75	83	0.5	0.1	0.4	0.1
13	K	3	11	C	FS					38				38	36	47	85	103				
13	L	3	12	C	PC							112		112	33	99	146	163				
13	M	4	13	C	FS					30				30	32	50	52	79				
13	N	4	14	C	PC							47		47	29	77	103	116				
13	O	4	15	C	BB						42			42	48	46	64	81				
13	P	4	16	C	CR								87	87	54	71	84	81	0.5	0.1	0.4	0.1
14	A	1	1	C	CR								103	103	59	61	73	81	0.4	0.2	0.4	0.1

			2010 All Biomass values in g									All measurements in CM							
			Bioma	Bioma	Bioma	Bioma	Bioma	Bioma	Bioma	Bioma	Biomass								
Column	Basin	Species	RB	GB	SB	LS	FS	BB	PC	CR	sum	June Leaf Height	July Leaf Height	August Leaf Height	September Leaf Height	July, Bulrush D (L)	July, Bulrush D (S)	August, Bulrush D (L)	August, Bulrush D (S)
2	C	PC							50		50	39	85	122	122				
3	C	FS					19				19	32	53	59	86				
4	C	BB						72			72	48	68	75	76				
5	C	BB						53			53	77	56	74	76				
6	C	PC							75		75	47	99	134	117				
7	C	CR	5							58	63	49	59	62	74	0.4	0.1	0.3	0.1
8	C	FS					32				32	39	57	84	95				
9	C	FS					14				14	40	55	84	88				
10	C	BB						61			61	65	50	68	90				
11	C	PC							19		19	44	61	102	105				
12	C	CR								0	0	58	58	55	56	0.5	0.1	0.2	0.1
13	C	BB						37			37	55	55	58	60				
14	C	CR								27	27	51	53	42	50	0.4	0.1	0.2	0.1
15	C	FS					15				15	24	32	59	71				
16	C	PC							80		80	58	108	151	140				
1	D	RB	303								303	47	119	159	166				
2	D	SB			37						37	43	122	206	219	0.8	0.2	1.1	0.2
3	D	GB		208							208	40	107	162	180				
4	D	LS				14					14	45	80	132	121				
5	D	LS				8					8	61	99	120	154				
6	D	RB	280								280	44	125	172	147				
7	D	SB			40						40	56	129	168	196	0.9	0.2	0.9	0.3
8	D	GB		114							114	50	117	169	192				
9	D	SB			47						47	56	136	186	194	0.8	0.2	0.9	0.3
10	D	LS				31					31	69	102	149	146				
11	D	RB	219								219	44	104	169	168				
12	D	GB		119							119	60	124	199	208				
13	D	RB	182								182	42	117	157	140				
14	D	GB		232							232	60	122	187	208				
15	D	SB			61						61	66	139	191	190	0.7	0.3	1.1	0.2
16	D	LS				14					14	51	91	117	126				
1	D	SB			63						63	46	130	177	209	0.9	0.4	0.9	0.3
2	D	GB		107							107	50	114	169	180				
3	D	LS				39					39	61	104	165	177				
4	D	RB	218								218	38	118	164	158				
5	D	GB		114							114	52	108	155	191				
6	D	SB			17						17	34	125	161	178	0.9	0.5	1	0.3
7	D	RB	173								173	20	94	120	160				
8	D	LS				17					17	57	90	139	161				
9	D	RB	140								140	41	110	181	181				
10	D	SB			13						13	58	131	174	202	1	0.3	0.9	0.3
11	D	LS				10					10	50	98	134	136				
12	D	GB		213							213	64	129	190	212				
13	D	GB		116							116	45	109	174	205				
14	D	SB			14						14	61	134	170	194	1.2	0.3	1.1	0.3
15	D	RB	106								106	35	109	145	124				
16	D	LS				8					8	60	94	126	133				
1	D	LS				22					22	73	99	132	157				
2	D	SB			37						37	56	128	170	187	0.9	0.3	1	0.2
3	D	RB	127								127	43	130	153	169				
4	D	GB		82							82	50	112	157	178				
5	D	RB	122								122	31	126	151	130				
6	D	SB			12						12	39	117	209	210			1	0.3
7	D	LS				13					13	56	89	120	169				
8	D	GB		166							166	41	105	169	202				
9	D	SB			60						60	73	130	187	191	1.1	0.2	1	0.4
10	D	RB	120								120	21	113	182	173				
11	D	GB		51							51	53	107	170	192				
12	D	LS				10					10	66	94	150	174				
13	D	RB	113								113	14	65	176	186				

			2010 All Biomass values in g									All measurements in CM							
			Bioma	Bioma	Bioma	Bioma	Bioma	Bioma	Bioma	Bioma	Biomass								
Column	Basin	Species	RB	GB	SB	LS	FS	BB	PC	CR	sum	June Leaf Height	July Leaf Height	August Leaf Height	September Leaf Height	July, Bulrush D (L)	July, Bulrush D (S)	August, Bulrush D (L)	August, Bulrush D (S)
14	D	GB		207							207	64	95	178	197				
15	D	LS				4					4	61	68	141	99				
16	D	SB			125						125	63	129	160	213	1	0.3	1.2	0.2
1	D	SB			97						97	33	126	174	192	0.8	0.2	1.2	0.3
2	D	RB	129								129	36	99	161	158				
3	D	GB		110							110	43	117	178	190				
4	D	LS				27					27	81	90	163	178				
5	D	SB			29						29	50	160	199	200	1	0.2	0.8	0.4
6	D	GB		250							250	56	115	183	190				
7	D	LS				7					7	55	90	142	81				
8	D	RB	61								61	38	86	185	133				
9	D	RB	136								136	35	110	176	157				
10	D	LS				10					10	70	87	131	120				
11	D	SB			24						24	45	122	175	167	1	0.3	0.8	0.3
12	D	GB		105							105	56	99	174	179				
13	D	GB		192							192	54	105	159	191				
14	D	SB			141						141	60	134	170	185	1.2	0.3	0.9	0.3
15	D	LS				15					15	58	85	140	165				
16	D	RB	71								71	30	94	139	128				
1	D	RB	92								92	36	120	138	141				
2	D	LS				12					12	54	80	131	150				
3	D	SB			47						47	26	100	183	180	0.8	0.2	1.1	0.3
4	D	GB		161							161	45	111	202	201				
5	D	LS				16					16	45	90	153	154				
6	D	SB			14						14	58	131	155	160	1.1	0.5	1	0.3
7	D	RB	112								112	29	115	159	130				
8	D	GB		147							147	44	96	179	195				
9	D	SB			13						13	43	100	141	170	0.8	0.2	0.5	0.4
10	D	GB		76							76	49	94	173	187				
11	D	RB	99								99	26	98	161	158				
12	D	LS				12					12	52	77	139	156				
13	D	RB	109								109	9	49	176	175				
14	D	LS				0					0	22	60	114	156				
15	D	GB		220							220	58	80	176	181				
16	D	SB			100						100	64	125	161	191	0.9	0.3	1.1	0.2
1	D	LS				31					31	66	96	143	154				
2	D	SB			42						42	47	131	179	183	1.2	0.3	1	0.3
3	D	GB		187							187	54	118	202	208				
4	D	RB	211								211	29	110	178	143				
5	D	LS				15					15	70	100	155	171				
6	D	GB		224							224	51	99	191	181				
7	D	SB			29						29	57	134	171	200	0.9	0.3	1.1	0.2
8	D	RB	136								136	22	100	127	175				
9	D	RB	92								92	40	98	180	147				
10	D	SB			72						72	50	111	186	160	1.2	0.4	1.1	0.4
11	D	GB		124							124	27	94	174	178				
12	D	LS				5					5	61	70	136	119				
13	D	LS				6					6	48	55	99	136				
14	D	GB		153							153	52	91	169	183				
15	D	RB	121								121	12	85	144	168				
16	D	SB			174						174	49	111	170	184	1.1	0.2	1.2	0.3
1	D	RB	274								274	47	112	137	153				
2	D	GB		195							195	50	102	154	185				
3	D	SB			12						12	23	86	147	153	0.7	0.3	0.6	0.4
4	D	LS				21					21	59	87	140	157				
5	D	RB	165								165	45	96	149	148				
6	D	GB		304							304	57	101	181	182				
7	D	LS				13					13	58	71	126	124				
8	D	SB			72						72	58	120	177	184			1	0.3
9	D	GB		182							182	53	89	166	175				

			2010 All Biomass values in g									All measurements in CM							
			Bioma	Bioma	Bioma	Bioma	Bioma	Bioma	Bioma	Bioma	Biomass								
Column	Basin	Species	RB	GB	SB	LS	FS	BB	PC	CR	sum	June Leaf Height	July Leaf Height	August Leaf Height	September Leaf Height	July, Bulrush D (L)	July, Bulrush D (S)	August, Bulrush D (L)	August, Bulrush D (S)
10	D	RB	73								73	27	105	154	130				
11	D	LS				27					27	64	81	117	160	0	0		
12	D	SB			121						121	52	110	156	201	1.1	0.2	1	0.7
13	D	GB		117							117	36	82	129	151				
14	D	RB	88								88	27	85	146	172				
15	D	SB			214						214	48	110	172	188	0.9	0.3	1.1	0.5
16	D	LS				14					14	69	66	103	136				
1	D	FS	252	45			6				303	23	44	64	63				
2	D	BB						19			19	56	49	95	105				
3	D	PC							34		34	29	86.5	135	80				
4	D	CR								47	47	57	65	101	124	0.3	0.1	0.3	0.1
5	D	CR	127	76						67	270	64	74	102	132	0.3	0.1	0.3	0.1
6	D	BB						35			35	47	56	95	140				
7	D	FS					10				10	29	46	95	104				
8	D	PC							55		55	41	91	159	173				
9	D	PC	116	71		5			17		209	39	81.5	124	122				
10	D	CR								0	0	43	Not CR	Not CR					
11	D	FS					7				7	29	39.5	83	86				
12	D	BB						56			56	41	57	123	130				
13	D	FS	94	25	14	5	7				145	28	36	84	61				
14	D	PC							15		15	26	88	142	128				
15	D	CR								78	78	60	65	101	109	0.4	0.1	0.3	0.1
16	D	BB						28			28	54	49	104	96				
1	D	CR	169	22						114	305	52	72	107	109	0.4	0.1	0.3	0.1
2	D	FS					6				6	22	36	72	70				
3	D	BB						80			80	50	54	102	121				
4	D	PC							15		15	48	63	111	132				
5	D	PC	93	47					84		224	74	91	156	172	0	0		
6	D	CR								88	88	59	64	93	118	0.4	0.1	0.3	0.1
7	D	FS					0				0	30	36	63	42				
8	D	BB						80			80	49	46	96	118				
9	D	FS	71	69	12		2				154	26	44	90	109				
10	D	BB						106			106	52	54	122	120				
11	D	CR								58	58	55	58	101	113	0.4	0.1	0.3	0.1
12	D	PC							17		17	35	82	145	141				
13	D	PC	103	9					20		132	44	107	136	141				
14	D	BB						59			59	54	52	113	125				
15	D	FS					0				0	36	45	73	53				
16	D	CR								74	74	52	67	83	97	0.4	0.1	0.4	0.1
1	D	BB	120	6				77			203	42	49	88	109	0	0		
2	D	CR								70	70	50	63	85	103	0.3	0.1	0.4	0.1
3	D	PC							29		29	27	77	130	147				
4	D	FS					5				5	42	46	35	85				
5	D	FS	46	20			5				71	14	29	62	76				
6	D	BB						60			60	44	36	83	110				
7	D	CR								124	124	61	64	84	102	0.4	0.1	0.4	0.1
8	D	PC							70		70	50	79	84	124	0.4	0.1		
9	D	CR	60	36						93	189	57	75	89	100			0.4	0.1
10	D	FS					4				4	25	40	64	93				
11	D	BB						56			56	36	44	109	110				
12	D	PC							46		46	62	89	142	135				
13	D	CR	94	9						45	148	62	57	81	110	0.3	0.1	0.3	0.1
14	D	PC							31		31	34	82	123	125				
15	D	FS					16				16	38	49	83	107				
16	D	BB						68			68	51	50	96	109				
1	D	PC	21						129		150	55	106	128	147				
2	D	FS					32				32	31	60	90	106				
3	D	BB						136			136	42	46	35	103				
4	D	CR								111	111	54	54	98	121	0.3	0.1	0.4	0.1
5	D	BB	35	5				50			90	47	37	76	100				

			2010 All Biomass values in g									All measurements in CM							
			Bioma	Bioma	Bioma	Bioma	Bioma	Bioma	Bioma	Bioma	Biomass								
Column	Basin	Species	RB	GB	SB	LS	FS	BB	PC	CR	sum	June Leaf Height	July Leaf Height	August Leaf Height	September Leaf Height	July, Bulrush D (L)	July, Bulrush D (S)	August, Bulrush D (L)	August, Bulrush D (S)
6	D	CR								128	128	55	67	89	118	0.4	0.1	0.5	0.1
7	D	PC							33		33	53	74	113	132				
8	D	FS					17				17	20	41	70	102				
9	D	FS	38	12			24				74	41	54	65	107				
10	D	BB						77			77	39	40	77	118				
11	D	PC							46		46	40	76	101	140				
12	D	CR								52	52	61	56	81	116	0.2	0.1	0.4	0.1
13	D	BB	81	7				56			144	44	35	86	110				
14	D	CR								50	50	59	57	81	105	0.2	0.1	0.3	0.1
15	D	FS					20				20	37	46	85	102				
16	D	PC							76		76	71	94	125	140				
1	D	FS	1				27				28	26	42	70	88				
2	D	BB						25			25	48	42	60	84				
3	D	CR								107	107	51	56	84	100	0.4	0.1	0.5	0.1
4	D	PC							52		52	41	90	139	137				
5	D	CR	29							101	130	54	58	84	101	0.4	0.1	0.4	0.1
6	D	FS					23				23	32	47	82	110				
7	D	BB						114			114	74	60	85	104				
8	D	PC							73		73	52	83	127	131				
9	D	CR	48							125	173	60	63	84	110	0.3	0.1	0.4	0.1
10	D	FS					32				32	27	34	68	107				
11	D	PC							37		37	53	68	111	107				
12	D	BB						84			84	42	46	84	98				
13	D	CR	40							49	89	63	55	80	102	0.2	0.1	0.4	0.1
14	D	BB						74			74	49	47	78	106				
15	D	PC							85		85	26	65	117	131				
16	D	FS					17				17	41	46	76	80				
1	D	BB						46			46	47	43	63	97				
2	D	FS					24				24	27	51	79	94				
3	D	PC							71		71	42	72	107	111				
4	D	CR								100	100	56	57	70	101	0.3	0.1	0.3	0.1
5	D	FS					26				26	30	45	83	101	0	0		
6	D	PC	11						51		62	20	70	132	135	0	0		
7	D	CR								91	91	58	56	81	101	0.4	0.1	0.3	0.1
8	D	BB						81			81	58	46	72	102				
9	D	BB						66			66	40	45	84	95				
10	D	CR	61							67	128	59	56	75	101	0.3	0.1	0.3	0.1
11	D	FS					20				20	34	36	75	96				
12	D	PC							57		57	30	77	35	127				
13	D	FS					22				22	27	35	75	100				
14	D	PC							40		40	21	52	105	133				
15	D	BB						71			71	56	45	68	92				
16	D	CR								123	123	60	58	72	90	0.4	0.1	0.4	0.1
1	D	CR								123	123	41	60	84	84	0.4	0.1	0.4	0.1
2	D	PC							124		124	62	120	150	150				
3	D	FS	3				13				16	21	17	70	77				
4	D	BB						52			52	48	44	55	94				
5	D	BB						106			106	56	51	74	100				
6	D	PC							123		123	62	89	117	121				
7	D	CR								127	127	62	64	75	103	0.5	0.1	0.4	0.1
8	D	FS					47				47	34	61	84	104				
9	D	FS					42				42	41	45	67	102				
10	D	BB						71			71	46	43	72	91				
11	D	PC							55		55	49	69	96	117				
12	D	CR								78	78	49	55	65	72	0.4	0.1	0.3	0.1
13	D	BB						84			84	48	47	76	94				
14	D	CR								80	80	53	52	71	97	0.3	0.1	0.3	0.1
15	D	FS					24				24	36	41	65	79				
16	D	PC							35		35	51	83	90	100				

SAFL Climate Change Basins - Water Level Data for 2010

*** Rows = Number of Rows partially underwater** depth in cm

		Normal		Dry		Wet		Futr			Rows Only						Water Levels Only				
Date	Dates	Normal	Rows	Dry	Rows	Wet	Rows	Futr	Rows		Date	Normal	Dry	Wet	Futr		Date	Normal	Dry	Wet	Futr
6/23/2010	1	25	1	25	1	25	1	23	1		1	1	1	1	1		1	25	25	25	23
6/24/2010	2	29	3	31	3	33	3	30	3		2	3	3	3	3		2	29	31	33	30
6/25/2010	3	39	4	36	4	38	4	35	4		3	4	4	4	4		3	39	36	38	35
6/28/2010	4	45	5	42.5	5	43	6	40	5		4	5	5	6	5		4	45	42.5	43	40
6/29/2010	5	45	5	42.5	5	43	6	40	5		5	5	5	6	5		5	45	42.5	43	40
6/30/2010	6	45	5	42.5	5	43	6	40	5		6	5	5	6	5		6	45	42.5	43	40
7/1/2010	7	51	9	51	8	53	8	53	8		7	9	8	8	8		7	51	51	53	53
7/6/2010	8	56	11	56.5	10	61.5	10	61.5	11		8	11	10	10	11		8	56	56.5	61.5	61.5
7/12/2010	9	56	11	55.5	9	67.5	12	66.5	12		9	11	9	12	12		9	56	55.5	67.5	66.5
7/19/2010	10	59.5	13	55.5	9	73.5	14	66.5	12		10	13	9	14	12		10	59.5	55.5	73.5	66.5
7/26/2010	11	62.5	14	55.5	9	80	14	64.5	11		11	14	9	14	11		11	62.5	55.5	80	64.5
8/2/2010	12	64.5	14	55.5	9	84.5	14	61	11		12	14	9	14	11		12	64.5	55.5	84.5	61
8/9/2010	13	65	14	54	8	88	14	54.5	9		13	14	8	14	9		13	65	54	88	54.5
8/16/2010	14	67	14	52.5	7	88.8	14	55.5	8		14	14	7	14	8		14	67	52.5	88.8	55.5
8/23/2010	15	67.9	14	49.6	7	88.8	14	55.5	8		15	14	7	14	8		15	67.9	49.6	88.8	55.5
8/30/2010	16	68	14	45.5	6	88.8	14	56.4	8		16	14	6	14	8		16	68	45.5	88.8	56.4
9/6/2010	17	68	14	42.4	6	87.8	14	58.5	8		17	14	6	14	8		17	68	42.4	87.8	58.5
9/13/2010	18	67.8	14	38.7	4	86.6	14	60	9		18	14	4	14	9		18	67.8	38.7	86.6	60
9/20/2010	19	66.6	14	35	3	85	14	61.4	10		19	14	3	14	10		19	66.6	35	85	61.4
9/27/2010	20	65.6	14	31.9	1	83.1	14	61.1	10		20	14	1	14	10		20	65.6	31.9	83.1	61.1
10/4/2010	21	64.3	14	28.9	1	81.7	14	59.2	9		21	14	1	14	9		21	64.3	28.9	81.7	59.2
10/11/2010	22	62.1	14	26.9	0	80.8	14	56.6	9		22	14	0	14	9		22	62.1	26.9	80.8	56.6
10/18/2010	23	91	14	91		91		91			23						23	91	91	91	91
10/25/2010	24	91	14	91		91		91			24						24	91	91	91	91

Appendix B

Uni-directional Flow Flume Data

2012 09 28 flume data	Element	water depth at element (inches)	manometer reading	cfs from manometer	Torque (in-oz) tracking	Torque (in-oz) peak		Zero		Simplified Re	Simplified Cd	Integrated Re upper avg	Integrated Cd
f0	aluminum	4	0		0.12								
f1	aluminum	6.25	7.5	0.453985021	0.95	0.702		0.12		1.43E+03	1.07802868	1704.415594	1.03434205
f2	aluminum	6.75	15.5	0.662525868	1.145	1.548		0.12		1.93E+03	1.13493149	2216.2896	1.17956882
f3	aluminum	7	18	0.716172297	1.268	1.69		0.12		2.01E+03	1.10164361	2303.241905	1.15287723
f4	aluminum	7.25	22	0.795053977	1.541	2.205		0.12		2153.15884	1.11970285	2452.811383	1.18799912
f5	aluminum	7.5	27.5	0.893012747	1.683	2.296		0.12		2337.835	0.98724482	2642.610179	1.06456354
f6	aluminum	8	38	1.056794254	2.41	3.126	tilted shaf	0.12					
f7	aluminum	4	0	0	-0.217	-0.21	new zero						
f8	aluminum	8	37	1.042220862	1.839	2.416		-0.21		2557.92164	0.97003969	2872.692095	1.06132574
f9	steel	4	0	0	1.082	1.091							
f10	steel	8	37	1.042220862	3.26	4.116		1.082		2131.60137	1.2373332	2393.91008	1.35377303
f11	steel	7.7	29	0.918053016	2.787	3.961		1.082		1950.80227	1.23328413	2208.145697	1.32724434
f12	steel	7.25	22	0.795053977	2.468	3.195		1.082		1794.29903	1.31054875	2044.009486	1.39048567
f13	steel	6.75	14.5	0.639913751	1.931	2.234		1.082		1551.15032	1.20919825	1792.096252	1.2452592
f14	steel	6.5	10	0.527347783	1.801	2.019		1.082		1327.45554	1.48778161	1563.897412	1.47141722
f15	wood	4	0	0	-0.014	-0.009							
f16	wood	6	10.5	0.540916703	0.317	0.491		-0.014		1475.07926	0.63202972	1702.245269	0.65056398
f17	wood	6.8	17	0.69517137	0.793	1.068		-0.014		1672.70433	0.97644021	1914.541009	1.02464987
f18	wood	7.25	22	0.795053977	0.889	1.151		-0.014		1794.29903	0.85384237	2044.009486	0.90592248
f19	wood	7.5	28	0.90143063	1.05	1.501		-0.014		1966.56028	0.79147911	2220.539597	0.8552712
f20	wood	8	36.5	1.034863379	1.297	1.798		-0.014		2116.55349	0.7554139	2378.862194	0.82524223
f21	straw	4	0	0	-0.031	-0.024							
f22	straw	7.8	36.5	1.034863379	1.703	2.283		-0.03		2170.82409	0.99060998	2429.833185	1.09010369
f23	straw	7.5	28	0.90143063	1.231	1.572		-0.03		1966.56028	0.93802176	2220.539597	1.01362499
f24	straw	7.25	22	0.795053977	1.075	1.314		-0.03		1794.29903	1.04484587	2044.009486	1.10857624
f25	straw	6.75	17	0.69517137	0.903	1.129		-0.03		1685.09473	1.12597979	1926.040665	1.18460134
f26	straw	6.5	11.5	0.567155946	0.62	0.752		-0.03		1427.66183	1.16282114	1664.103707	1.17533226
f27	polytube	4	0	0	0.202	0.204							
f28	polytube	6	10.5	0.540916703	0.659	1.029		0.202		1770.09512	0.72718424	2042.694323	0.74850891
f29	polytube	7	17	0.69517137	1.535	2.11		0.202		1949.89533	1.35762761	2244.336127	1.40987506
f30	polytube	7.25	21	0.776026784	1.777	2.786		0.202		2101.62955	1.30265398	2401.282092	1.37393484
f31	polytube	7.5	28	0.90143063	2.011	2.774		0.202		2359.87234	1.12138605	2664.647517	1.21176818
f32	polytube	7.75	34	0.997328423	2.198	3.118		0.202		2526.7016	1.0215979	2836.514728	1.11756984
f33	foam	4	0	0	-0.069	-0.052							
f34	foam	7.75	34	0.997328423	0.907	1.66		-0.069		3445.50218	0.36632849	3867.974629	0.40074248
f35	foam	7.5	28	0.90143063	0.727	1.545		-0.069		3218.00773	0.36185208	3633.61025	0.39101685
f36	foam	7.25	22	0.795053977	0.772	1.475		-0.069		2936.12569	0.48596627	3344.742795	0.51560778
f37	foam	6.9	16	0.673569478	0.67	1.166		-0.069		2613.66152	0.58500777	3012.293451	0.605717
f38	foam	6.5	11	0.554179295	0.574	1.087		-0.069		2282.72174	0.73626661	2669.626624	0.73919029

Appendix C

Wave Flume Data

Explanation of Data

The following data was collected in 2012 in the hydraulics laboratory at the University of Minnesota Department of Bioproducts and Biosystems Engineering. The columns abbreviations are:

Torque = the summary torque value measured
Upstream RMS Peak to Peak = the RMS Peak to Peak wave height from the upstream sensor
Downstream RMS Peak to Peak = the RMS Peak to Peak wave height from the downstream sensor
D = water depth
L = calculated wave period
U = calculated summary orbital velocity
RE RMSP = Reynolds number calculated from RMS wave height calculated velocity values
KC RMSP = Kuelegan Carpenter number calculated from RMS wave height velocity values
CD RMS P = Drag Coefficient calculated from RMS wave height velocity values
CD rms simple adjustment = moment arm adjustment applied for velocity profile
RE Peak= Reynolds number calculated from peak wave height calculated velocity values
KC Peak = Kuelegan Carpenter number calculated from peak wave height velocity values
CD Peak = Drag Coefficient calculated from peak wave height velocity values
CDPeak simple adjustment = moment arm adjustment applied for velocity profile
RE Int = Reynolds number calculated from integrated torque and wave profiles
KC Int = Kuelegan Carpenter number calculated from integrated torque and wave profiles
CD Int = Drag Coefficient calculated from integrated torque and wave profiles
T Freq 1 = first frequency (s) of the torque data
T % 1 = the amount of the spectral density occupied by the first frequency
T Freq 2 = Second frequency (s) of the torque data
T % 2 = the amount of the spectral density occupied by the second frequency
H Freq 1 = first frequency (s) of the wave height data
H % 1 = the amount of the spectral density occupied by the first frequency
H Freq 2 = Second frequency (s) of the wave height data
H % 2 = the amount of the spectral density occupied by the second frequency

date	test	Element type	Torque (N-M)	Upstream RMS Peak to peak(M)	Downstream RMS Peak to peak (M)
9/21/2012	w1	wood	0.007024084	0.03507171	0.031507347
9/21/2012	w10	aluminum	0.014962441	0.04138964	0.035552997
9/21/2012	w11	aluminum	0.00565712	0.03351604	0.029523111
9/21/2012	w2	wood	0.005172888	0.02345265	0.022820159
9/21/2012	w3	Straw	0.008008464	0.03392028	0.031787829
9/21/2012	w4	straw	0.004286669	0.01985838	0.022617114
9/21/2012	w5	Vinyl tube	0.002996283	0.03360134	0.035979008
9/21/2012	w6	poly tube	0.004889461	0.03931128	0.036334248
9/21/2012	w7	poly tube	0.004491866	0.03204597	0.029739068
9/21/2012	w8	Foam	0.003009362	0.04221585	0.036586311
9/21/2012	w9	Foam	0.002771546	0.0289447	0.027440147
10/3/2012	w1	softstem bulrush	0.002089879	0.02013784	0.021919276
10/3/2012	w2	softstem bulrush	0.003118731	0.02906613	0.026162822
10/3/2012	w4	softstem bulrush	0.005442522	0.0442406	0.041285126
10/3/2012	w5	river bulrush	0.041385764	0.04476754	0.039602626
10/3/2012	w6	river bulrush	0.024426644	0.02643881	0.029478257
10/23/2012	w1	aluminum with dense network	0.005926283	0.03772942	0.031355299
10/23/2012	w2	aluminum with dense network	0.004823476	0.04253503	0.037482324
10/23/2012	w3	aluminum with dense network	0.003485645	0.03644443	0.033532663
10/23/2012	w4	aluminum with dense network	0.003359573	0.03403175	0.02993988
10/30/2012	w1	aluminum with dense network	0.007763928	0.04011417	0.036355449
10/30/2012	w13	aluminum	0.00994301	0.03870568	0.030211342
10/30/2012	w14	aluminum	0.008445495	0.04247121	0.039340882
10/30/2012	w15	aluminum	0.008478694	0.03348326	0.028762557
10/30/2012	w16	aluminum	0.007345864	0.03268758	0.021359668
10/30/2012	w17	aluminum	0.006130423	0.02433531	0.028176136
10/30/2012	w18	aluminum	0.006853099	0.03001271	0.023749948
10/30/2012	w19	Straw	0.008160018	0.03123183	0.02784904
10/30/2012	w2	aluminum with dense network	0.007927424	0.03382435	0.029725632
10/30/2012	w20	Straw	0.010440581	0.0325194	0.03005051
10/30/2012	w21	Straw	0.007822434	0.0321499	0.02369253
10/30/2012	w22	Straw	0.006045995	0.02905761	0.029223682
10/30/2012	w23	Straw	0.006710736	0.0295105	0.019042919
10/30/2012	w24	Straw	0.003804552	0.02101244	0.027219326
10/30/2012	w3	aluminum with dense network	0.00543126	0.03285284	0.022433367
10/30/2012	w4	aluminum with dense network	0.004606234	0.03160486	0.015072311
10/30/2012	w5	aluminum with dense network	0.003014865	0.02274002	0.029732733
10/30/2012	w6	aluminum with dense network	0.002153674	0.02868017	0.022331559
11/6/2012	w10	Poly Tube	0.010768108	0.03461126	0.027670955
11/6/2012	w11	Poly Tube	0.014986558	0.03219769	0.027475354
11/6/2012	w12	Poly Tube	0.009218113	0.0227313	0.028694294
11/6/2012	w13	Foam	0.003082335	0.02487193	0.024519337
11/6/2012	w14	Foam	0.002725596	0.03726171	0.032458567
11/6/2012	w15	Foam	0.002915785	0.02882645	0.027855671
11/6/2012	w16	Foam	0.005362584	0.03404694	0.021854049
11/6/2012	w17	Foam	0.003040312	0.03804137	0.033558737
11/6/2012	w18	Foam	0.003729073	0.02901724	0.014667733
11/6/2012	w7	Poly Tube	0.015231866	0.03973888	0.033096007
11/6/2012	w8	Poly Tube	0.017431134	0.04502197	0.041548127
11/6/2012	w9	Poly Tube	0.01186565	0.03548486	0.033188021
11/13/2012	w2	Straw with Dense network of 310 obstructions per meter	0.010334595	0.03507367	0.027027765
11/13/2012	w3	Straw with Dense network of 310 obstructions per meter	0.005707197	0.03693378	0.03065397
11/13/2012	w4	Straw with Dense network of 310 obstructions per meter	0.006787901	0.04469358	0.037838799
11/13/2012	w5	Straw with Dense network of 310 obstructions per meter	0.004560441	0.03763758	0.034524746
11/13/2012	w6	Straw with Dense network of 310 obstructions per meter	0.006214063	0.03261476	0.013207286
11/13/2012	w7	Straw with Dense network of 310 obstructions per meter	0.002423453	0.02262235	0.02755215
11/15/2012	w1	Foam with Dense network of 310 obstructions per meter	0.003804648	0.03926987	0.031289807
11/15/2012	w3	Foam with Dense network of 310 obstructions per meter	0.00322092	0.03571494	0.033484989

date	test	Element type	Torque (N-M)	Upstream RMS Peak to peak(M)	Downstream RMS Peak to peak (M)
11/15/2012	w1	Foam with Dense network of 310 obstructions per meter	0.003804648	0.03926987	0.031289807
11/15/2012	w3	Foam with Dense network of 310 obstructions per meter	0.00322092	0.03571494	0.033484989
11/15/2012	w4	Foam with Dense network of 310 obstructions per meter	0.003065035	0.03657728	0.025891453
11/15/2012	w5	Foam with Dense network of 310 obstructions per meter	0.003025597	0.02812976	0.023544935
11/15/2012	w6	Foam with Dense network of 310 obstructions per meter	0.002326656	0.01822208	0.019148513
11/20/2012	w10	Foam with Dense network of 155 obstructions per meter	0.001221297	0.02638283	0.023229847
11/20/2012	w3	Foam with Dense network of 310 obstructions per meter	0.002233643	0.03534191	0.027152721
11/20/2012	w4	Foam with Dense network of 155 obstructions per meter	0.001840715	0.03810138	0.029526303
11/20/2012	w6	Foam with Dense network of 155 obstructions per meter	0.002947516	0.03523523	0.027514011
11/20/2012	w7	Foam with Dense network of 155 obstructions per meter	0.00146338	0.03900654	0.031817525
11/20/2012	w8	Foam with Dense network of 155 obstructions per meter	0.001755362	0.03148062	0.023609193
11/20/2012	w9	Foam with Dense network of 155 obstructions per meter	0.00200803	0.02738704	0.021316656
11/27/2012	w10	Poly tube with medium network of 198 obstructions per meter	0.010287179	0.03710146	0.02961895
11/27/2012	w11	Poly tube with medium network of 198 obstructions per meter	0.007534208	0.03072002	0.024485168
11/27/2012	w12	Poly tube with medium network of 198 obstructions per meter	0.006283774	0.03025757	0.012337638
11/27/2012	w13	Poly tube with medium network of 198 obstructions per meter	0.005088827	0.02331627	0.022501187
11/27/2012	w2	Foam with thin network of 86 obstructions per meter	0.002610214	0.03586682	0.031417939
11/27/2012	w3	Foam with thin network of 86 obstructions per meter	0.003829187	0.03433717	0.025669721
11/27/2012	w4	Foam with thin network of 86 obstructions per meter	0.002802775	0.03740717	0.032058774
11/27/2012	w5	Foam with thin network of 86 obstructions per meter	0.003247201	0.03147375	0.021521648
11/27/2012	w6	Foam with thin network of 86 obstructions per meter	0.003336094	0.02517912	0.02256126
11/27/2012	w7	Foam with thin network of 86 obstructions per meter	0.002747146	0.02845312	0.023680186
11/27/2012	w8	Poly tube with medium network of 198 obstructions per meter	0.008959914	0.03147738	0.029582072
11/27/2012	w9	Poly tube with medium network of 198 obstructions per meter	0.010154175	0.03461078	0.023359713
12/4/2012	w1	Poly tube with medium network of 155 obstructions per meter	0.011901122	0.0356477	0.02749279
12/4/2012	w10	Poly tube with light network of 86 obstructions per meter	0.007622869	0.03019243	0.019967631
12/4/2012	w11	Poly tube with light network of 86 obstructions per meter	0.008641536	0.02499454	0.022118122
12/4/2012	w12	Poly tube with light network of 86 obstructions per meter	0.005747824	0.02631842	0.021956203
12/4/2012	w13	Straws with medium network of 155 obstructions per meter	0.006412518	0.0337727	0.030305323
12/4/2012	w14	Straws with medium network of 155 obstructions per meter	0.006694845	0.03508422	0.024632695
12/4/2012	w15	Straws with medium network of 155 obstructions per meter	0.005692418	0.02898794	0.022865767
12/4/2012	w16	Straws with medium network of 155 obstructions per meter	0.003511367	0.03253456	0.029375274
12/4/2012	w17	Straws with medium network of 155 obstructions per meter	0.00441006	0.02884492	0.013483464
12/4/2012	w18	Straws with medium network of 155 obstructions per meter	0.002289549	0.02249345	0.022550001
12/4/2012	w19	Straws with light network of 86 obstructions per meter	0.005982505	0.0313611	0.030883976
12/4/2012	w2	Poly tube with medium network of 155 obstructions per meter	0.010324022	0.03775187	0.03207895
12/4/2012	w20	Straws with light network of 86 obstructions per meter	0.006706779	0.03470884	0.02567645
12/4/2012	w21	Straws with light network of 86 obstructions per meter	0.005742599	0.02995203	0.022618786
12/4/2012	w22	Straws with light network of 86 obstructions per meter	0.003751054	0.03417146	0.030200262
12/4/2012	w23	Straws with light network of 86 obstructions per meter	0.004391289	0.02894821	0.014360144
12/4/2012	w24	Straws with light network of 86 obstructions per meter	0.002270435	0.02454588	0.024230369
12/4/2012	w3	Poly tube with medium network of 155 obstructions per meter	0.007892879	0.03234243	0.024694136
12/4/2012	w4	Poly tube with medium network of 155 obstructions per meter	0.006682754	0.03208994	0.016967866
12/4/2012	w5	Poly tube with medium network of 155 obstructions per meter	0.007676931	0.02217016	0.022982427
12/4/2012	w6	Poly tube with medium network of 155 obstructions per meter	0.004360471	0.01691634	0.017093288
12/4/2012	w7	Poly tube with light network of 86 obstructions per meter	0.010201765	0.03507233	0.029990154
12/4/2012	w8	Poly tube with light network of 86 obstructions per meter	0.010751151	0.03423363	0.023772099
12/4/2012	w9	Poly tube with light network of 86 obstructions per meter	0.00872244	0.03616644	0.03161329
12/11/2012	w1	Aluminum rod with medium network of 142 obstructions per meter	0.01188271	0.03436819	0.026742115
12/11/2012	w2	Aluminum rod with medium network of 142 obstructions per meter	0.009724476	0.03158186	0.026195604
12/11/2012	w3	Aluminum rod with medium network of 142 obstructions per meter	0.009315737	0.03184931	0.019132658
12/11/2012	w4	Aluminum rod with medium network of 142 obstructions per meter	0.009649986	0.02851787	0.020994763
12/11/2012	w5	Aluminum rod with medium network of 142 obstructions per meter	0.008268359	0.02360977	0.023692462
12/11/2012	w6	Aluminum rod with medium network of 142 obstructions per meter	0.00587348	0.01739589	0.010774066
12/11/2012	w7	Aluminum rod with medium network of 86 obstructions per meter	0.010465486	0.03320154	0.024699751
12/11/2012	w8	Aluminum rod with medium network of 86 obstructions per meter	0.007963208	0.03553661	0.031775466
12/11/2012	w9	Aluminum rod with medium network of 86 obstructions per meter	0.008303711	0.03017929	0.021125673
12/11/2012	w10	Aluminum rod with medium network of 86 obstructions per meter	0.007893986	0.03051323	0.016061913
12/11/2012	w11	Aluminum rod with medium network of 86 obstructions per meter	0.006909171	0.02324315	0.024161411
12/11/2012	w12	Aluminum rod with medium network of 86 obstructions per meter	0.00465229	0.01746059	0.016925904

date	test	Upstream water level (M)	downstream water level (m)	stem width (m)	Period (s)	2x H downstream peak to peak wave height(m)	d	L=	u =	Re HrmsP	KC HrmsP	Cd HrmsP	Cd HrmsP Simple adjustment
9/21/2012	w1	0.22	0.225	0.0055	0.88	0.063014694	0.225	1.054174	0.258019	1419.103	41.283	1.771741	1.812121259
9/21/2012	w10	0.215	0.22	0.0066	0.82	0.071105995	0.22	0.943428	0.303145	2000.757	37.66346	2.534621	1.942837142
9/21/2012	w11	0.22	0.225	0.0066	1.01	0.059046222	0.225	1.278326	0.228829	1510.271	35.01776	1.318452	1.58032419
9/21/2012	w2	0.22	0.225	0.0055	1.07	0.045640318	0.225	1.379844	0.173597	954.7819	33.77245	2.394419	1.505304263
9/21/2012	w3	0.22	0.225	0.0055	0.88	0.063575658	0.225	1.054376	0.260266	1431.462	41.64254	1.985021	1.811859244
9/21/2012	w4	0.22	0.225	0.0055	1.07	0.045234228	0.225	1.37984	0.172053	946.2893	33.47205	2.019986	1.505306883
9/21/2012	w5	0.22	0.225	0.006477	0.85	0.071958016	0.225	1.001586	0.299536	1940.094	39.30917	0.495219	1.884508142
9/21/2012	w6	0.22	0.225	0.0066	0.84	0.072668497	0.225	0.98386	0.30432	2008.515	38.73169	0.779065	1.910865581
9/21/2012	w7	0.22	0.225	0.0066	1	0.059478135	0.225	1.261314	0.231299	1526.571	35.04525	1.033778	1.594418643
9/21/2012	w8	0.22	0.225	0.009	0.82	0.073172622	0.225	0.948439	0.310307	2792.767	28.27246	0.348088	1.966769843
9/21/2012	w9	0.22	0.225	0.009	1.01	0.054880293	0.225	1.27833	0.212683	1914.151	23.86781	0.548335	1.580320718
10/3/2012	w1	0.195	0.205	0.0035	0.95	0.043838552	0.205	1.141846	0.1789	626.1514	48.55868	1.779568	1.607396473
10/3/2012	w2	0.195	0.205	0.0035	0.8	0.052325644	0.205	0.893159	0.229887	804.6049	52.54563	1.927739	1.926666888
10/3/2012	w4	0.195	0.205	0.005	0.85	0.082570251	0.205	0.977069	0.352335	1761.677	59.89701	0.9353	1.797513269
10/3/2012	w5	0.195	0.205	0.009	0.85	0.079205252	0.205	0.977069	0.337977	3041.789	31.92001	4.294063	1.797513269
10/3/2012	w6	0.195	0.205	0.009	0.95	0.058956514	0.205	1.141841	0.240596	2165.367	25.39628	4.472279	1.6074015
10/23/2012	w1	0.219	0.234	0.0066	0.81	0.062710598	0.234	0.938606	0.265449	1751.965	32.57786	1.242674	2.04122019
10/23/2012	w2	0.209	0.224	0.0066	0.83	0.074964649	0.224	0.965129	0.316219	2087.046	39.76695	0.725562	1.933592058
10/23/2012	w3	0.203	0.216	0.0066	0.84	0.067065326	0.216	0.973833	0.283747	1872.733	36.11331	0.668575	1.870272197
10/23/2012	w4	0.192	0.207	0.0066	0.84	0.059879761	0.207	0.963046	0.256184	1690.811	32.60517	0.82903	1.82987517
10/30/2012	w1	0.225	0.24	0.0066	0.81	0.072710899	0.24	0.943789	0.30609	2020.191	37.56553	1.191007	2.07061585
10/30/2012	w13	0.225	0.237	0.0066	0.77	0.060422685	0.237	0.867596	0.263034	1736.025	30.68731	2.236599	2.195862766
10/30/2012	w14	0.219	0.234	0.0066	0.81	0.078681764	0.234	0.93861	0.333053	2198.148	40.87466	1.124956	2.041214346
10/30/2012	w15	0.218	0.23	0.0066	0.86	0.057525114	0.23	1.024658	0.236819	1563.003	30.85819	2.117961	1.881060452
10/30/2012	w16	0.212	0.225	0.0066	0.87	0.042719336	0.225	1.036689	0.175847	1160.589	23.1798	3.366808	1.835267996
10/30/2012	w17	0.21	0.222	0.0066	0.93	0.056352272	0.222	1.136551	0.226175	1492.754	31.8701	1.607094	1.698689744
10/30/2012	w18	0.206	0.22	0.0066	1.02	0.047499895	0.22	1.285622	0.18485	1220.008	28.56767	2.495622	1.552938078
10/30/2012	w19	0.201	0.215	0.0055	0.71	0.055698079	0.215	0.74604	0.260001	1430.006	33.56379	2.784328	2.310347073
10/30/2012	w2	0.221	0.234	0.0066	0.86	0.059451263	0.234	1.029083	0.243696	1608.393	31.75431	1.834096	1.898185027
10/30/2012	w20	0.199	0.214	0.0055	0.75	0.06010102	0.214	0.815427	0.271142	1491.281	36.97391	3.057751	2.140227481
10/30/2012	w21	0.196	0.21	0.0055	0.78	0.047385059	0.21	0.864206	0.209777	1.15E+03	29.75017	3.71286	2.013274767
10/30/2012	w22	0.195	0.209	0.0055	0.81	0.058447364	0.209	0.914547	0.253912	1396.516	37.3943	1.880562	1.917923889
10/30/2012	w23	0.193	0.207	0.0055	0.88	0.038085838	0.207	1.029913	0.159619	877.9044	25.53904	4.867508	1.740031928
10/30/2012	w24	0.191	0.205	0.0055	0.95	0.054438651	0.205	1.141838	0.22216	1221.878	38.37304	1.336892	1.607403578
10/30/2012	w3	0.217	0.23	0.0066	0.87	0.044866735	0.23	1.042652	0.18363	1211.957	24.20576	2.226456	1.856018111
10/30/2012	w4	0.212	0.225	0.0066	0.88	0.030144621	0.225	1.054214	0.123425	814.6041	16.45665	4.231165	1.812068787
10/30/2012	w5	0.208	0.222	0.0066	0.94	0.059465465	0.222	1.153711	0.237648	1568.478	33.84687	0.708276	1.680654626
10/30/2012	w6	0.205	0.218	0.0066	1.03	0.044663118	0.218	1.298274	0.173804	1147.104	27.12391	0.890003	1.534809221
11/6/2012	w10	0.216	0.231	0.0066	0.87	0.05534191	0.231	1.043755	0.226263	1493.336	29.82559	2.893303	1.860260179
11/6/2012	w11	0.215	0.229	0.0066	0.92	0.054950708	0.229	1.129511	0.219538	1448.951	30.60228	4.064608	1.742596106
11/6/2012	w12	0.21	0.224	0.0066	0.96	0.057388588	0.224	1.19127	0.226843	1497.165	32.99536	2.303502	1.65299573
11/6/2012	w13	0.202	0.217	0.009	0.7	0.049038673	0.217	0.729469	0.230818	2077.358	17.95248	0.823935	2.369763882
11/6/2012	w14	0.197	0.211	0.009	0.73	0.064917134	0.211	0.778497	0.298582	2687.241	24.21834	0.423078	2.199634641
11/6/2012	w15	0.193	0.208	0.009	0.76	0.055711342	0.208	0.828067	0.250802	2257.217	21.17882	0.617663	2.069153909
11/6/2012	w16	0.189	0.204	0.009	0.79	0.043708098	0.204	0.8754	0.193473	1741.261	16.98267	1.857172	1.950543134
11/6/2012	w17	0.185	0.201	0.009	0.83	0.067117474	0.201	0.938788	0.291062	2619.555	26.84235	0.446431	1.827318725
11/6/2012	w18	0.184	0.198	0.009	0.9	0.029335465	0.198	1.048866	0.123468	1111.212	12.3468	2.843741	1.666654723
11/6/2012	w7	0.235	0.249	0.0066	0.79	0.066192013	0.249	0.913081	0.280907	1853.985	33.62369	2.754247	2.185471351
11/6/2012	w8	0.23	0.244	0.0066	0.82	0.083096255	0.244	0.965552	0.346146	2284.561	43.00597	2.021983	2.058101599
11/6/2012	w9	0.225	0.24	0.0066	0.87	0.066376042	0.24	1.053723	0.268808	1774.136	35.43385	2.163327	1.897957578
11/13/2012	w2	0.223	0.237	0.0055	0.79	0.054055531	0.237	0.904495	0.231579	1273.687	33.26322	3.479338	2.12291455
11/13/2012	w3	0.22	0.232	0.0055	0.74	0.061307939	0.232	0.809548	0.274881	1511.847	36.98402	1.521811	2.286845172
11/13/2012	w4	0.214	0.228	0.0055	0.82	0.075677599	0.228	0.951348	0.319949	1759.719	47.70147	1.191087	1.981138616
11/13/2012	w5	0.211	0.225	0.0055	0.84	0.069049492	0.225	0.983843	0.28917	1590.433	44.1641	0.965746	1.910890812
11/13/2012	w6	0.209	0.222	0.0055	0.9	0.026414573	0.222	1.084826	0.107489	591.1908	17.58915	8.953235	1.757225168
11/13/2012	w7	0.206	0.22	0.0055	0.96	0.0551043	0.22	1.184563	0.219047	1204.759	38.23367	0.796527	1.640154419

date	test	Upstream water level (M)	downstream water level (m)	stem width (m)	Period (s)	2x H downstream peak to peak wave height(m)	d	L=	u =	Re HrmsP	KC HrmsP	Cd HrmsP	Cd HrmsP Simple adjustment
11/15/2012	w1	0.23	0.244	0.009	0.8	0.062579614	0.244	0.92834	0.264518	2380.659	23.51268	0.572002	2.124165175
11/15/2012	w3	0.228	0.242	0.009	0.88	0.066969977	0.242	1.074217	0.269098	2421.879	26.31177	0.420065	1.881091866
11/15/2012	w4	0.227	0.241	0.009	0.88	0.051782906	0.241	1.073273	0.208256	1874.305	20.36282	0.670486	1.876793105
11/15/2012	w5	0.227	0.241	0.009	0.95	0.04708987	0.241	1.199948	0.182864	1645.774	19.30228	0.789695	1.726513346
11/15/2012	w6	0.226	0.24	0.009	1.04	0.038297025	0.24	1.358081	0.143851	1294.656	16.62274	0.904575	1.580536396
11/20/2012	w10	0.208	0.223	0.009	0.97	0.046459695	0.223	1.206691	0.183185	1648.669	19.74332	0.341673	1.633615215
11/20/2012	w3	0.219	0.234	0.009	0.79	0.054305443	0.234	0.902232	0.233234	2099.103	20.47273	0.459285	2.107182173
11/20/2012	w4	0.211	0.226	0.009	0.74	0.059052605	0.226	0.805986	0.265939	2393.453	21.86612	0.329319	2.250703357
11/20/2012	w6	0.211	0.226	0.009	0.78	0.055028021	0.226	0.87778	0.239846	2158.61	20.78662	0.604772	2.099530593
11/20/2012	w7	0.21	0.224	0.009	0.83	0.063635051	0.224	0.964914	0.268488	2416.391	24.76055	0.223963	1.933930467
11/20/2012	w8	0.208	0.223	0.009	0.88	0.047218386	0.223	1.05151	0.193829	1744.463	18.95219	0.48444	1.804226825
11/20/2012	w9	0.208	0.222	0.009	0.94	0.042633312	0.222	1.153704	0.170381	1533.43	17.79536	0.67303	1.680661928
11/27/2012	w10	0.201	0.216	0.0066	0.82	0.0592379	0.216	0.939122	0.253706	1674.458	31.52102	2.538953	1.923946887
11/27/2012	w11	0.201	0.214	0.0066	0.88	0.048970337	0.214	1.039541	0.203335	1342.014	27.11139	2.701292	1.7681958
11/27/2012	w12	0.2	0.214	0.0066	0.9	0.024675277	0.214	1.073627	0.101459	669.6288	13.83531	8.836623	1.726697973
11/27/2012	w13	0.2	0.212	0.0066	0.98	0.045002374	0.212	1.203832	0.179694	1185.983	26.68189	2.125964	1.584603541
11/27/2012	w2	0.211	0.225	0.009	0.76	0.062835878	0.225	0.841293	0.278428	2505.852	23.5117	0.413012	2.166040338
11/27/2012	w3	0.21	0.223	0.009	0.79	0.051339442	0.223	0.893249	0.222713	2004.414	19.54922	0.909339	2.049688365
11/27/2012	w4	0.208	0.223	0.009	0.85	0.064117548	0.223	0.999234	0.267527	2407.744	25.26645	0.422159	1.875866693
11/27/2012	w5	0.206	0.222	0.009	0.89	0.043043296	0.222	1.067648	0.175998	1583.978	17.4042	1.079178	1.778157478
11/27/2012	w6	0.205	0.219	0.009	0.95	0.04512252	0.219	1.165938	0.180335	1623.016	19.03538	1.004081	1.653375644
11/27/2012	w7	0.201	0.216	0.009	1.03	0.047360372	0.216	1.294353	0.184858	1663.723	21.15598	0.74445	1.529336181
11/27/2012	w8	0.203	0.217	0.0066	0.76	0.059164145	0.217	0.8354	0.264008	1742.451	30.40089	2.233709	2.120372079
11/27/2012	w9	0.203	0.215	0.0066	0.78	0.046719426	0.215	0.868748	0.205749	1357.942	24.31577	4.071348	2.040078979
12/4/2012	w1	0.213	0.228	0.0066	0.81	0.054985581	0.228	0.933436	0.234039	1544.658	28.72297	3.301945	2.0113403
12/4/2012	w10	0.201	0.215	0.0066	0.89	0.039935263	0.215	1.057919	0.164791	1087.62	22.22181	4.089468	1.751030334
12/4/2012	w11	0.2	0.212	0.0066	0.94	0.044236245	0.212	1.137544	0.179299	1183.37	25.53646	3.768293	1.64672352
12/4/2012	w12	0.199	0.211	0.0066	1.03	0.043912407	0.211	1.283779	0.172812	1140.557	26.9691	2.503381	1.516123945
12/4/2012	w13	0.198	0.211	0.0055	0.75	0.060610647	0.211	0.813307	0.274154	1507.847	37.38463	1.864022	2.122242709
12/4/2012	w14	0.197	0.211	0.0055	0.8	0.049265389	0.211	0.8996	0.214893	1181.909	31.2571	2.920248	1.956615279
12/4/2012	w15	0.195	0.208	0.0055	0.8	0.045731534	0.208	0.896529	0.200161	1100.888	29.11439	2.906743	1.941449347
12/4/2012	w16	0.195	0.209	0.0055	0.84	0.058750547	0.209	0.965398	0.25074	1379.07	38.29485	1.073903	1.838999092
12/4/2012	w17	0.194	0.208	0.0055	0.91	0.026966929	0.208	1.081245	0.111324	612.2807	18.41902	6.319687	1.68531969
12/4/2012	w18	0.192	0.206	0.0055	0.96	0.045100002	0.206	1.159969	0.18308	1006.939	31.95574	1.16652	1.59535227
12/4/2012	w19	0.195	0.207	0.0055	0.76	0.061767952	0.207	0.827284	0.278331	1530.82	38.46026	1.692288	2.063314475
12/4/2012	w2	0.211	0.224	0.0066	0.83	0.064157899	0.224	0.965121	0.270636	1786.197	34.03451	2.120176	1.933604624
12/4/2012	w20	0.193	0.206	0.0055	0.79	0.051352899	0.206	0.877423	0.226789	1247.34	32.57516	2.737202	1.96096935
12/4/2012	w21	0.193	0.206	0.0055	0.8	0.045237573	0.206	0.894432	0.198464	1091.55	28.86743	3.01422	1.931353925
12/4/2012	w22	0.192	0.205	0.0055	0.85	0.060400524	0.205	0.977071	0.257734	1417.539	39.83168	1.095162	1.797510448
12/4/2012	w23	0.191	0.205	0.0055	0.91	0.028720289	0.205	1.07638	0.119098	655.0375	19.70526	5.593225	1.674475517
12/4/2012	w24	0.19	0.204	0.0055	0.97	0.048460739	0.204	1.172468	0.196653	1081.589	34.68237	1.005261	1.57443316
12/4/2012	w3	0.21	0.224	0.0066	0.89	0.049388272	0.224	1.07013	0.201473	1329.72	27.16828	2.701827	1.786193256
12/4/2012	w4	0.208	0.222	0.0066	0.9	0.033935732	0.222	1.085027	0.13807	911.2597	18.82768	4.862422	1.756985151
12/4/2012	w5	0.208	0.22	0.0066	0.95	0.045964855	0.22	1.167611	0.183438	1210.693	26.40401	3.028397	1.656649458
12/4/2012	w6	0.206	0.22	0.0066	1.05	0.034186576	0.22	1.335704	0.131818	869.9967	20.97099	3.04803	1.515857112
12/4/2012	w7	0.204	0.216	0.0066	0.76	0.059980307	0.216	0.834624	0.267898	1768.13	30.84891	2.48201	2.11466895
12/4/2012	w8	0.203	0.215	0.0066	0.79	0.047544197	0.215	0.886113	0.20791	1372.204	24.88616	4.154975	2.007897658
12/4/2012	w9	0.202	0.215	0.0066	0.83	0.06322658	0.215	0.95533	0.269441	1778.31	33.88424	1.89126	1.891990977
12/11/2012	w1	0.21	0.225	0.0066	0.81	0.053484229	0.225	0.930633	0.228334	1507.006	28.02284	3.51406	1.996600785
12/11/2012	w2	0.21	0.223	0.0066	0.87	0.052391207	0.223	1.034238	0.21617	1426.724	28.49518	2.979401	1.826987028
12/11/2012	w3	0.207	0.221	0.0066	0.9	0.038265317	0.221	1.083609	0.155889	1028.865	21.25754	5.345267	1.753222832
12/11/2012	w4	0.207	0.22	0.0066	0.94	0.041989527	0.22	1.15062	0.168258	1110.503	23.96403	4.571401	1.673784249
12/11/2012	w5	0.206	0.22	0.0066	0.97	0.047384925	0.22	1.201536	0.187635	1238.392	27.57668	3.056392	1.624214185
12/11/2012	w6	0.203	0.217	0.0066	1.09	0.021548132	0.217	1.395224	0.082572	544.9733	13.63684	10.34212	1.464982915
12/11/2012	w7	0.202	0.217	0.0066	0.8	0.049399501	0.217	0.905294	0.214122	1413.207	25.95422	3.717527	1.987350593
12/11/2012	w8	0.201	0.215	0.0066	0.84	0.063550932	0.215	0.972564	0.269229	1776.912	34.26552	1.70554	1.865934352
12/11/2012	w9	0.2	0.214	0.0066	0.88	0.042251345	0.214	1.039684	0.175413	1157.723	23.38835	4.000058	1.768014929
12/11/2012	w10	0.2	0.213	0.0066	0.91	0.032123826	0.213	1.088977	0.131671	869.0264	18.15459	6.553084	1.703632673
12/11/2012	w11	0.199	0.211	0.0066	0.96	0.048322822	0.211	1.169004	0.194646	1284.667	28.31222	2.520809	1.611283575
12/11/2012	w12	0.198	0.211	0.0066	1.05	0.033851807	0.211	1.316259	0.132455	874.2038	21.07241	3.396514	1.49303131

date	test	Re Peak	KC Peak	Cd Peak	Cd peak Simple adjustment	Re Hrms	KC Hrms	Cd Hrms	Cd Hrms Simple adjustment	Cd IntT	Re IntT	KC IntT	URMS
9/21/2012	w1	1622.115	47.18881	1.121316	1.81212126					0.403533	1298.632	37.77838	0.236115
9/21/2012	w10	2493.749	46.94385	1.871396	1.94283714					0.423782	2005.48	37.75238	0.303861
9/21/2012	w11	1083.248	25.11664	2.957707	1.58032419					0.559753	1115.284	25.85943	0.168982
9/21/2012	w2	877.3705	31.03426	2.366287	1.50530426					0.41782	1069.853	37.84274	0.194519
9/21/2012	w3	1588.401	46.20803	1.271556	1.81185924					0.517642	1240.504	36.08738	0.225546
9/21/2012	w4	883.6364	31.2559	2.184328	1.50530688					0.44402	937.5187	33.16182	0.170458
9/21/2012	w5	2297.483	46.55039	0.416894	1.88450814					0.118174	1754.781	35.55446	0.270925
9/21/2012	w6	2256.431	43.51244	0.578429	1.91086558					0.17237	1827.971	35.25013	0.276965
9/21/2012	w7	1051.862	24.14743	2.113867	1.59441864					0.442515	1120.773	25.7294	0.169814
9/21/2012	w8	2373.378	24.02679	0.561799	1.96676984					0.147069	1936.041	19.59943	0.215116
9/21/2012	w9	1479.576	18.44903	1.022431	1.58032072					0.251308	1366.074	17.03376	0.151786
10/3/2012	w1	532.0171	41.25847	1.440996	1.60739647					0.606145	516.7669	40.0758	0.147648
10/3/2012	w2	993.6268	64.88991	1.389518	1.92666689					0.339971	853.1999	55.71917	0.243771
10/3/2012	w4	1867.681	63.50116	1.134373	1.79751327					0.210285	1567.116	53.28193	0.313423
10/3/2012	w5	3307.43	34.7076	3.93291	1.79751327					1.089208	2737.079	28.72243	0.30412
10/3/2012	w6	2474.81	29.02555	5.531495	1.6074015					0.870939	2223.574	26.07895	0.247064
10/23/2012	w1	2056.155	38.23429	1.267283	2.04122019					0.217329	1629.116	30.29348	0.246836
10/23/2012	w2	2517.104	47.96135	0.790493	1.93359206					0.150521	1910.017	36.3938	0.289396
10/23/2012	w3	2034.776	39.2381	0.672915	1.8702722					0.182137	1651.098	31.83936	0.250166
10/23/2012	w4	1933.703	37.28904	1.041317	1.82987517					0.171785	1518.712	29.28645	0.230108
10/30/2012	w1	2357.242	43.83301	1.045829	2.0706124					0.236055	1892.24	35.18628	0.286703
10/30/2012	w13	2095.469	37.04112	1.613739	2.19586277					0.422263	1615.39	28.55488	0.244756
10/30/2012	w14	2564.499	47.68696	0.798265	2.04121435					0.23383	2021.516	37.59017	0.30629
10/30/2012	w15	1743.106	34.41393	1.940324	1.88106045					0.554877	1392.889	27.49965	0.211044
10/30/2012	w16	1241.656	24.79892	3.054035	1.835268					0.956063	1019.205	20.35602	0.154425
10/30/2012	w17	1710.609	36.52126	1.296569	1.69868974					0.339514	1490.817	31.82873	0.225881
10/30/2012	w18	842.2479	19.72206	7.472648	1.55293808					1.019945	923.8352	21.63251	0.139975
10/30/2012	w19	1592.929	37.38776	2.687591	2.31034707					0.575135	1238.259	29.06328	0.225138
10/30/2012	w2	2064.593	40.76102	1.667101	1.89818509					0.35989	1487.072	29.35908	0.225314
10/30/2012	w20	1707.468	42.33391	3.088148	2.14022748					0.619206	1364.948	33.8417	0.248172
10/30/2012	w21	1405.998	36.25384	3.078325	2.01327477					0.820346	1074.31	27.70123	0.195329
10/30/2012	w22	1606.058	43.00518	1.699008	1.91792389					0.431525	1284.07	34.38336	0.233467
10/30/2012	w23	831.4199	24.18676	6.613991	1.74003193					1.916379	686.621	19.97443	0.12484
10/30/2012	w24	1489.003	46.76209	1.198382	1.60740358					0.270219	1251.943	39.31722	0.227626
10/30/2012	w3	1319.927	26.36217	2.262163	1.85601811					0.721563	987.8823	19.73043	0.149679
10/30/2012	w4	811.6195	16.39635	3.622696	1.81206879					1.573122	650.9868	13.15125	0.098634
10/30/2012	w5	1595.597	34.43208	0.563453	1.68065463					0.172056	1461.229	31.53249	0.221398
10/30/2012	w6	1028.738	24.32508	0.998893	1.53480922					0.307321	953.3045	22.54141	0.14444
11/6/2012	w10	1603.747	32.03076	3.378829	1.86026018					0.809082	1279.503	25.55482	0.193864
11/6/2012	w11	1597.827	33.74657	4.695715	1.74259611					0.982356	1368.894	28.91144	0.207408
11/6/2012	w12	1571.702	34.63806	3.534067	1.65299573					0.536263	1393.077	30.70142	0.211072
11/6/2012	w13	2197.576	18.9914	1.089452	2.36976388					0.181307	1752.059	15.14125	0.194673
11/6/2012	w14	3108.074	28.01104	0.454611	2.19963464					0.085633	2457.136	22.14456	0.273015
11/6/2012	w15	2351.484	22.06331	0.834838	2.06915391					0.157288	1901.615	17.84232	0.211291
11/6/2012	w16	1931.593	18.83899	2.06472	1.95054313					0.459164	1549.406	15.11149	0.172156
11/6/2012	w17	2764.116	28.32366	0.562388	1.82731872					0.137203	2142.29	21.95186	0.238032
11/6/2012	w18	1173.886	13.04318	3.270543	1.66665472					0.878163	1020.971	11.34412	0.113441
11/6/2012	w7	2373.04	43.03722	2.070694	2.18547135					0.449562	1922.233	34.86143	0.291247
11/6/2012	w8	2767.847	52.10364	1.773932	2.0581016					0.413241	2160.258	40.66602	0.327312
11/6/2012	w9	2014.432	40.23315	2.220436	1.89795758					0.532261	1596.846	31.89292	0.241946
11/13/2012	w2	1531.32	39.9915	3.484236	2.12291455					0.665867	1222.52	31.92698	0.222276
11/13/2012	w3	1687.186	41.27331	1.7844	2.28684517					0.296161	1362.301	33.32571	0.247691
11/13/2012	w4	2128.657	57.70245	1.19118	1.98113862					0.264287	1576.305	42.72959	0.286601
11/13/2012	w5	1813.115	50.34765	1.165275	1.91089081					0.222464	1403.215	38.96531	0.25513
11/13/2012	w6	465.5654	13.85153	17.7915	1.75722517					4.156668	438.6792	13.05161	0.07976
11/13/2012	w7	1351.545	42.89201	0.890687	1.64015442					0.183677	1146.306	36.37864	0.208419

date	test	Re Peak	KC Peak	Cd Peak	Cd peak Simple adjustment	Re Hrms	KC Hrms	Cd Hrms	Cd Hrms Simple adjustment	Cd IntT	Re IntT	KC IntT	URMS
11/15/2012	w1	2780.983	27.4665	0.573113	2.12416517					0.124941	2096.11	20.70232	0.232901
11/15/2012	w3	2526.455	27.44791	0.452804	1.88109187					0.109538	2109.842	22.92174	0.234427
11/15/2012	w4	1881.394	20.43984	0.852	1.8767931					0.205645	1526.132	16.5802	0.16957
11/15/2012	w5	1708.163	20.03401	0.852	1.72869029					0.229247	1423.132	16.69105	0.158126
11/15/2012	w6	869.5773	11.16494	2.185381	1.5805364					0.422963	932.704	11.97546	0.103634
11/20/2012	w10	1363.578	16.32927	0.622363	1.63361522					0.145774	1197.749	14.34341	0.133083
11/20/2012	w3	2523.818	24.61502	0.283219	2.10718217					0.09326	1968.946	19.2033	0.218772
11/20/2012	w4	2967.208	27.10783	0.173256	2.25070336					0.058606	2271.74	20.75417	0.252416
11/20/2012	w6	2337.199	22.50636	0.35528	2.09953059					0.150704	1813.483	17.46317	0.201498
11/20/2012	w7	2758.498	28.26609	0.198839	1.93393047					0.052198	2206.898	22.61389	0.245211
11/20/2012	w8	1815.392	19.72278	0.499086	1.79827775					0.151562	1430.1	15.53689	0.1589
11/20/2012	w9	1678.03	19.47344	0.566485	1.68066193					0.177793	1424.543	16.53174	0.158283
11/27/2012	w10	1665.533	31.35301	3.278563	1.92394689					0.784185	1343.025	25.28193	0.203489
11/27/2012	w11	1431.432	28.91781	3.449776	1.7681958					0.722688	1170.478	23.64603	0.177345
11/27/2012	w12	811.2007	16.76035	8.741501	1.72669797					1.928178	692.5919	14.30975	0.104938
11/27/2012	w13	1026.722	23.09889	4.178655	1.58460354					1.004486	838.292	18.85965	0.127014
11/27/2012	w2	3016.856	28.3063	0.339948	2.16604034					0.072786	2368.988	22.22754	0.263221
11/27/2012	w3	1979.168	19.30299	1.331233	2.04968836					0.260535	1606.191	15.66532	0.178466
11/27/2012	w4	2850.329	29.91085	0.437928	1.87586669					0.101098	2158.392	22.64979	0.239821
11/27/2012	w5	1565.682	17.20317	1.54433	1.77815748					0.372849	1249.518	13.72927	0.138835
11/27/2012	w6	1686.784	19.78327	1.252925	1.65337564					0.267317	1513.146	17.74678	0.168127
11/27/2012	w7	1256.283	15.97496	2.013725	1.52933618					0.362384	1166.83	14.83747	0.129648
11/27/2012	w8	1992.394	34.76169	2.616121	2.12037208					0.473116	1518.197	26.48828	0.23003
11/27/2012	w9	1375.284	24.6263	5.456285	2.04007898					1.113457	1141.075	20.43247	0.17289
12/4/2012	w1	1763.835	32.79858	3.537105	2.0113403	1092.403	20.31328	4.66895	2.01134	0.79154	1371.835	25.50932	0.207854
12/4/2012	w10	1257.844	25.69976	4.543994	1.75103033	769.1798	15.71556	5.782508	1.75103	0.957986	995.0108	20.32965	0.150759
12/4/2012	w11	1190.708	25.6948	5.616768	1.64672352	836.8957	18.05973	5.328366	1.646724	1.185874	971.8023	20.97094	0.147243
12/4/2012	w12	926.3215	21.90338	4.986054	1.51612394	806.6176	19.07291	3.539781	1.516124	1.360393	763.387	18.0507	0.115665
12/4/2012	w13	1936.039	48.00097	1.841887	2.12224271	1066.37	26.43892	2.635727	2.122243	0.330387	1441.749	35.74585	0.262136
12/4/2012	w14	1285.321	33.99195	3.607503	1.95661528	835.8621	22.10544	4.12923	1.956615	0.707886	1058.731	27.99949	0.192497
12/4/2012	w15	1418.785	37.52158	2.568265	1.94144935	778.5627	20.59009	4.110135	1.941449	0.553242	1101.366	29.12703	0.200248
12/4/2012	w16	1559.5	43.30512	1.287622	1.83899909	975.2973	27.08264	1.518498	1.838999	0.278107	1187.775	32.98283	0.215959
12/4/2012	w17	707.9133	21.29591	6.201894	1.68531969	433.0132	13.02618	8.936037	1.68532	1.54521	614.8129	18.4952	0.111784
12/4/2012	w18	871.8742	27.6694	2.365304	1.59535227	712.1207	22.59953	1.649459	1.595352	0.504557	725.2857	23.01733	0.13187
12/4/2012	w19	1816.394	45.63502	1.854506	2.06331448	1082.616	27.19962	2.392895	2.063314	0.315607	1459.865	36.6776	0.26543
12/4/2012	w2	1994.335	38.00042	2.460007	1.93360462	1263.223	24.06967	2.997929	1.933605	0.526671	1557.356	29.67414	0.235963
12/4/2012	w20	1460.708	38.14742	3.102926	1.96096935	882.1357	23.03759	3.870404	1.960969	0.562877	1193.132	31.15947	0.216933
12/4/2012	w21	1318.602	34.87213	3.056451	1.93135392	771.9589	20.41544	4.262107	1.931354	0.617836	1068.463	28.25688	0.194266
12/4/2012	w22	1392.459	39.12695	1.739962	1.79751045	1002.503	28.16951	1.548559	1.79751	0.302966	1213.689	34.10367	0.220671
12/4/2012	w23	731.837	22.01559	6.374358	1.67447552	463.2514	13.93583	7.90882	1.674476	1.469818	626.9441	18.86014	0.11399
12/4/2012	w24	823.5098	26.40676	2.657049	1.57443316	764.9147	24.52784	1.421439	1.574433	0.549769	738.1787	23.67052	0.134214
12/4/2012	w3	1451.882	29.66426	3.430514	1.78619326	940.3957	19.21378	3.820384	1.786193	0.668078	1186.403	24.24011	0.179758
12/4/2012	w4	1112.308	22.98157	4.569385	1.75698515	644.4552	13.31519	6.875465	1.756985	1.168585	867.3173	17.91978	0.131412
12/4/2012	w5	1045.829	22.80849	6.305468	1.65664946	856.2187	18.67327	4.282153	1.656649	0.95647	985.7654	21.49856	0.149358
12/4/2012	w6	715.3233	17.24264	5.292996	1.51585711	615.2735	14.83097	4.309915	1.515857	1.380664	654.9814	15.78812	0.09924
12/4/2012	w7	2048.364	35.73821	2.746032	2.11466895	1250.445	21.81677	3.509562	2.114669	0.501535	1659.76	28.95817	0.251479
12/4/2012	w8	1309.872	23.75572	6.096497	2.00789766	970.4413	17.59983	5.875134	2.007898	1.379857	1060.737	19.23743	0.160718
12/4/2012	w9	1865.979	35.55469	2.475481	1.89199098	1257.645	23.96339	2.674242	1.891991	0.477787	1542.859	29.3979	0.233766
12/11/2012	w1	1543.963	28.71005	4.550989	1.99660079	1065.775	19.81813	4.968881	1.996601	0.929565	1266.882	23.55773	0.191952
12/11/2012	w2	1519.937	30.35687	3.126821	1.82698703	1008.999	20.15218	4.212873	1.826987	0.718117	1301.485	25.99384	0.197195
12/11/2012	w3	1186.37	24.51178	4.950258	1.75322283	727.6272	15.03362	7.558208	1.753223	1.210733	991.4107	20.48369	0.150214
12/11/2012	w4	1013.063	21.86131	6.456384	1.67378425	785.3629	16.94768	6.463961	1.673784	1.374151	957.7043	20.66671	0.145107
12/11/2012	w5	1086.564	24.19576	5.173641	1.62421419	875.8077	19.5026	4.321738	1.624214	0.987993	1038.399	23.12321	0.157333
12/11/2012	w6	396.639	9.92508	21.71318	1.46498292	385.4125	9.644161	14.62375	1.464983	2.124486	601.9602	15.06283	0.091206
12/11/2012	w7	1692.06	31.07547	3.60915	1.98735059	999.4393	18.35518	5.256583	1.987351	0.828023	1281.143	23.52879	0.194113
12/11/2012	w8	2050.566	39.5426	1.627338	1.86593435	1256.656	24.23304	2.411633	1.865934	0.389909	1624.524	31.32691	0.24614
12/11/2012	w9	1216.022	24.56611	4.706776	1.76801493	818.7576	16.54056	5.656082	1.768015	1.057376	1027.072	20.74892	0.155617
12/11/2012	w10	1107.901	23.14486	4.779687	1.70363267	614.5873	12.83917	9.26606	1.703633	1.415194	882.5721	18.43757	0.133723
12/11/2012	w11	1219.566	26.87749	3.587135	1.61128357	908.5338	20.02278	3.564424	1.611284	0.781817	1109.937	24.46141	0.168172
12/11/2012	w12	689.0437	16.60918	6.217863	1.49303131	618.2488	14.90269	4.802671	1.493031	1.325398	700.9709	16.89668	0.106208

date	test	T Freq 1	T %1	T Freq 2	T %2	T Freq 3	T %3	T Freq 4	T %4	T Freq 5	T %5
9/21/2012	w1	1.085069	0.716786	2.19184	0.091749	3.284144	0.04321	0		0	
9/21/2012	w10	1.17	0.430021	2.329	0.196624	3.493333	0.295033	0.013333	0	0.013333	0
9/21/2012	w11	0.953333	0.485929	1.9	0.052988	2.85	0.02809	3.81	0.280252	4.756667	0.04207
9/21/2012	w2	0.911458	0.568143	1.815683	0.150771	2.727141	0.057575	3.631366	0.020106	6.329572	0.067461
9/21/2012	w3	1.099333	0.75504	2.19	0.080263	3.29	0.04777	4.383333	0.020009	4.7	0.000889
9/21/2012	w4	0.916667	0.513327	1.836667	0.173584	2.756	0.066883	3.673333	0.06904	5.51	0.049685
9/21/2012	w5	1.1	0.892351	3.296667	0.020838	0		0		0	
9/21/2012	w6	1.15	0.60569	2.3	0.06137	3.463333	0.061037	4.62	0.036312	10.19	0.017681
9/21/2012	w7	0.946667	0.733531	1.83	0.012879	3.79	0.021412	5.7	0.021136	2.183333	0.001629
9/21/2012	w8	1.156667	0.760916	1.713333	0.000634	3.463333	0.014214	8.896667	0.000884	9.736667	0.021278
9/21/2012	w9	0.946667	0.791639	1.88	0.020397	2.826667	0.018369	9.466667	0.035446	9.64	0.017047
10/3/2012	w1	0		0		0		0		0	
10/3/2012	w2	0		0		0		0		0	
10/3/2012	w4	0		0		0		0		0	
10/3/2012	w5	0		0		0		0		0	
10/3/2012	w6	0		0		0		0		0	
10/23/2012	w1	1.236667	0.505972	2.473333	0.108967	3.703333	0.050508	4.933333	0.018957		
10/23/2012	w2	1.17	0.506174	2.35	0.190256	3.52	0.087254	4.693333	0.03085		
10/23/2012	w3	1.156667	0.476104	2.27	0.092304	3.396667	0.017883	3.956667	0.00085		
10/23/2012	w4	1.15	0.628225	2.313333	0.11127	3.476667	0.052065	4.643333	0.049251		
10/30/2012	w1	1.176667	0.62034	2.343333	0.117217	3.506667	0.021553	0.333333	0.00325		
10/30/2012	w13	1.243333	0.678769	2.036667	0.00259	3.716667	0.042101	5.02	0.043011	0	
10/30/2012	w14	1.186667	0.49924	2.356667	0.097808	3.53	0.026064	4.723333	0.123368	5.893333	0.048567
10/30/2012	w15	1.113333	0.736606	2.226667	0.06458	3.34	0.033243	4.453333	0.051077	5.57	0.049784
10/30/2012	w16	1.096667	0.838253	1.713333	0.000571	3.26	0.018355	4.223333	0.005976	4.793333	0.002218
10/30/2012	w17	1.033333	0.512779	2.066667	0.141849	3.096	0.027253	4.143333	0.096858	5.176667	0.121908
10/30/2012	w18	0.953333	0.39302	1.91	0.032604	3.833333	0.034918	4.796	0.269316	5.07	0.024621
10/30/2012	w19	1.35	0.480697	2.703333	0.440606						
10/30/2012	w2	1.113333	0.733544	2.233333	0.144281	2.646667	0.000701	4.453333	0.017367	4.976667	0.000762
10/30/2012	w20	1.28	0.43653	2.566667	0.481925						
10/30/2012	w21	1.236667	0.77047	2.456667	0.167436	3.116667	0.001351				
10/30/2012	w22	1.2	0.679518	2.386667	0.20615	3.573333	0.052962				
10/30/2012	w23	1.096667	0.731999	2.176667	0.023182	3.296667	0.198778				
10/30/2012	w24	1.033333	0.408684	2.053333	0.264138	3.08	0.248481	4.1	0.015235		
10/30/2012	w3	1.106667	0.853208	2.196667	0.024312	3.306667	0.032258	3.673333	0.000549	4.88	0.00081
10/30/2012	w4	1.09	0.862901	1.44	0.000435	3.283333	0.023885	4.883333	0.000285		
10/30/2012	w5	1.026667	0.486805	2.053333	0.106187	4.113333	0.045447	5.15	0.152236	6.183333	0.075243
10/30/2012	w6	0.953333	0.602842	1.903333	0.043908	2.85	0.026025	4.766667	0.076911	5.726667	0.076548
11/6/2012	w10	1.106667	0.816622	2.213333	0.097171	2.74	0.001116	0		0	
11/6/2012	w11	1.041667	0.820242	2.083333	0.094998	3.11	0.042342	3.296667	0.001389	0	
11/6/2012	w12	1.016667	0.595971	2.036667	0.225386	3.056667	0.082403	4.086667	0.033448	4.416667	0.000292
11/6/2012	w13	1.38	0.605729	1.993333	0.000582	9.663333	0.08208	0		0	
11/6/2012	w14	1.313333	0.534477	2.63	0.048708	3.956667	0.025348	9.25	0.144375	9.923333	0.011142
11/6/2012	w15	1.27	0.744783	1.9	0.000434	3.816667	0.016449	8.933333	0.020454	10.22	0.02362
11/6/2012	w16	1.236667	0.512047	1.62	0.000502	9.85	0.267587	0		0	
11/6/2012	w17	1.163333	0.735287	1.523333	0.000834	9.263333	0.030664			0	
11/6/2012	w18	1.076667	0.71926	9.763333	0.091285	0		0		0	
11/6/2012	w7	1.226667	0.844503	2.466667	0.058231	0		0		0	
11/6/2012	w8	1.176667	0.828593	2.343333	0.095426	3.506667	0.017662	0		0	
11/6/2012	w9	1.113333	0.825738	2.226667	0.089419	0		0		0	
11/13/2012	w2	1.22	0.749839	2.443333	0.079925	3.666667	0.06378	4.89	0.033419	5.633333	0.001727
11/13/2012	w3	1.313333	0.633734	2.63	0.114781	3.946667	0.03704	5.22	0.025785	0	
11/13/2012	w4	1.17	0.580446	2.343333	0.147227	3.513333	0.068493	4.693333	0.052256	5.916667	0.026773
11/13/2012	w5	1.156667	0.54272	2.313333	0.12332	3.47	0.059113	4.626667	0.034655	10.43667	0.091999
11/13/2012	w6	1.083333	0.863999	1.436667	0.000729	3.196667	0.010198	0		0	
11/13/2012	w7	1.01	0.456776	2.03	0.226045	3.043333	0.035813	4.063333	0.028471	5.083333	0.08041

date	test	T Freq 1	T %1	T Freq 2	T %2	T Freq 3	T %3	T Freq 4	T %4	T Freq 5	T %5
11/15/2012	w1	1.22	0.630153	9.566667	0.08262	0		0		0	
11/15/2012	w3	1.1	0.796302	9.996667	0.038394	0		0		0	
11/15/2012	w4	1.09	0.838695	1.343333	0.002096	9.366667	0.004137	0		0	
11/15/2012	w5	1.026667	0.845287	1.343333	0.001015	0		0		0	
11/15/2012	w6	0.93	0.795165	1.863333	0.033903	10.24	0.01999	0.333333	0.001764	0.333333	0.001764
11/20/2012	w10	0.998	0.727306	1.46	0.000942	30	0.004721	30	0.004721	30	0.004721
11/20/2012	w3	1.21	0.866475	2.41	0.021388	4.11	0.000379	30	0.000321	30	0.000321
11/20/2012	w4	1.3	0.737151	2.61	0.030233	30	0.000717	30	0.000717	30	0.000717
11/20/2012	w6	1.22	0.720918	1.82	0.000511	9.787	0.025047	30	0.000916	30	0.000916
11/20/2012	w7	1.164	0.79632	2.315	0.018318	30	0.002532	30	0.002532	30	0.002532
11/20/2012	w8	1.09	0.774326	2.177	0.018974	30	0.003838	30	0.003838	30	0.003838
11/20/2012	w9	1.027	0.793852	1.37	0.001157	9.67	0.002089	10.57	0.003286	11.73	0.003457
11/27/2012	w10	1.164	0.793989	2.329	0.097585	3.47	0.030694	4.058	0.000348	30	1.17E-05
11/27/2012	w11	1.099	0.659074	2.206	0.141333	3.305	0.058981	4.405	0.045331	10.308	0.000288
11/27/2012	w12	1.0706	0.787879	2.126	0.056518	3.204	0.05733	3.428	0.000922	4.49	0.00078
11/27/2012	w13	1.005	0.705911	2.01	0.07033	3.016	0.075134	4.02	0.028523	5.034	0.052224
11/27/2012	w2	1.265	0.540576	10.185	0.138468	30	0.000866	30	0.000866	30	0.000866
11/27/2012	w3	1.215	0.72982	9.765	0.069581	30	0.0003	30	0.0003	30	0.0003
11/27/2012	w4	1.15	0.686806	2.893	0.000312	9.237	0.063595	10.387	0.046029	30	0.000257
11/27/2012	w5	1.085	0.823439	9.23	0.002769	30	0.000302	30	0.000302	30	0.000302
11/27/2012	w6	1.027	0.827366	1.555	0.000513	10.257	0.057504	30	0.000588	30	0.000588
11/27/2012	w7	0.9476	0.62345	1.888	0.043917	9.476	0.110409	9.96	0.010745	30	0.000331
11/27/2012	w8	1.273	0.735819	2.546	0.12821	3.819	0.042838	4.499	0.00082	30	2.48E-05
11/27/2012	w9	1.222	0.856567	2.452	0.06277	2.98	0.000696	30	2.68E-05	30	2.68E-05
12/4/2012	w1	1.2225	0.825612	2.4377	0.068542	3.66	0.040733	4.23	0.000997	30	6.76E-06
12/4/2012	w10	1.0923	0.814181	2.177	0.054928	2.62	0.00187	30	1.39E-05	30	1.39E-05
12/4/2012	w11	1.0344	0.811086	2.0471	0.05098	3.074	0.038347	30	7.47E-06	30	7.47E-06
12/4/2012	w12	0.94039	0.487767	1.88078	0.307295	3.75	0.028375	4.629	0.00572	5.63	0.020029
12/4/2012	w13	1.2659	0.578246	2.539	0.160016	3.8122	0.062702	5.078	0.062928	5.57	0.011382
12/4/2012	w14	1.2297	0.8264	2.4522	0.054692	3.674	0.027111	4.9045	0.018247	30	2.37E-05
12/4/2012	w15	1.208	0.763112	2.4088	0.047325	3.624	0.064465	4.817	0.030231	30	3.96E-05
12/4/2012	w16	1.1501	0.675686	2.3003	0.128309	3.443	0.044267	30	4.8E-05	30	4.8E-05
12/4/2012	w17	1.0706	0.778266	2.1267	0.031942	3.21	0.038282	4.28	0.024075	5.309	0.017342
12/4/2012	w18	1.00549	0.521162	2.01	0.188161	3.016	0.061028	4.029	0.027924	5.02	0.029395
12/4/2012	w19	1.28	0.568842	2.5607	0.146402	3.8339	0.048709	5.121	0.075518	5.88	0.008257
12/4/2012	w2	1.1501	0.741965	2.3148	0.122643	3.4288	0.045475	3.964	0.001032	30	5.94E-06
12/4/2012	w20	1.2297	0.75219	2.4739	0.07756	3.696	0.02566	4.933	0.027113	6.17	0.017753
12/4/2012	w21	1.208	0.776264	2.416	0.045065	3.638	0.059402	4.839	0.014624	5.3	0.007157
12/4/2012	w22	1.1501	0.637651	2.3075	0.101952	3.457	0.046375	5.76	0.016607	30	5.43E-05
12/4/2012	w23	1.0778	0.730082	2.1484	0.045958	3.226	0.055548	4.304	0.033929	5.316	0.016264
12/4/2012	w24	0.998	0.423026	2.003	0.201387	3.009	0.054238	4.007	0.023279	5.0202	0.063964
12/4/2012	w3	1.0923	0.726028	2.1918	0.090272	3.284	0.03066	3.696	0.00295	30	8.76E-06
12/4/2012	w4	1.0778	0.774682	2.162	0.075419	3.2335	0.033879	3.79	0.001265	30	1.02E-05
12/4/2012	w5	1.0127	0.763334	2.03269	0.088364	3.045	0.035164	5.071	0.025634	30	6.11E-06
12/4/2012	w6	0.9259	0.529294	1.859	0.159993	2.792	0.105724	3.718	0.059332	4.64	0.021222
12/4/2012	w7	1.25868	0.812577	2.4956	0.056651	3.776	0.023503	4.499	0.000997	30	8.29E-06
12/4/2012	w8	1.2225	0.844115	2.4377	0.057471	3.667	0.032445	30	1.33E-05	30	1.33E-05
12/4/2012	w9	1.157	0.780346	2.307	0.084128	3.443	0.025904	3.877	0.000992	30	7.99E-06
12/11/2012	w1	1.208	0.585722	2.416	0.046187	3.6313	0.223742	4.1087	0.024939	30	1.26E-06
12/11/2012	w2	1.0923	0.41774	2.1918	0.084968	3.2986	0.189037	3.73	0.062869	4.3909	0.138051
12/11/2012	w3	1.08506	0.440893	2.1701	0.066652	3.269	0.126517	3.2769	0.126202	4.34	0.155114
12/11/2012	w4	1.04166	0.424823	2.07609	0.048982	3.1105	0.070133	4.15219	0.329666	30	8.85E-07
12/11/2012	w5	1.01273	0.306471	2.03269	0.049324	3.0454	0.032256	4.0653	0.466422	5.0708	0.013559
12/11/2012	w6	0.89699	0.427478	1.801215	0.192288	2.7054	0.059524	3.600966	0.173789	30	1.43E-06
12/11/2012	w7	1.21527	0.58839	2.4305	0.059023	3.653	0.198214	30	1.43E-06	30	1.43E-06
12/11/2012	w8	1.15017	0.426423	2.32204	0.106629	3.47945	0.174744	3.48668	0.174629	4.6151	0.050513
12/11/2012	w9	1.0923	0.513853	2.17737	0.082326	3.28414	0.140814	3.25	0.13558	4.36	0.063327
12/11/2012	w10	1.07783	0.46614	2.15567	0.060751	3.2335	0.149137	4.3113	0.136514	30	2.1E-06
12/11/2012	w11	1.01273	0.352503	2.02546	0.034081	3.03819	0.036301	4.06539	0.436056	5.07	0.025199
12/11/2012	w12	0.925925	0.359483	1.85185	0.086829	2.785	0.093308	3.718	0.208255	4.65	0.076259

date	test	H Freq1	H%1	H Freq 2	H% 2	H Freq 3	H% 3	H Freq 4	H% 4
9/21/2012	w1	1.092303	0.935012	2.19184	0.032093	0		0	
9/21/2012	w10	1.163333	0.923212	2.32	0.046143	3.493333	0.002625	0.013333	0
9/21/2012	w11	0.946667	0.946234	1.893333	0.031495	0		0	
9/21/2012	w2	0.911458	0.51189	1.815683	0.421653	2.727141	0.021515	0	
9/21/2012	w3	1.099333	0.940461	2.183333	0.025101	0.013333	0	0.013333	0
9/21/2012	w4	0.916667	0.60047	1.836667	0.350172	2.756	0.011789	3.673333	0.001354
9/21/2012	w5	1.1	0.954325	1.583333	0.000692	2.666667	0.000744	0	
9/21/2012	w6	1.15	0.961357	1.583333	0.000836	0.013333	0	0.013333	0
9/21/2012	w7	0.946667	0.928168	1.893333	0.049338	0.013333	0	0.013333	0
9/21/2012	w8	1.156667	0.956723	2.233333	0.011339	3.463333	0.000754	8.896667	5.42E-06
9/21/2012	w9	0.946667	0.899611	1.886667	0.075259	2.826667	0.00522	9.466667	3.17E-06
10/3/2012	w1	0		0		0		0	
10/3/2012	w2	0		0		0		0	
10/3/2012	w4	0		0		0		0	
10/3/2012	w5	0		0		0		0	
10/3/2012	w6	0		0		0		0	
10/23/2012	w1	1.163333	0.857985	2.343333	0.016837	0.013333	0.002678	0.013333	0.002678
10/23/2012	w2	1.156667	0.955261	2.313333	0.024041	2.856667	0.000197	3.52	0.001671
10/23/2012	w3	1.15	0.964242	2.25	0.016841	0		0	
10/23/2012	w4	1.143333	0.957739	2.286667	0.022011	0		0	
10/30/2012	w1	1.163333	0.923483	2.126667	0.001856	0		0	
10/30/2012	w13	1.23	0.909934	2.45	0.03447	0		0	
10/30/2012	w14	1.163333	0.958496	1.583333	0.00116	0		0	
10/30/2012	w15	1.096667	0.927456	2.196667	0.040871	0		0	
10/30/2012	w16	1.09	0.901255	2.176667	0.044327	2.486667	0.00098	3.27	0.011243
10/30/2012	w17	1.02	0.908324	2.04	0.064582	0		0	
10/30/2012	w18	0.946667	0.933796	1.816667	0.013515	2.22	0.000423	0	
10/30/2012	w19	1.336667	0.937262	2.666667	0.019738	0		0	
10/30/2012	w2	1.113333	0.937723	2.206667	0.027154	2.583333	0.000551	0	
10/30/2012	w20	1.263333	0.949336	1.763333	0.000747				
10/30/2012	w21	1.213333	0.914254	2.43	0.049068				
10/30/2012	w22	1.183333	0.939752	2.343333	0.030334	2.856667	9.43E-05	3.573333	0.009747
10/30/2012	w23	1.083333	0.871251	2.16	0.052974	3.253333	0.030068		
10/30/2012	w24	1.016667	0.849188	2.023333	0.128473	0		0	
10/30/2012	w3	1.09	0.930989	2.176667	0.029625	0		0	
10/30/2012	w4	1.083333	0.895807	2.103333	0.033122	2.583333	0.000388	3.333333	0.008043
10/30/2012	w5	1.02	0.872461	2.03	0.108222	0		0	
10/30/2012	w6	0.94	0.804763	1.886667	0.137498	2.826667	0.03575	0	
11/6/2012	w10	1.09	0.928444	2.183333	0.026445	0		0	
11/6/2012	w11	1.026667	0.886065	2.053333	0.078081	0		0	
11/6/2012	w12	1.003333	0.856247	2.016667	0.121109	0		0	
11/6/2012	w13	1.366667	0.933293	2.036667	0.00186	0		0	
11/6/2012	w14	1.3	0.94773	0		0		0	
11/6/2012	w15	1.256667	0.942553	2.516667	0.025292	0		0	
11/6/2012	w16	1.213333	0.914451	2.43	0.04185	0		0	
11/6/2012	w17	1.18	0.97523	0		0		0	
11/6/2012	w18	1.07	0.519611	2.153333	0.33772	3.216667	0.053605	0	
11/6/2012	w7	1.22	0.849378	2.436667	0.071147	0		0	
11/6/2012	w8	1.156667	0.937297	2.313333	0.027207	0		0	
11/6/2012	w9	1.096667	0.931727	2.196667	0.029623	0		0	
11/13/2012	w2	1.206667	0.927439	2.413333	0.029137	3.563333	0.005067	0	
11/13/2012	w3	1.3	0.945381	1.943333	0.001029	2.6	0.009769	3.1	0.000411
11/13/2012	w4	1.156667	0.965217	1.67	0.000344	0		0	
11/13/2012	w5	1.14	0.970348	1.583333	0.000543	0		0	
11/13/2012	w6	1.076667	0.79184	2.153333	0.124672	3.233333	0.023076	0	
11/13/2012	w7	1.003333	0.842141	2.01	0.140141	0		0	

date	test	H Freq1	H%1	H Freq 2	H% 2	H Freq 3	H% 3	H Freq 4	H% 4
11/15/2012	w1	1.213333	0.88756	0		0		0	
11/15/2012	w3	1.096667	0.956736	2.183333	0.022314	0		0	
11/15/2012	w4	1.076667	0.960799	1.583333	0.000581	0		0	
11/15/2012	w5	1.01	0.917742	2.023333	0.0613	0		0	
11/15/2012	w6	0.923333	0.889267	1.82	0.078788	0.333333	0.000279	0.333333	0.000279
11/20/2012	w10	0.998	0.951747	1.97	0.030567	30	1.26E-06	30	1.26E-06
11/20/2012	w3	1.2	0.932984	2.35	0.025751	30	2.77E-06	30	2.77E-06
11/20/2012	w4	1.29	0.938454	30	1.4E-06	30	1.4E-06	30	1.4E-06
11/20/2012	w6	1.2	0.947727	2.4	0.014735	30	1.92E-06	30	1.92E-06
11/20/2012	w7	1.15	0.961133	2.27	0.018342	30	7.14E-07	30	7.14E-07
11/20/2012	w8	1.085	0.923848	2.163	0.039041	30	1.26E-06	30	1.26E-06
11/20/2012	w9	1.027	0.864209	2.039	0.101478	30	1E-06	30	1E-06
11/27/2012	w10	1.164	0.968797	1.69	0.000411	30	4.38E-07	30	4.38E-07
11/27/2012	w11	1.09	0.91484	2.177	0.052636	30	1.38E-06	30	1.38E-06
11/27/2012	w12	1.056	0.791682	2.119	0.136324	30	1.22E-06	30	1.22E-06
11/27/2012	w13	0.998	0.947392	1.98	0.030243	2.47	0.000167	30	8.55E-07
11/27/2012	w2	1.251	0.942782	1.96	0.002418	30	9.65E-07	30	9.65E-07
11/27/2012	w3	1.208	0.954135	30	1.33E-06	30	1.33E-06	30	1.33E-06
11/27/2012	w4	1.142	0.964703	2.271	0.017216	30	5.15E-07	30	5.15E-07
11/27/2012	w5	1.085	0.914638	2.155	0.045224	2.56	0.00124	30	1.23E-06
11/27/2012	w6	1.0127	0.864437	2.032	0.104795	2.38	0.000357	30	1.02E-06
11/27/2012	w7	0.933	0.933232	1.85	0.035798	2.039	0.001045	30	7.24E-07
11/27/2012	w8	1.258	0.95884	1.866	0.000847	30	7.13E-07	30	7.13E-07
11/27/2012	w9	1.21	0.956758	1.779	0.001158	30	1.52E-06	30	1.52E-06
12/4/2012	w1	1.208	0.945282	2.358	0.011415	30	6.65E-07	30	6.65E-07
12/4/2012	w10	1.077	0.839201	2.1556	0.11173	2.56	0.001656	30	1.35E-06
12/4/2012	w11	1.0199	0.938449	2.018	0.025912	2.38	0.000603	30	9.58E-07
12/4/2012	w12	0.9331	0.862363	1.8663	0.091832	2.785	0.019492	30	4.68E-07
12/4/2012	w13	1.258	0.94168	2.5028	0.02591	30	7.35E-07	30	7.35E-07
12/4/2012	w14	1.2225	0.938295	2.4233	0.023782	30	8.56E-07	30	8.56E-07
12/4/2012	w15	1.1935	0.9043	2.387	0.055497	30	1.68E-06	30	1.68E-06
12/4/2012	w16	1.1357	0.962502	2.271	0.017846	30	3.11E-07	30	3.11E-07
12/4/2012	w17	1.0706	0.739058	2.1267	0.187522	30	2.23E-06	30	2.23E-06
12/4/2012	w18	0.991	0.930555	1.989	0.045673	30	4.48E-07	30	4.48E-07
12/4/2012	w19	1.2659	0.942986	2.517	0.027498	30	8.81E-07	30	8.81E-07
12/4/2012	w2	1.1429	0.961745	2.228	0.010424	30	7.65E-07	30	7.65E-07
12/4/2012	w20	1.2297	0.91825	2.437	0.04262	30	1.43E-06	30	1.43E-06
12/4/2012	w21	1.2008	0.911944	2.394	0.043571	30	2.69E-06	30	2.69E-06
12/4/2012	w22	1.1429	0.964755	2.26	0.014402	30	2.82E-07	30	2.82E-07
12/4/2012	w23	1.063	0.664075	2.1267	0.253896	3.19	0.016972	30	2.56E-06
12/4/2012	w24	0.991	0.866709	1.98	0.091748	30	6.4E-07	30	6.4E-07
12/4/2012	w3	1.085	0.894884	2.17	0.063764	30	5.04E-07	30	5.04E-07
12/4/2012	w4	1.0706	0.779068	2.1412	0.150532	3.2045	0.018441	30	8.69E-07
12/4/2012	w5	1.0054	0.880065	2.011	0.094078	30	6.17E-07	30	6.17E-07
12/4/2012	w6	0.9186	0.72509	1.8446	0.220715	2.0399	0.00146	30	7.09E-07
12/4/2012	w7	1.244	0.933308	2.488	0.036941	30	7.73E-07	30	7.73E-07
12/4/2012	w8	1.208	0.955672	1.779	0.001164	30	1.82E-06	30	1.82E-06
12/4/2012	w9	1.1429	0.965004	1.692	0.000803	30	1.2E-06	30	1.2E-06
12/11/2012	w1	1.2008	0.944708	1.6	0.001834	30	1.97E-06	30	1.97E-06
12/11/2012	w2	1.085	0.883781	2.177	0.059002	30	1.4E-06	30	1.4E-06
12/11/2012	w3	1.0706	0.776668	2.1484	0.131204	30	1.46E-06	30	1.46E-06
12/11/2012	w4	1.02719	0.897566	2.04716	0.041422	30	1.29E-06	30	1.29E-06
12/11/2012	w5	1.00549	0.835619	2.01099	0.13212	30	8.37E-07	30	8.37E-07
12/11/2012	w6	0.88975	0.524047	1.78674	0.319608	2.67	0.036221	30	3.79E-06
12/11/2012	w7	1.208	0.934424	30	1.15E-06	30	1.15E-06	30	1.15E-06
12/11/2012	w8	1.1429	0.956974	1.6059	0.00806	30	5.15E-07	30	5.15E-07
12/11/2012	w9	1.0778	0.850352	2.1556	0.075547	30	1.25E-06	30	1.25E-06
12/11/2012	w10	1.0633	0.675319	2.1339	0.199092	3.1973	0.030394	30	1.34E-06
12/11/2012	w11	1.00549	0.809648	2.01099	0.155617	30	7.18E-07	30	7.18E-07
12/11/2012	w12	0.91869	0.687149	1.837	0.2523	30	1.19E-06	30	1.19E-06

Appendix D

Moduli of Elasticity Data

Plant ID	Plant type	Diameter at base	Diameter at load	Height of load application	Load applied	Deflection	total plant height		Force	Average Radius	I - solid cylinder	E
Units:		cm	cm	cm	g	cm	cm		kg m/S^2	m		
Dowel 1	clear straw with dowel	0.6	0.6	10	14.19	0.1	16.2		0.139204	0.003	6.36E-11	7.29E+08
Dowel 1	clear straw with dowel	0.6	0.6	16	14.19	0.3	16.2		0.139204	0.003	6.36E-11	9.96E+08
Dowel 1	clear straw with dowel	0.6	0.6	10	28.37	0.2	16.2		0.27831	0.003	6.36E-11	7.29E+08
Dowel 2	clear straw with dowel	0.6	0.6	10	14.19	0.05	34		0.139204	0.003	6.36E-11	1.46E+09
Dowel 3	clear straw with dowel	0.6	0.6	20	14.19	0.3	34		0.139204	0.003	6.36E-11	1.95E+09
Dowel 4	clear straw with dowel	0.6	0.6	30	14.19	1	34		0.139204	0.003	6.36E-11	1.97E+09
Dowel 5	clear straw with dowel	0.6	0.6	10	28.37	0.1	34		0.27831	0.003	6.36E-11	1.46E+09
Dowel 6	clear straw with dowel	0.6	0.6	20	28.37	0.7	34		0.27831	0.003	6.36E-11	1.67E+09
Dowel 7	clear straw with dowel	0.6	0.6	30	28.37	2.2	34		0.27831	0.003	6.36E-11	1.79E+09
straw 1	clear straw	0.6	0.6	10	14.19	0.6	34		0.139204	0.003	6.36E-11	1.22E+08
straw 1	clear straw	0.6	0.6	16	14.19	2.1	34		0.139204	0.003	6.36E-11	1.42E+08
straw 1	clear straw	0.6	0.6	10	28.37	1.3	34		0.27831	0.003	6.36E-11	1.12E+08
straw 1	clear straw	0.6	0.6	20	14.19	5	34		0.139204	0.003	6.36E-11	1.17E+08
Steel 1	clear straw with steel rod	0.6	0.6	10	14.19	0	34		0.139204	0.003	6.36E-11	
Steel 2	clear straw with steel rod	0.6	0.6	15	14.19	0	34		0.139204	0.003	6.36E-11	
Steel 3	clear straw with steel rod	0.6	0.6	20	14.19	0.05	34		0.139204	0.003	6.36E-11	1.17E+10
Steel 4	clear straw with steel rod	0.6	0.6	30	14.19	0.1	34		0.139204	0.003	6.36E-11	1.97E+10
Steel 5	clear straw with steel rod	0.6	0.6	10	28.37	0	34		0.27831	0.003	6.36E-11	
Steel 6	clear straw with steel rod	0.6	0.6	15	28.37	0	34		0.27831	0.003	6.36E-11	
Steel 7	clear straw with steel rod	0.6	0.6	20	28.37	0.05	34		0.27831	0.003	6.36E-11	2.33E+10
Steel 8	clear straw with steel rod	0.6	0.6	30	28.37	0.2	34		0.27831	0.003	6.36E-11	1.97E+10
Steel 9	clear straw with steel rod	0.6	0.6	20	100	0.1	34		0.981	0.003	6.36E-11	4.11E+10
Steel 10	clear straw with steel rod	0.6	0.6	30	100	0.3	34		0.981	0.003	6.36E-11	4.63E+10
	Foam	0.9	0.9	5	14.19	100	30		0.139204	0.0045	3.22E-10	18009.44
	Foam	0.9	0.9	5	14.19	5	30		0.139204	0.0045	3.22E-10	360188.8
	Foam	0.9	0.9	3	14.19	1.4	30		0.139204	0.0045	3.22E-10	277859.9
	Aluminum	0.66	0.66						0	0.0033	9.31E-11	#DIV/0!
	Polyethelene tubing	0.66	0.66	10	14.19	0.4	30		0.139204	0.0033	9.31E-11	1.25E+08
	Vinyl Tubing	0.65	0.65	10	14.19	10	30		0.139204	0.00325	8.76E-11	5295498

Appendix E

R code for time series analysis

```
# Time Series Analysis: Correlogram and Spectrum Analysis
library(car)
# Set number of nobs
nobs = 10001
# SECTION 1: Data Entry and computations
# Enter time series data from comma delimited file
# Column 1: Time  (sec), Column 2: torque on element (N-M) Column 3: upstream wave
height (m), Column 4: downstream wave height (m)

data=read.csv('input.csv',header=TRUE)
ytorq = data[,2]
tvalue = data[,1]
upheight = data[,3]
dnheight = data[,4]



# Time and frequency characteristics of data
Delta_t <- (tvalue[nobs]-tvalue[1])/(nobs-1)
sprintf('Maximum time = %.2f, Minimum time = %.2f, Delta time = %.4f', tvalue[nobs],
tvalue[1], Delta_t)
sprintf('Normalized max time = %.2f, Normalized min time = %.2f, Normalized delta t =
%.4f',
tvalue[nobs]/tvalue[nobs], tvalue[1]/tvalue[nobs], Delta_t/tvalue[nobs])
# Maximum (Nyquist) and minimum frequencies
fmax <- 1.0 /(2*Delta_t)
fmin <- 1.0 /((nobs-1)*Delta_t)
Delta_f <- (fmax - fmin)/(nobs-1)
sprintf('Maximum frequency = %.2f, Minimum frequency = %.4f, Delta frequency =
%.4f', fmax, fmin, Delta_f)
sprintf('Maximum alternative frequency = %.2f, Minimum alternative frequency = %.4f,
Delta alternative frequency = %.4f',
fmax/2/pi/tvalue[nobs], fmin/2/pi/tvalue[nobs], Delta_f/2/pi/tvalue[nobs])

#Torque
# SECTION 2:  Autocorrelation function and correlogram
AutoCorrelation <- acf(ytorq, lag.max = 120, type = "correlation")
LagVector <- AutoCorrelation$lag[,1,1]
LagVector
CorrVector <- AutoCorrelation$acf[,1,1]
CorrVector
LagTime <- LagVector * Delta_t
plot.new
```

```
plot(LagTime, CorrVector, type = "l", panel.first=grid(), xlab='Time', ylab='Correlation')
# SECTION 2:  Autocorrelation function and correlogram
# Method #1 - Default estimation method
AutoCorrelation <- acf(ytorq, lag.max = 120, type = "correlation")
LagVector <- AutoCorrelation$lag[,1,1]
#LagVector
TCorrVector <- AutoCorrelation$acf[,1,1]
#CorrVector
TLagTime <- LagVector * Delta_t
plot.new
plot(TLagTime, TCorrVector, type = "l", panel.first=grid(), xlab='Time',
ylab='Correlation')

#tqcorr.dat= rbind(TLagTime,TCorrVector)
#tqcorr.mat= t(tqcorr.dat)
#write.csv(tqcorr.mat, file="tqcorr.csv")
#write.csv(LagTime, file="Torquelagtime.csv")
#write.csv(CorrVector, file="TorqueCorrelation.csv")


# SECTION 3: Spectrum Computations
require(graphics)
# Method #1 - Default estimation method, no log scale for y
ns_results_ytorq.spec <-spectrum(ytorq, log=c("no") )
ns_results_ytorq.spec$freq
OurFrequency = tvalue[nobs] * 2 * pi * ns_results_ytorq.spec$freq
OurFrequency
ns_results_ytorq.spec$spec
plot(OurFrequency, ns_results_ytorq.spec$spec, type = "l", panel.first=grid(),
xlab='Frequency', ylab='Spectral Density')
# Moving average smoothing using 5 adjacent spikes (no log scale)
results_ytorq.spec <-spectrum(ytorq, span = 5, log=c("no"))
results_ytorq.spec$freq
TOurFrequency = tvalue[nobs] * 2 * pi * results_ytorq.spec$freq
#OurFrequency
#results_ytorq.spec$spec
plot(TOurFrequency,results_ytorq.spec$spec, type = "l", panel.first=grid(),
xlab='Frequency', ylab='Spectral Density')

#tqspec.dat= rbind(TOurFrequency,results_ytorq.spec$spec)
#tqspec.mat= t(tqspec.dat)
#write.csv(tqspec.mat, file="tqspec.csv")
#write.csv(OurFrequency, file="TorqueFrequency.csv")
#write.csv(results_ytorq.spec$spec, file="Torquespectraldensity.csv")
```

```
#upstream wave height
# SECTION 2:  Autocorrelation function and correlogram
AutoCorrelation <- acf(upheight, lag.max = 120, type = "correlation")
LagVector <- AutoCorrelation$lag[,1,1]
LagVector
CorrVector <- AutoCorrelation$acf[,1,1]
CorrVector
LagTime <- LagVector * Delta_t
plot.new
plot(LagTime, CorrVector, type = "l", panel.first=grid(), xlab='Time', ylab='Correlation')
# SECTION 2:  Autocorrelation function and correlogram
# Method #1 - Default estimation method
AutoCorrelation <- acf(upheight, lag.max = 120, type = "correlation")
LagVector <- AutoCorrelation$lag[,1,1]
#LagVector
UCorrVector <- AutoCorrelation$acf[,1,1]
#CorrVector
ULagTime <- LagVector * Delta_t
plot.new
plot(ULagTime, UCorrVector, type = "l", panel.first=grid(), xlab='Time',
ylab='Correlation')


#upcorr.dat= rbind(ULagTime,UCorrVector)
#upcorr.mat= t(upcorr.dat)
#write.csv(upcorr.mat, file="upcorr.csv")
#write.csv(LagTime, file="upheightlagtime.csv")
#write.csv(CorrVector, file="upheightCorrelation.csv")


# SECTION 3: Spectrum Computations
require(graphics)
# Method #1 - Default estimation method, no log scale for y
ns_results_upheight.spec <-spectrum(upheight, log=c("no") )
ns_results_upheight.spec$freq
OurFrequency = tvalue[nobs] * 2 * pi * ns_results_upheight.spec$freq
OurFrequency
ns_results_upheight.spec$spec
plot(OurFrequency, ns_results_upheight.spec$spec, type = "l", panel.first=grid(),
xlab='Frequency', ylab='Spectral Density')
# Moving average smoothing using 5 adjacent spikes (no log scale)
```

```
results_upheight.spec <-spectrum(upheight, span = 5, log=c("no"))
results_upheight.spec$freq
UOurFrequency = tvalue[nobs] * 2 * pi * results_upheight.spec$freq
#OurFrequency
results_upheight.spec$spec
plot(UOurFrequency,results_upheight.spec$spec, type = "l", panel.first=grid(),
xlab='Frequency', ylab='Spectral Density')

#upspec.dat= rbind(UOurFrequency,results_upheight.spec$spec)
#upspec.mat= t(upspec.dat)
#write.csv(upspec.mat, file="upheightspec.csv")
#write.csv(OurFrequency, file="upheightFrequency.csv")
#write.csv(results_upheight.spec$spec, file="upheightspectraldensity.csv")



#downstream wave height
# SECTION 2:  Autocorrelation function and correlogram
AutoCorrelation <- acf(dnheight, lag.max = 120, type = "correlation")
LagVector <- AutoCorrelation$lag[,1,1]
LagVector
CorrVector <- AutoCorrelation$acf[,1,1]
CorrVector
LagTime <- LagVector * Delta_t
plot.new
plot(LagTime, CorrVector, type = "l", panel.first=grid(), xlab='Time', ylab='Correlation')
# SECTION 2:  Autocorrelation function and correlogram
# Method #1 - Default estimation method
AutoCorrelation <- acf(dnheight, lag.max = 120, type = "correlation")
LagVector <- AutoCorrelation$lag[,1,1]
#LagVector
DCorrVector <- AutoCorrelation$acf[,1,1]
#CorrVector
DLagTime <- LagVector * Delta_t
plot.new
plot(DLagTime, DCorrVector, type = "l", panel.first=grid(), xlab='Time',
ylab='Correlation')

#dncorr.dat= rbind(DLagTime,DCorrVector)
#dncorr.mat= t(dncorr.dat)
#write.csv(dncorr.mat, file="dncorr.csv")
#write.csv(LagTime, file="dnheightlagtime.csv")
#write.csv(CorrVector, file="dnheightCorrelation.csv")
```

```
# SECTION 3: Spectrum Computations
require(graphics)
# Method #1 - Default estimation method, no log scale for y
ns_results_dnheight.spec <-spectrum(dnheight, log=c("no") )
ns_results_dnheight.spec$freq
OurFrequency = tvalue[nobs] * 2 * pi * ns_results_dnheight.spec$freq
OurFrequency
ns_results_dnheight.spec$spec
plot(OurFrequency, ns_results_dnheight.spec$spec, type = "l", panel.first=grid(),
xlab='Frequency', ylab='Spectral Density')
# Moving average smoothing using 5 adjacent spikes (no log scale)
results_dnheight.spec <-spectrum(dnheight, span = 5, log=c("no"))
results_dnheight.spec$freq
DOurFrequency = tvalue[nobs] * 2 * pi * results_dnheight.spec$freq
#OurFrequency
results_dnheight.spec$spec
plot(DOurFrequency,results_dnheight.spec$spec, type = "l", panel.first=grid(),
xlab='Frequency', ylab='Spectral Density')

#dnspec.dat= rbind(DOurFrequency,results_dnheight.spec$spec)
#dnspec.mat= t(dnspec.dat)
#write.csv(dnspec.mat, file="dnheightspec.csv")
#write.csv(OurFrequency, file="dnheightFrequency.csv")
#write.csv(results_dnheight.spec$spec, file="dnheightspectraldensity.csv")




# SECTION 4: RMS averages
#creates a time series from the data
torque.ts=ts(ytorq)
dsh.ts = ts(dnheight)
ush.ts = ts(upheight)

#creates an RMS average for peak to peak amplitude
torque.sqr=torque.ts^2
torque.mean = mean(torque.sqr, na.rm = TRUE)
torque.amp = 1.414*torque.mean^0.5
dsh.sqr = dsh.ts^2
dsh.mean = mean(dsh.sqr, na.rm = TRUE)
dsh.amp = 1.414*dsh.mean^0.5
ush.sqr = ush.ts^2
```

```
ush.mean = mean(ush.sqr, na.rm = TRUE)
ush.amp = 1.414*ush.mean^0.5

torque.amp
ush.amp
dsh.amp

#Section 5: cross spectrum analysis

torque.spc=spec.pgram(ts.intersect(torque.ts,dsh.ts), spans=c(3,3))
plot(torque.spc, plot.type = "phase")
plot(torque.spc, plot.type = "coherency")


#Section 6: Peak detection
library(pastecs)
torque.tp = turnpoints(torque.ts)
torque.peak = extract(torque.tp,no.tp=0,peak=1, pit=-1)
#peaks.dat = rbind(tvalue,torque.peak,ytorq,upheight,dnheight)
#peaks=t(peaks.dat)
#write.csv(peaks, file="torquepeak.csv")
ush.tp = turnpoints(ush.ts)
ush.peak = extract(ush.tp,no.tp=0,peak=1, pit=-1)
dsh.tp = turnpoints(dsh.ts)
dsh.peak = extract(dsh.tp,no.tp=0,peak=1, pit=-1)
```

Appendix F

Visual Basic Code
for Wave Analysis of Time Series Data

```
Public Sub wavetheta()
Dim wks As Worksheet
Set wks = ActiveWorkbook.Sheets("DragD")

Dim dblpeak As Double
Dim dblRow As Double

Dim dblCount As Double
Dim dblTheta As Double
Dim dblThetainc As Double
Dim Wave As Double
Dim dblIndex As Double
Dim dblrowwrite As Double
Dim dblOldWave As Double

dblOldWave = 0
dblTheta = 0
dblCount = 0
dblRow = 10

For Wave = 1 To 600

Do
dblpeak = wks.Cells(dblRow, 4)
dblRow = dblRow + 1
Loop Until dblpeak = 1

'dblCount = dblRow - wks.Cells(dblRow, 1)
dblCount = wks.Cells(dblRow, 1) - dblOldWave
dblOldWave = dblRow
dblThedainc = 6.28 / dblCount

For Index = 0 To dblCount

dblTheda = dblTheta + (dblThedainc * Index)
dblrowwrite = dblRow - (dblCount - Index) - 2
If dblrowwrite < 3 Then dblrowwrite = 3
wks.Cells(dblrowwrite, 9) = dblTheda

Next Index

dblCount = 0
```

```
Next Wave


'


'Do
'dblpeak = wks.Cells(dblRow, 4)
'dblRow = dblRow + 1
'Loop Until dblpeak = 1



'Do
'dblCount = dblRow
'dblpeak = wks.Cells(dblCount, 4)
'dblTheta = 0
'dblCount = dblCount + 1

'If dblCount > 200 Then dblpeak = 1
'Loop Until dblpeak = 1


'For dblRow = 1 To 11000


'wks.Cells(dblRow, 9) = dblTheda
'Next Index


End Sub
```

Appendix G

Visual Basic Code
for Mendez and Losada (2004) Energy Dissipation

```
Public Sub mendez()
   Dim wks As Worksheet
   Set wks = ActiveWorkbook.Sheets("Sheet1")

   Dim dblTanH As Double, dblZeta As Double


   Dim dblperiod As Double, dblgammaB As Double, dblB As Double, dblG As Double,
dblViscosity As Double, dblDensityWater As Double, dblDensitySoil As Double,
dblDfiftyGrain As Double, dblTheta As Double
   dblperiod = wks.Range("c2")
   dblgammaB = wks.Range("c3")
   dblB = wks.Range("c4")
   dblG = wks.Range("c5")
   dblViscosity = wks.Range("c6")
   dblDensityWater = wks.Range("c7")
   dblDensitySoil = wks.Range("c8")
   dblDfiftyGrain = wks.Range("c9")
   dblTheta = wks.Range("c11")

   Dim dbldv As Double, dblbv As Double, dblN As Double, dblX As Double, dblh As
Double, dblHrms As Double
   Dim dblalpha As Double, dblCD As Double, dblQ As Double, dlbK As Double, dblU
As Double, dblA1 As Double, dlbwavelength As Double, dblCel As Double
   Dim dblEnergyD As Double, dblev As Double, dbleb As Double, dblwavenumb As
Double, dblwavefrq As Double, dblEnergyChangewithx As Double
   Dim intColCount As Integer, intColEnd As Integer, dblXnew As Double, dblhnew As
Double, dblHrmsnew As Double

   intColEnd = wks.Cells(15, 3)
   intColCount = 3

   Do
   dbldv = wks.Cells(16, intColCount)
   dblbv = wks.Cells(17, intColCount)
   dblN = wks.Cells(18, intColCount)
   dblX = wks.Cells(19, intColCount)
   dblh = wks.Cells(20, intColCount)
   dblHrms = wks.Cells(21, intColCount)


   If dblh < 0 Then dblh = 0.00001 Else dblh = dblh
   dblalpha = dbldv / dblh
```

```
    'this is for CD determiniation using Kleug-carpenter relationship
    'dblU = (dblHrms / 2) * ((dblG / (dblh)) ^ 0.5) * Cos(dblTheta)
    'dblK = dblU * dblperiod / dblbv
    'dblQ = dblK / (dblalpha ^ 0.76)
    'dblCD = Exp(-0.0138 * dblQ) / (dblQ ^ 0.3)
    'this replaces the complex relationship with a average value for CD
    dblCD = wks.Range("c12")


    dblZeta = ((4 * 3.14 ^ 2 * dblh) / (dblperiod ^ 2 * dblG))
    dblTanH = (((2.718282 ^ dblZeta) - (2.718282 ^ -dblZeta)) / 2) / (((2.718282 ^
dblZeta) + (2.718282 ^ -dblZeta)) / 2)
    dblL = (dblG * (dblperiod ^ 2)) / (2 * 3.14) * dblTanH
    dblCel = dblL / dblperiod

    ' unsure if these two are supposed to be in radians or not
    dblwavenumb = (2 * 3.14) / dblL
    dblwavefrq = (2 * 3.14) / dblperiod


    'this calculates energy loss from breaking and vegetation
    dbleb = (3 * (3.14 ^ 0.5) / 16) * dblG * dblDensityWater * ((dblB ^ 3 * dblperiod) /
((dblgammaB ^ 4) * dblh ^ 5)) * (dblHrms ^ 7)
    Dim dblsinh As Double, dblcosh As Double
    dblZeta = (dblwavenumb * dblh * dblalpha)
    dblsinh = (((2.718282 ^ dblZeta) - (2.718282 ^ -dblZeta)) / 2)
    dblcosh = (((2.718282 ^ dblZeta) + (2.718282 ^ -dblZeta)) / 2)
    dblev = (1 / (2 * (3.14 ^ 0.5))) * dblDensityWater * dblCD * dblbv * dblN *
(((dblwavenumb * dblG / (2 * dblwavefrq)) ^ 3)) * ((dblsinh ^ 3 + 3 * dblsinh) / (3 *
(dblcosh ^ 3))) * (dblHrms ^ 3)


    ' this corrects the total energy for losses
    dblEnergyChangewithx = -dbleb - dblev
    dblEnergyD = 0.125 * dblDensityWater * dblG * (dblHrms ^ 2)

    dblXnew = wks.Cells(19, intColCount + 1)
    dblhnew = wks.Cells(20, intColCount + 1)
    If dblhnew < 0 Then dblhnew = 0.000001 Else dblhnew = dblhnew

    dblEnergyD = dblEnergyD + dblEnergyChangewithx * (dblXnew - dblX) / dblCel
    dblHrmsnew = (dblEnergyD * 8 / (dblDensityWater * dblG)) ^ 0.5
```

```
    wks.Cells(22, intColCount) = dblEnergyChangewithx
    wks.Cells(23, intColCount) = dblEnergyD
    wks.Cells(24, intColCount) = dblev
    wks.Cells(25, intColCount) = dbleb

    intColCount = intColCount + 1
    wks.Cells(21, intColCount) = dblHrmsnew
    Loop Until intColCount = (intColEnd + 3)

   ' Debug.Print dblL
    'Debug.Print dblev
   ' Debug.Print dbleb


End Sub
```

Appendix H

Spreadsheet for Energy Dissipation after Mendez and Losada (2004)

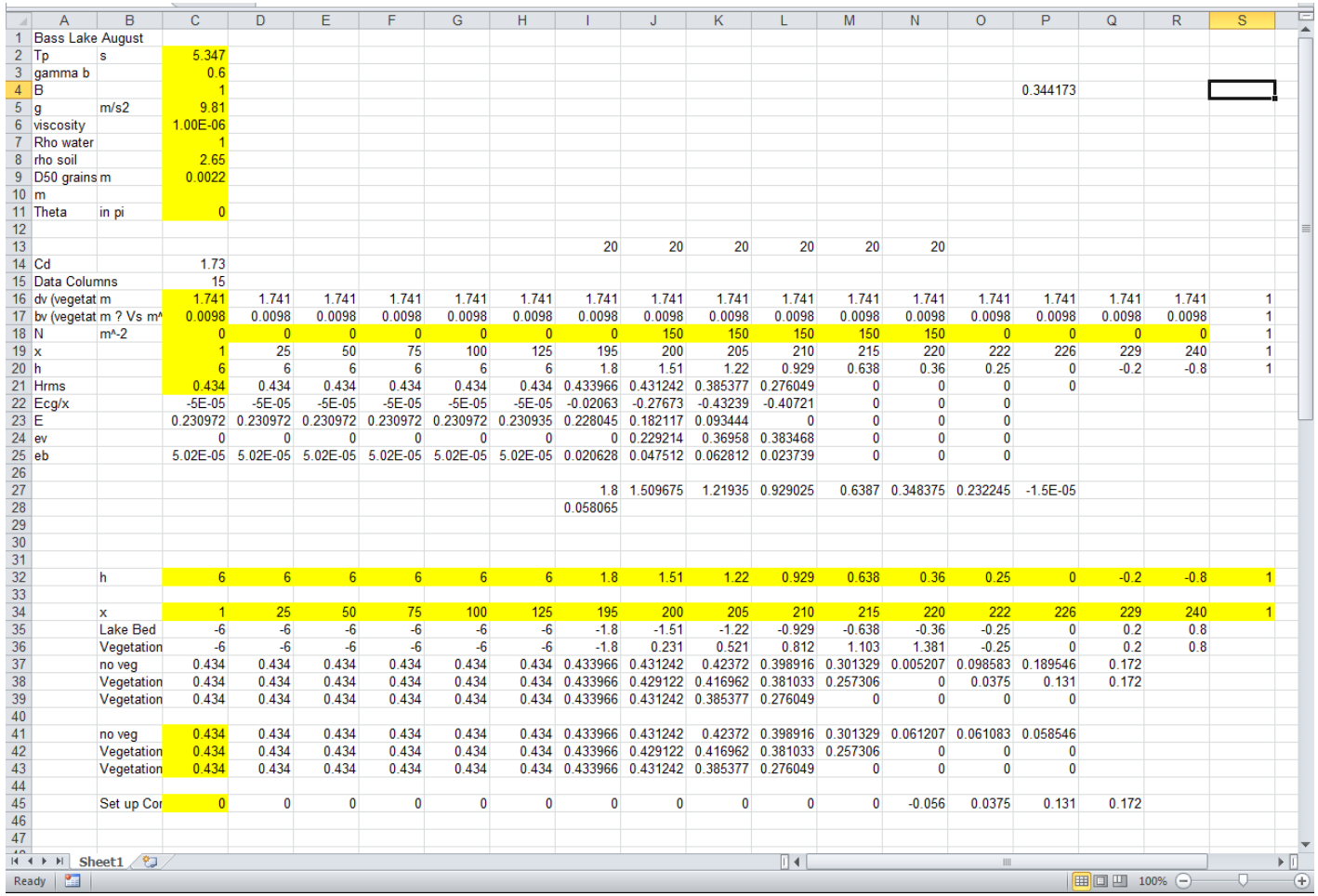

	A	B	C	D	E	F	G	H	I	J	K	L	M	N	O	P	Q	R	S
1	Bass Lake August																		
2	Tp	s	5.347																
3	gamma b		0.6																
4	B		1													0.344173			
5	g	m/s2	9.81																
6	viscosity		1.00E-06																
7	Rho water		1																
8	rho soil		2.65																
9	D50 grains	m	0.0022																
10	m																		
11	Theta	in pi	0																
12																			
13									20	20	20	20	20	20					
14	Cd		1.73																
15	Data Columns		15																
16	dv (vegetat	m	1.741	1.741	1.741	1.741	1.741	1.741	1.741	1.741	1.741	1.741	1.741	1.741	1.741	1.741	1.741	1.741	1
17	bv (vegetat	m ? Vs m^	0.0098	0.0098	0.0098	0.0098	0.0098	0.0098	0.0098	0.0098	0.0098	0.0098	0.0098	0.0098	0.0098	0.0098	0.0098	0.0098	1
18	N	m^-2	0	0	0	0	0	0	0	150	150	150	150	150	0	0	0	0	1
19	x		1	25	50	75	100	125	195	200	205	210	215	220	222	226	229	240	1
20	h		6	6	6	6	6	6	1.8	1.51	1.22	0.929	0.638	0.36	0.25	0	-0.2	-0.8	1
21	Hrms		0.434	0.434	0.434	0.434	0.434	0.434	0.433966	0.431242	0.385377	0.276049	0	0	0	0			
22	Ecg/x		-5E-05	-5E-05	-5E-05	-5E-05	-5E-05	-5E-05	-0.02063	-0.27673	-0.43239	-0.40721	0	0	0				
23	E		0.230972	0.230972	0.230972	0.230972	0.230972	0.230935	0.228045	0.182117	0.093444	0	0	0	0				
24	ev		0	0	0	0	0	0	0	0.229214	0.36958	0.383468	0	0	0				
25	eb		5.02E-05	5.02E-05	5.02E-05	5.02E-05	5.02E-05	5.02E-05	0.020628	0.047512	0.062812	0.023739	0	0	0				
26																			
27									1.8	1.509675	1.21935	0.929025	0.6387	0.348375	0.232245	-1.5E-05			
28									0.058065										
29																			
30																			
31																			
32		h	6	6	6	6	6	6	1.8	1.51	1.22	0.929	0.638	0.36	0.25	0	-0.2	-0.8	1
33																			
34		x	1	25	50	75	100	125	195	200	205	210	215	220	222	226	229	240	1
35		Lake Bed	-6	-6	-6	-6	-6	-6	-1.8	-1.51	-1.22	-0.929	-0.638	-0.36	-0.25	0	0.2	0.8	
36		Vegetation	-6	-6	-6	-6	-6	-6	-1.8	0.231	0.521	0.812	1.103	1.381	-0.25	0	0.2	0.8	
37		no veg	0.434	0.434	0.434	0.434	0.434	0.434	0.433966	0.431242	0.42372	0.398916	0.301329	0.005207	0.098583	0.189546	0.172		
38		Vegetation	0.434	0.434	0.434	0.434	0.434	0.434	0.433966	0.429122	0.416962	0.381033	0.257306	0	0.0375	0.131	0.172		
39		Vegetation	0.434	0.434	0.434	0.434	0.434	0.434	0.433966	0.431242	0.385377	0.276049	0	0	0	0			
40																			
41		no veg	0.434	0.434	0.434	0.434	0.434	0.434	0.433966	0.431242	0.42372	0.398916	0.301329	0.061207	0.061083	0.058546			
42		Vegetation	0.434	0.434	0.434	0.434	0.434	0.434	0.433966	0.429122	0.416962	0.381033	0.257306	0	0	0			
43		Vegetation	0.434	0.434	0.434	0.434	0.434	0.434	0.433966	0.431242	0.385377	0.276049	0	0	0	0			
44																			
45		Set up Cor	0	0	0	0	0	0	0	0	0	0	0	-0.056	0.0375	0.131	0.172		
46																			
47																			

Appendix I

Spreadsheet for
Young and Verhagen (1996) Wave Heights

bass lake Wildwood resort, itasca county u10 for August peak gust (IF Airport)

Wave generated from winds, fetch limited Young and Verhagen						
mean depth (d)	3.23				10.6	3.231707
fetch (x)	1854				6080	1853.659
U10	29.9					
g	9.81					
A1	0.040271					
B1	0.017432					
gx/u10^2	20.344					
gd/u10^2	0.035443					
g^2E/u10^4						
E						
U10^2/g	91.13252					
tanh A1	0.040249					
B1/A1	0.432872					
tanh B1/A1	0.407719					
Hs	0.614956					
A2	0.010661					
B2	0.004996					
g/U10	0.328094					
tanh A2	0.01066					
B2/A2	0.468594					
tanh B2/A2	0.437063					
1/Ts	0.185954					
Ts	5.377678					

intermediate wave celerity and Length						
T	5.377678					
g	9.81					
d	3.23					
L=	19.0301		II-1-11			
C=	3.53872		II-1-7	c=	5.629059	II-1-18

wave velocity						
H	0.614956					
g	9.81					
d	3.23					
Theta	0	in pi				
U=	0.535855	m/s	FigII-1-9	U =	0.761933	II-1-22
ubm =	0.535855	m/s				

viscosity	1.00E-06		rough turbulent
Rho water	1		Wave friction factor

rho soil	2.65		
		in	
D50 grainsize	0.003	meters	

wave shear			
Hrms	0.43484		
			ex III-6-
Abm=	0.169804		2
w=	1.168383		
kn	0.003		
x(final)=	1.39		
fw=	0.120756		
u*wm =	0.13167	m/s	III-6-15
turbulent check			
	395.0106		
	rough	turbulent	
Zo smooth=	1.46E-08		III-6-4
Zo rough =	0.0001		III-6-4
Zo =	0.000167		
phi =	19.44989		III-6-12
Maximum bottom shear			
twm =	0.017337	N/M^2	III-6-
twm" =	0.017337		III-6-53

Shields paramter (no current)		
Ustar	0.13167	
D50	0.003	in m
Tau star	0.357027	

Shields Critical		
viscosity	1.00E-06	
Rep =	6.61E+02	
Tau Star Crit	0.046322	
Movement	yes	

Wave Runup		
Slope 1/	16.857	
Lo=	45.15218	
omega =	1.322376	
Hb=	0.813204	breaker height
a	29.61045	
b	1.186768	

x(0)		0.4
initial		1.280888
	1	0.780708
iteration		1.662687
	2	0.601436
iteration		1.506362
	3	0.663851
iteration		1.564223
	4	0.639295
iteration		1.54196
	5	0.648525
iteration		1.550401
	6	0.644994
iteration		1.547183
	7	0.646336
iteration		1.548407
	8	0.645825
iteration		1.547941
	9	0.64602
iteration		1.548118
	10	0.645945
iteration		1.548051
	11	0.645974
iteration		1.548076
	12	0.645963
iteration		1.548067
	13	0.645967
iteration		1.54807
	14	0.645965
iteration		1.548069
	15	0.645966
iteration		1.548069
	16	0.645966
iteration		1.548069
	17	0.645966

Eo	0.50832

gamma b	1.101892			
db	0.738007	breaker depth	xb	
set down	-0.056		13.38463	
still water depth	0.198417	suspect		
gradient	0.013999			

Shields Critical on beach slope		
viscosity	1.00E-06	
Rep =	6.61E+02	
Beach angle:	0.059253	radians
Tau Star Crit	0.042322	
Movement	yes	